Mekelle University

Ethiopian Institute of Technology – Mekelle

School of Electrical and Computer Engineering

Electrical Power Engineering

Distributed Power Flow Controller Based Power Quality Improvement for Grid Connected Wind Farm- Case Study Ashegoda Wind Farm

By

Ashenafi Selema

Thesis Submitted to school of Electrical and Computer Engineering in partial fulfillment of the requirements for the degree of Master of Science in Electrical Power Engineering

Advisor:

Zenachew Muluneh (Ph.D.)

September 23, 2025

Mekelle, Ethiopia

Mekelle University

Ethiopian Institute of Technology-Mekelle (EiT-M)

School of Electrical and Computer Engineering

M.Sc. Program in Electrical Power Engineering

Final Thesis Acceptance Approval Form

1. Name: **Ashenafi Selema** **ID.No. EITM/PR176052/12**
2. Thesis Title: **(Distributed Power Flow Controller Based Power Quality Improvement for Grid Connected Wind Farm. Case study: Ashegoda Wind Farm)**
3. This is to certify that **Mr. Ashenafi Selema** has incorporated all the comments forwarded to her by the external and internal examiners during the thesis defense held on 16th October, 2025.

3.1. Mr. Ashenafi Selema (Student)	Signature	21 Oct. 25 Date
3.2. Dr. Zenachew Muluneh (Advisor)	Signature	21 Oct. 25 Date
3.3 Mr. Solomon Kiros (Internal Examiner)	Signature	21 Oct. 25 Date
3.4. Dr. Teshome Goa (External Examiner)	Signature	21 Oct. 25 Date
3.5. Mr. Solomon Kiros (Head, Electrical Power Engineering Chair)	Signature	21 Oct. 25 Date
3.6. Mr. Adhena Nigus (Dean, School of ECE)	Signature	21 Oct. 25 Date

Declaration

I, the undersigned, declare that this MSc. thesis is my original work, has not been presented for fulfillment of a degree in this or any other university, and all sources and materials used for the thesis have been acknowledged.

Name: Ashenafi Selema _____
Signature

Place: Mekelle, Ethiopia

Date of submission: October 21, 2025

Acknowledgement

First and foremost, I am very grateful to the almighty God for the unlimited wisdom, strength, and determination to complete this thesis work.

I would like to express my sincere gratitude to my advisor Dr. Zenachew Muluneh, for his invaluable guidance, encouragement constructive suggestion and advice throughout the course of the master's thesis research. Dr. Zenachew's expertise and patience have been pivotal in shaping this thesis.

My thanks also go to Mekelle University EiTM and Ashegoda Wind farm staff members for providing all the necessary resources, support, and providing learning environment during my research studies.

Last but not least, I would like to express my deepest appreciation to my parents, friends, and colleagues for their constant source of motivation and support in both academically and personally.

Table of Contents

Abstract

Grid penetration level of renewable energy is growing and merging dramatically. However, poor power quality creates a major integration and operation problems. Ashegoda wind farm represents Ethiopian first large scale wind power installation, having a total rated capacity of 120 MW. The substation is equipped with two 230kv buses that interconnect Lachi and Alamata substations. In the analyzed system, both transmission lines experienced high reactive power flow approximately 43MVAr and more than 3% current total harmonic distortion (THD), which leads to additional power loss, voltage drop, equipment overheating, and network congestions. On the other hand, the on-load tap changer (OLTC) transformer used to support voltage sag, swell, under-voltage, and over-voltage has slow response time up to 10 seconds per tap, and creates transformer overheating and mechanical fatigue. To solve such integration challenges, the incorporation of a distributed power flow controller (DPFC) with in the system is necessary for improved power quality and reliability. This study analyzed and modeled the integration, impact, cost benefit analysis, and Genetic Algorithm (GA) based optimal sizing and placement of DPFC for Ashegoda wind farm. The objective was to model, simulate, and asses its impact on voltage stability, reactive power compensation, and steady state and dynamic performance. The result indicated that, without DPFC the 230kv system operated at under-voltage of 0.89 pu with 5% current THD at bus 690v. After integration of 8MVA series and 25MVA shunt DPFC controller, the voltage profile is improved to 0.96 pu and current THD is minimized to 1.8%. Integrating DPFC exhibited excellent performance in maintaining voltage stability and limiting short-circuit current levels under different fault scenarios. The cost benefit analysis was carried out over a 20-year period. The total net present value (NPV) is estimated around $15,310,316.0 US dollars, while the total investment cost amounts $7,883,000.00 US dollars. By implementing the system, Ethiopian electric utility is expected to gain $7.5 million US dollars profit without considering scrap value. Generally, the researcher proved that DPFC is technically and economically feasible. MATLAB/Simulink 2018a and Excel-2013 was employed to model, simulate, and analyze the proposed DPFC system.

Keywords: DFIG wind farm, DPFC, FACT, Genetic Algorithm, Power quality, WEC.

List of tables

List of Figure

List of abbreviation

AC	Alternating Current
CBA	Cost Benefit Analysis
DC	Direct Current
DFIG	Doubly Fed Induction Generator
DPFC	Distributed Power Flow Controller
FACTS	Flexible Alternative Current Transmission Systems
GA	Genetic Algorithm
IGBT	Insulated Gate Bipolar transistor
MW	Mega Watt
OLTC	On-Load Tap Changer
PE	Power Electronics
PSAT	Power System Analysis Toolbox
pu	Per-Unit
RMS	Root Mean Square
SSSC	Static Synchronous Series Compensator
STATCOM	Static Compensator
SVC	Static Var Compensator
TCR	Thyristor Controlled Reactor
TCSC	Thyristor controlled Series Capacitor
THD	Total Harmonic Distortion
TSC	Thyristor Switched Capacitor
TSSC	Thyristor Switched Series Capacitor
UPFC	Unified Power Flow controller
VoLL	Value of loss load
WEC	Wind Energy Conversion

Chapter One
Introduction

1.1 Background

Modern power systems compromises generation, transmission and distribution networks, which make them complex systems. The generation system is responsible for the production and conversion of different energy resources into their equivalent electrical energy per the load requirements. As the name indicates, the transmission line is used to transmit the generated energy to the distribution networks at high-voltage to minimize transmission loses, and distribution networks are used to connect the end users with the grid system at low-voltage.

The increase in electrical energy consumption and demand opened a new era for renewable energy. Due to price and climatic concern of non- renewable energy, the energy sector is shifting towards renewable energy sources. The demand for reliable and good power quality leads to the improvement of renewable energy sources. Recently the most utilized renewable energy sources are water, wind and solar energy [1, 2]. Manufacturing industries and utilities are working on the improvement and optimization of those energy resources to minimize fossil fuel dependency. However, wind and solar energy resources are intermittent in nature and this bring integration difficulties with the old grid system. Not only this but some transmission lines are also more loaded than the planed and creates a line congestion. Due to economic and environmental reasons the installation of new transmission line is restricted [3, 4]. Hence, the utilities are forced to rely on already existing infrastructure instead of building new transmissions lines.

The importance of power system stability is increasingly becoming one of the most limiting factors for system performance. By the stability of a power system, we actually mean that the ability of the system to remain in its steady state operating condition, or synchronism, during system disturbances. If the oscillatory response of a power system during the transient period following a disturbance is damped and the system settles in a finite time to a new steady operating condition, we say the system is stable.

The transmission network are very often pushed to their physical limits, where outage of lines or other equipment could result in the rapid failure of the entire system. In order to maximize the efficiency of generation, transmission and distribution of power system, the use of Flexible Alternative Current Transmission Systems (FACTS) devices is an important and effective option [4, 5].

FACT devices are installing in power system to increase the power flow capacity of the transmission system, to maximize continuous control over the voltage profile and to damp power system oscillation. The ability to control power rapidly can increase stability margins as well as the damping of the power system, to minimize losses and operate under the thermal limits. Since, transmission line power flow is a function of line impedance, bus voltage magnitude and phase angle. If these parameters are controlled, then the power flow through the transmission line can be controlled in a predetermined manner.

Flexible AC Transmission System uses advanced power electronics to control parameters in the power system in order to fully utilize the existing transmission facilities. The FACTS controllers offer a great opportunity to regulate the AC transmission, increasing or diminishing the power flow in specific lines and responding almost instantaneously to the stability problems. Based on the technology and control mechanism FACT devices can be classified as follows:

i. Thyristor based FACT controller (Thyristor Switched Capacitor (TSC), Thyristor Controlled Reactor (TCR), Static Var Compensator (SVC), Thyristor controlled Series Capacitor (TCSC))
ii. Voltage source controller (VSC) based FACT controller(Static Synchronous Series Compensator (SSSC), STATCOM, UPFC)

The FACTS based power flow controlling devices can be connected in to three different connection configurations with the power system [6]. Namely:

i. Static Shunt Compensator (STATCOM, TSR,TSC)
ii. Static Series Compensating Devices (TSSC, SSSC, TCSC)
iii. Combined Compensator (UPFC, IPFC)

From all those VSI based FACTS controllers the unified power flow controller (UPFC) operates based on multiple operation. UPFC is considers and known as one of the best FACTS devices. It is a combination of series and shunt compensation, and can therefore provide active and reactive control to achieve maximum power transfer, system stability and improve power quality and reliability [5, 6].

UPFC is capable of handling the bus voltages, line impedance and phase angel for high rating power systems [7]. Real-time adaptability and economic constrains still are becoming the main integration challenges in UPFC system. In UPFC the common dc link is responsible for the power exchange between series and shunt converters. This section is vulnerable to failure form the whole system. A failure that happens at one amongst the device can have an effect on the total system. To attain the specified reliability for power systems, bypass circuits and redundant backup electrical device unit are needed [8]. In DPFC the common dc link that allow power transfer between the shunt and the series converters is eliminated. This make the series and shunt converters to work independently. The active power that used to exchange through the common DC link in the UPFC, is now transferred through the transmission line at the 3rd harmonic frequency [9].

1.2 Problem statement

The dramatic increase in electrical power demand stressed the electrical transmission and distribution lines and causes load imbalances, fault vulnerability, and existence of low frequency power oscillations on the grid system. This results in overall low power quality, which can damages utility converters, controllers, measuring device, and sensitive equipment. Hence, provision of a reliable and quality power is mandatory by using DPFC.

The poor power quality on the Ashegoda network causes a severe damage on the line-side IGBT converter of the DFIG. This is mainly caused by the harmonic distortion caused by the power electronics converters in the wind farm and high reactive power demand (33MVAr at the sample day) by Lachi substation. When the THD reaches above 3%, the converters and the controlling equipment start to create excess heat and start to malfunction [10]. Even under worst case scenarios they burnout. As a matter of fact, every unit of wind turbines have their own harmonic filter and reactive power compensators but it is not enough and need additional support to stabilize the system. By integrating one of the economical and powerful FACT device which is DPFC, the power quality, reactive and active power control can be maintained with the desirable values. Hence, the total penetration level of the wind farm will be improved.

Ashegoda wind farm does not have any kind of FACT devices. They use On-Load Tap Changer (OLTC) to prevent voltage fluctuations. OLTC works by changing transformer turns ratio in a discrete steps to control steady state bus voltage. The transformer is slower to react. It needs up to 10 seconds per single tap to respond for such kind of voltage dynamics [11]. According to IEC 61400-27 and IEEE grid performance standards, for grid connected renewable systems the fault response time should be within 100 milliseconds. Adding DPFC can provide fast and continues control with fault response time of 20 to 40 micro-seconds [12]. Doubly fed induction generators (DFIG) required rapid voltage support (in the order of milliseconds) to maintain its stability, reactive power balance, and converter protection. Hence, employing OLTC can lower the power output and experience poor fault ride through performance. Overall, the utility face difficulties to collect the capital, maintenance and operation costs for the farm, and the payback time will delay.

1.3 Research questions

The researcher answered the following questions in the research:

- What are power quality problems, their effects and mitigation technique in wind farm?
- How does DPFC perform power quality improvement in a power system?
- How to use GA in optimal sizing and placement of DPFC system?
- How DPFC performs in steady state and its dynamic response?
- Is DPFC economically feasible?

1.4 Objectives

1.4.1 General objectives

The main aim of the research is to improve power quality for grid connected wind farm by using distributed power flow controller for Ashegoda wind farm.

1.4.2 Specific objectives

- To model, design, and analyze the existing wind farm.
- To model and design DPFC and its controller for Ashegoda wind farm.
- To identify DPFC optimal size and placement using genetic algorithm.
- To simulate and analyze DPFC dynamic and steady state responses.
- To evaluate the cost benefit analysis.

1.5 Scope of the study

Under the research, the researcher modeled, designed, and simulated the DPFC system and evaluated the cost benefit analysis (CBA). Genetic Algorithm is used for optimal sizing and placement of the converter to increase reliability and efficiency of the system. The DPFC can maximize the incoming and outgoing power transfer capability under smooth operation of the power plant. The extent of the research is up to modeling and simulation of the DPFC for the wind farm by using MATLAB Simulink.

1.6 Limitations of the study

The study aims to provide a basic foundation and insight of the DPFC system to wards wind farm. However there are some limitation that could affect the research. One of the limitations of the research is that, the converter is size is limited to inject 0.1pu. This is due to the system operates within the tolerable limits. For future research works including load forecasting and considering environmental dispatch and maximum power transfer for future GA based optimization is recommended. Besides, integration of DPFC system can create protection equipment improvement for the wind farm. Proper sizing of protection for the DPFC and the wind farm is required.

1.7 Significance of the Study

By implementing the proposed technology the performance, reliability, and profitability of the wind energy will be enhanced. Not only this the power quality and congestion of the power system will be also optimized and improved. The DPFC has great advantage on the power system steady state and dynamic performance. Generally the system overall efficiency and profitability will be enhanced.

1.8 Thesis organization

The thesis is organized in the following manner, the first chapter begins with an introduction of wind farm technology and power quality problems and improvement, followed by problem statement, research questions, general and specific objective of the research, its scope and limitations , significant of the study and finalized by providing thesis organization. In chapter two literature review and related study on FACT devices application on power quality improvement are described in detail with their compassion. Not only this the recent. The next chapter discuss about data collection, modeling and

sizing of DPFC system, after this optimal sizing and placement of DPFC with cost benefit analysis for 20 years are done. Chapter four presents the MATLAB Simulink and PSAT results. The steady state performance and dynamic response of the PDFC are examined. Finally, the fifth chapter winds-up by conclusion of the findings and gives a recommendation for future research work on DPFC systems.

Chapter Two

Theoretical Background and Literature Review

2.1 Literature Review

During the injection and consumption of the energy input and output of wind turbines, the issue of power quality will raised up. For optimal operation and integration this issue must be considered and resolved. As the wind is an intermittent energy resource, it causes a voltage dip, harmonics, voltage sag, poor power factor and poor voltage regulation in the total grid system. In reverse, the wind farm is also affected by the poor power quality that come from the grid. To mitigate such kind of problem FACT devices are used and plays a critical role in mitigating the problem. FACT devices are capable of controlling power flow, enhancing voltage stability, reducing transmission loss and mitigating congestion [13]. The proper installation of FACT devices on the wind farm will improve power quality, system stability, and lower integration difficulties.

Due to seasonal and energy consumption behaviors, the single phase power consumption is random, unpredictable, and asynchronous. This medium and low-voltage distribution network will susceptible to three-phase imbalances. The three phase imbalance increases the system power loss, reduce the feeders and transformers capacity, causes overheating and damage three phase equipment, and disturb grid system [14].

Modern WECS have FACT devices connected with them to minimize integration difficulties. The most commonly used FACT devices are unified power flow controller (UPFC), Static Synchronous Compensator (STATCOM), Static Var compensator (SVC) and Thyristor Switched Capacitor (TSC). In 2019*, R. Thilepa et al.* [15], presented the use of Distribution Static Compensator (DSATCOM) to improve power factor and terminal voltage for linear loads at 400V voltage and 50Hz frequency. The researchers showed the principles of system operation and good simulation results but in real word loads are non-linear. Hence, the research needs farther study for non-linear loads to evaluate its performance. As studied by *J. Hussain et al* [13], the use of DSTATCOM is not limited to power factor control but it also capable of improving the total power quality when it is integrated with battery and energy management system at the point of common coupling (PCC) and explained the economic disadvantages of UPFC and SVC for low- voltage applications. The battery energy storage system (BESS) is used for better support and control of the active power.

The series-shunt and series-series power flow controller are known for their versatility among FACTS class. The application of combined power flow controller devices are universal, comprehensive, and multifunctional used for active and reactive power compensation, voltage regulation, and maintain stability of large power systems for all conventional and non-conventional energy resource. UPFC and IPFC are the most commonly used type of combined power flow controllers [6].

In 2020, Eti-Lni R. Akpan and et al. [16], analyzed the power flow under IPFC on 5 high-voltage transmission line (330kv) and six bus system in south-southern part of Nigeria. The main aims of the research are to minimize power loss and regulating the voltage stability. They conduct the load study by using Newton-Raphson algorithm and simulated in MATLAB. The designed IPFC system minimized 80.9% and 75.5% of active and reactive power respectively. However, they did not consider the optimal sizing and placement of the IPFC. If they were the results gained under the IPFC will perform better. In 2024, Qiuyu Li and et al. [17], studied a novel location method for IPFC base on Entropy theory.

Djamel Eddine and *et al.* [18], reviewed the application and classification of FACT devices on power system with the vast advantage of UPFC. The researchers mentioned that, FACT devices play an important role in reliability improvement, dynamic and transient stability enhancement, power quality improvement, and in optimal power flow on the power system. The power flow controlling devices (PFCD) provide a critic role in the static and dynamic operation of transmission line. PFCD operates by adjusting the system parameter to the required standard. The power system parameters are voltage magnitude, line impedance and transmission angle [18, 19]. The PFCD can be divided in to three main categories based on their system connection and configurations. Those are Series PFCD, Shunt PFCD, and Combined PFCD.

The UPFC is a combination of series and shunt compensators. This device consists of two voltage source converter connected in back-to-back configuration trough a DC-link capacitor [5, 6, 18]. In 2018, Aamir Farooq et al. [5], analyzed the effects of UPFC on 500kv transmission line and assessed system active power, reactive power, and bus voltage with and without UPFC device. The entire system is a combination of 230kv and 500kv voltage transmission line. The researchers select bus-2 (B-2) on the 500kv system. However, they did not explained why they chose the 500kv system and B-2. The researchers did a good FACT device theoretical performance comparisons based on load flow control, voltage control, transient stability, and dynamic stability.

The application of UPFC system in wind, tidal and diesel standalone and hybrid system can be used for the reactive power compensation. In 2019, S. Singh [20] explains the back to back converter is used by many WEC manufacturers. The BTB converter uses two identical power converters on the generator side and grid side of the Dc link. The two level BTB conversion system is used in the DFIG. This helps to provide a full centrality of four quadrant operation. The use of frequency converter in the system is also mandatory to gain 50Hz or 60Hz frequency. The process can be attained with or without DC-link.

The UPFC and IPFC are suitable for power flow control. Though, the installation complexity, high cost, complex topology and less reliability introduce to the development of new FACT device called the Distributed Power Fellow Controller (DPFC) [19]. The main failing converter section in the UPFC system is the DC-link. Due to its failure rate, the system become unreliable. Recently the DPFC is the

power full device among the PFC family and this is due to the elimination of the DC-link, low capital cost and high reliability. The DPFC eliminates the DC-link between the series and shunt compensators.

In DPFC system transmission line is used for the active power exchange between converters at third harmonic frequency [19, 21, 22]. The converter uses a distributed series of single phase converters instead of using a one series large three phase converter and one single shunt converter. This minimizes the cost and maximizes the reliability as explained by *Mr. Mahesh Shende et.al.* [7]. The D-Facts are a single phase based converters. A mathematical model for the dynamic energy exchange of the third harmonics and optimal control strategy for proper DPFC operation is mandatory. In 2022, Vemuri Sowmya Sree et al. [21] proposed fuzzy logic controller (FLC) by eliminating PI controller for solar-wind hybrid energy systems. The FLC have a good performance over the PI controller for total harmonic distortion, voltage sag and swell mitigations.

As described by *Biplab Bhattacharyya and et.al*. [8], the optimal placement of FACT devices play an important role in minimizing the transmission loss during heavy load conditions. To achieve this Genetic Algorithm (GA) and Differential Evolution (DE) techniques can be used for optimal placement of the device. Overall, a lot of studies have been done but the optimal placement and sizing with a detailed cost benefit analysis (CBA) are barely studied. The researcher is going to study on those research gaps for the efficient, economical, and smooth operation of the Ashegoda wind farm.

The series device of the DPFC works same as distributed FACTS working principle. The operation principle is based on multiple low-rating single-phase converters replace the high-rating three-phase series converter, which greatly reduces the cost and increases the reliability. The DPFC can be considered as a UPFC that employs the DFACTS concept and the concept of exchanging power through harmonic. Therefore, the DPFC inherits all the advantages of the UPFC and the D-FACTS. This device is characterized by its high control capability, high reliability, and low cost. Generally, the DPFC can be considered as an improvement of UPFC [7].

Currently, the application of DPFC system is wide in power generation integration and power quality improvement for standalone and grid connected renewable energy systems. In 2020, prof. Radharaman Shaha and et al. demonstrates the power quality improvement in photovoltaic based distribution system by using DPFC. The research does not explains the working principles and difference form UPFC. It does not have any mathematical modeling and simulation for the proposed system.

In 2024, Thamatapu Eswara Rao et al. [3], studied the impacts of DPFC systems on the performance of wind-solar hybrid micro grid system. They used the fuzzy logic control technique and Lion optimization algorithm (LOA) to improve power quality problem and transient stability and they compared the voltage, reactive power and rotor speed and the total harmonic distortion (THD) under the fuzzy logic, PI, and LOA controlling techniques for series and shunt controller.

Table 2. 1. General compression of commonly used FACT devices

Device name	Voltage control	Load flow control	Transient stability	Dynamic stability	Complexity	Cost	Reference
STATCOM	High	Low	Medium	Low	Medium	Low	[5, 6, 13, 23]
SSSC	High	Medium	Medium	Medium	Low	Low	[23, 24]
TCSC	Low	Medium	High	Medium	Medium	Medium	[5, 6]
IPFC	Medium	High	High	Medium	High	Medium	[6]
UPFC	High	High	Medium	Medium	High	High	[5]
DPFC	High	High	Medium	Medium	Medium	Medium	[3, 7, 25, 9]

2.2 Conceptual survey

2.2.1 Basics of Wind Energy

The demand for sustainable and affordable electrical energy is dramatically increasing globally. However, the concern of greenhouse effect caused by conventional (non-renewable) energy source for the generation of electrical energy become a big obstacle to satisfy the growing demand. This obstacle opened a new era of renewable energy [3]. Clean energy generation exceeded 40% of global electricity generation in 2024 for the first time since 1940. The energy generated by renewables added 858 TWh in 2024 [1]. According to the International Renewable Energy Agency (IRENA) report of 2025, the global wind share 8.1% and solar energy share 6.9% together exceeded hydropower energy 14.3% for the first time in 2024. The total energy generated by solar showed a rapped increase for the past there consecutive years and reached 2131 TWh in 2024. The wind also played a central role and its generation reached 2494 TWh increased by 182 TWh (7.9%) from 2023 [2].

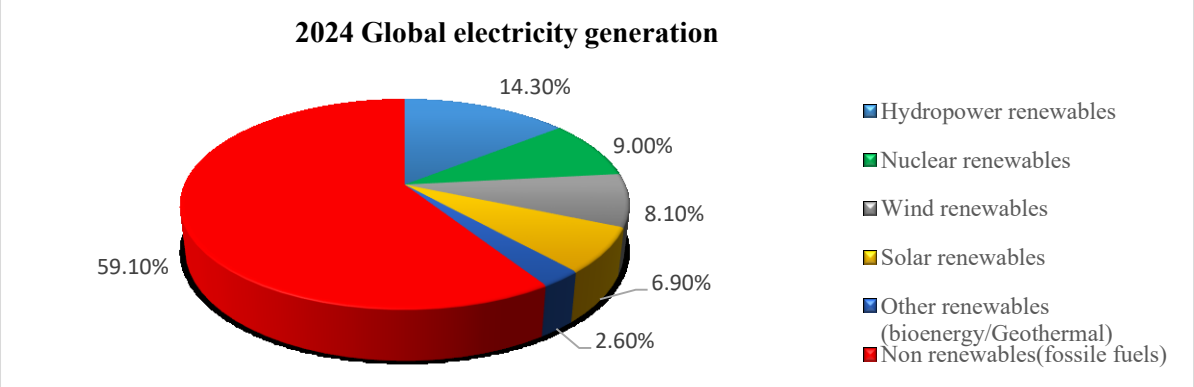

Figure 2. 1. Global electricity generation 2024

Wind energy is characterized by its abundance and environment-friendly energy form [25]. Wind energy is an energy produced from the motion of air. A small part of the solar energy on the Earth is converted into kinetic energy of flowing air. Wind motion is caused due to uneven distribution of temperature of solar radiation and the earth's rotation. Wind energy is cartelized by its renewable, unlimited and clean energy [26]. A wind turbine is used to transform the kinetic energy in the wind to mechanical energy in a shaft and finally into electrical energy in a generator. There are two primary physical principles by which energy can be extracted from the wind; these are through the creation of either lift or drag force (or through a combination of the two). The rated output power of the wind turbine is calculated by [18, 25]:

$$Pv = {}^{1}/_{2}\ \pi\rho R^2V^3 \tag{2.01}$$

$$Pm = {}^{1}/_{2}\ \pi\rho C_pR^2V^3$$

$$C_p(\beta,\lambda) = 0.5176\left({}^{116}/_{\lambda_i} - 0.4\beta - 5.0\right)e^{\ {}^{-21}/_{\lambda_i}} + 0.0068\lambda \tag{2.02}$$

$$\frac{1}{\lambda_i} = \frac{1}{(\lambda + 0.08\beta) - {}^{0.035}/_{(\beta^3+1)}}$$

We can calculate λ by:

$$\lambda = \frac{R\omega_m}{V} \tag{2.03}$$

Where P_v : Power of wind

P_m: Power generated by wind turbine

C_p : Coefficient of power (aerodynamic efficiency)

R : Blades radius

ρ : Air density

V : Wind speed

λ : Tip speed ratio and

β : Blade pitch angle / angle of inclination of the blades

ωm : Rotational speed/ angular speed of blades.

In 1919, Albert Betz demonstrated the maximum mechanical power generated by wind turbine cannot exceed 59.3% of the kinetic power of air. This is called the Betz limit [27].

$$C_{p_{max}} = \frac{P_m}{P_v} = 0.593 = 59.3\% \tag{2.04}$$

$C_{p_{max}}$ does not include energy loss of mechanical to electrical energy conversion. As a result, the efficiency of wind turbines is only 60 to 70% of Betz limit.

Today's wind turbine are showing a rapid developments in their overall technology and increased competitiveness over other renewable energy. It is becoming promising energy source in the world especially in offshore application due to its availability [28].

WACS can be classified as fixed and variable speed wind turbine system. The variable speed WECS are most commonly used. The variable speed technology is the most powerful and advanced technology used for the generation of mega wind energy. The conversion technology used in this is the multi-level converters. This is due to the high and medium power output handling capacity [12].

There are three major types of variable speed WECS. It is easy to integrate variable sped WACS with grid by using power electronics devices [13].

i. Doubly fed induction generator (DFIG)
ii. Gear/Gearless squirrel cage induction generator (SCIG)
iii. Gear /Gearless wound rotor synchronous generator (WRSG)

The DFIG can be used as a partial scale with power converter. 30% of the capacity of DFIG is delivered to the grid by using the rotor part using power electronics, the rest of the energy is delivered directly from the stator to the grid.

The power electronics is integrated with the internal system of WECS, generator, load and the grid. The power electronics semiconductors are insulated gate bipolar transistor (IGBT), integrated gate commutated thyristor (IGCT), MOSFET, MOS-gate thyristor and silicon carbide FET. FACT application in the smart grid is used for maximizing the system efficiency, controllability and minimizing the operation and running cost. Based on the use of power electronics WECs can be classified as WECS without power electronics, WECS with partial rated power electronics, and WECS with full scale power electronics [29, 30, 31].

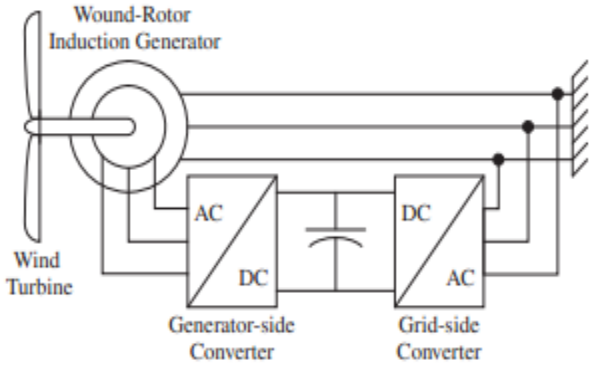

Figure 2. 2. Variable speed DFIG with partial application power electronics [32]

The DC-link capacitor is very important in every grid connected DFIG system. The DC-like voltage support, harmonic minimization and reactive power compensation. This power electronics can be used for maximizing the smart grid (the bidirectional power flow) [31].

Areas with annual wind speed of 7m/s and above are technically and economically suitable for grid-based electricity generation, those areas in Ethiopia are primarily found on high terrains such as ridges

and mountain tops which are mainly located at the edge of the highlands that form the great East African Rift Valley, North Eastern cliff of the country near Tigray regional state and the Eastern part of the country. In those areas the wind velocities are in the range of 7 m/s to 9 m/s**,** which is suitable for wind energy generation. The majority of the sites lie in altitudes between 2,000 and 2,400 m. According to Ethiopia electric power report, the total exploitable wind energy potential of the country is around 1,350 GW and less than 1% is exploited. All the wind generations delver power to the national grid [33, 34].

Table 2. 2 Existing and upcoming wind power plants (WPP) with their capacity

No.	Project	Generating capacity (MW)	Annual Energy production (GWh)	
1	Adama I WPP	51	157	Connected to grid
2	Adama II WPP	153	479	
3	Ashegoda WPP	120	450	
	Total	*324*	*1086*	
1	Ayisha WPP	300	592	Planed project
2	Messobo WPP	42	104	
3	Assela WPP	100	197	
4	Debre Birhan WPP	100	197	
	Over all	*866*	*2176*	

2.2.2 Ashegoda wind farm

Ashegoda Wind farm is one of the grid connected wind farms which is located in the northern part of Ethiopia 783 km from Addis Ababa and at 20 km south eastern of Mekelle, found at an altitude of 2200-2560 m above sea level. EEPCO signed a contract agreement for Ashegoda wind power construction project with Vergnet S.A in October 2008, in Engineering, Procurement and Construction Turnkey (EPCT) base with total installed capacity of 120 MW. With 210 Million Euro total capital cost, and start construction in October, 2009.

The project had three consecutive phases that is phase I, 30MW for 16 months, Phase II, 45MW within 26 months and Phase III, 45MW within the 36 months from the commencement works. But with the agreement the latter two phases combined in to one phase with a turbine different from the first phase that is three bladed and that has 54 turbines with rated power of 1.67MW each. The loan for the foreign portion of the project cost (91% of the capital cost of the project) is covered by French lenders BNP PARIBAS as Mandate Lead Arranger for COFACE Backed Loan amounting Euro 130 Million and Tied commercial facility Euro 33.6 Million and Agency France Development (AFD) Euro 45 Million. Construction Administration, Supervision, Operation and Maintenance consulting contract is signed with Lamaher International GmbH (LI).

The main contractor of the project (Vergnet S.A) gave some of the works to the subcontractors like:

- ALSTOM - Subcontractor for the substation works and phase two total works.
- In the substation work Ethiopian company SIGMA ELECTRIC had involved in the electromechanical works as sub-contractor for ALSTOM
- HYDRO - Subcontractor for the grouting of Guy wire foundation
- SINTEC ETHIOPIA - Subcontractor for the Electromechanical works in the WEC.
- RAMA - Subcontractor for the Civil works (turbine foundation, peripheral foundation, trenches, access road works and civil substation works).

The installed turbine parameters

Phase I installed turbine parameter

- Total Installed Capacity ……....30 MW
- Wind Turbine Type …….GEV HP – 62/1000
- Total number of Wind Turbine……..30
- Rated Power…….1 MW
- Rotor diameter…….62 m
- Tower height …….70 m
- No of blade …….....2

Phase II and III installed turbine parameter

- Total Installed Capacity ……....90 MW
- Wind Turbine Type ……ECO 74
- Total number of Wind Turbine……54
- Rated Power……..1.67 MW
- Rotor diameter……..….74 m
- Tower height ……..80 m
- No of blade ……...3

For constructing a wind farm the availability of high average wind speed at the site is needed. The wind velocity and direction depend on the imposed pressure gradients, and the local geography [25]. Ashegoda wind farm have the following parameters:

- Site Air density ……..…….0.922 kg/ m^3
- Site Temperature ……..15.5 ºc
- Annual average wind speed at 40 m……..8.11 m/s

Ashegoda substation has two incoming and outgoing circuit connections connected to the bus bars namely the Alamata and Mekelle incoming or outgoing connections. Bus bars are conducting bars to which number of circuit connections is connected. Each circuit has certain number of electrical components such as high voltage circuit breakers, Isolators, earth switches, current transformers, voltage transformers, relay, lighting arrester and bus bar coupler.

Ashegoda wind substation basically consists of number of incoming and outgoing circuit connections connected to bus bars. The 230kv bus bar in the substation is connected to the Mekelle and Alamata line and also there is a 33kv incoming line from the wind turbines to the power transformer. Ashegoda wind farm substation is organized as:

- 33kV Cable Network
- 33kV Overhead Lines Network
- 33kV Cluster Substations
- 230/33kV High Voltage Substation
- 230 kV National Network

The main barrier in the development and delivery of wind energy is the difficulty in grid integration. For grid integration and synchronization high voltage must maintain the same voltage, frequency and phase angle. Otherwise the system will face disturbances. For high penetration of wind energy the power quality, low voltage rid and active and reactive power control must be kept within the standards. In addition to this for efficient operation the grid power quality must satisfy the power quality requirements.

2.3 Power quality Problems

The definitions, criteria's, and ranges are defined by international code agencies, equipment manufacturers, electric power operators, and customers. The word power quality is mentioned in a paper published in 1968 [35]. The physical meaning of power quality is the difference between the supplied power quality and the required power quality for the reliable operation of equipment and loads. The delivered power quality is characterized by two factors namely *supply Continuity* and *voltage Quality* [36, 24]. The poor power quality leads to an extra power consumptions, power interruption due to false protection, data loss, and equipment damage.

In engineering terms, power is the rate of energy delivery at a time and it is proportional to the product of voltage and current. The power supply system can only control the quality of the voltage; it has no control over the currents that particular loads might draw. Therefore, the standards in the power quality area are devoted to maintaining the supply voltage within certain limits. Know a days there is a big concerns on power quality from electric utilities and end users. This is due to five major reasons. Those are [13, 37, 23]:

i. Many things are now interconnected in a network. The failure of any component has much more important consequences on entire system.
ii. Modern electrical devices are more sensitive to power quality variations than the past.
iii. Future concerned on the impact poor power quality on system capabilities.

iv. The increased awareness of power quality issues by end users and challenging the utilities to improve the quality of power delivered.
v. The economic impact of poor power quality on utilities, customers, and suppliers equipment.

AC power systems are designed to operate at sinusoidal voltage magnitude and frequency typically 50 or 60 Hz. Any significant deviation in waveform, magnitude, frequency, or purity is a potential power quality problem. While it is the voltage with which sector is ultimately concerned. Addressing current phenomena to understand the basis of many power quality problems is must. This is due to the behavior of current have a major impact on the system voltage. When current pass through the system impedance it can cause a variety of disturbances to the voltage. Such like,

i. Short circuit current can causes the voltage to sag or disappear completely.
ii. Currents from lightning strikes passing through the power system cause high-impulse voltages that frequently flash over insulation and lead to other phenomena, such as short circuits.
iii. Distorted currents from harmonic-producing loads also distort the voltage as they pass through the system impedance. Thus a distorted voltage is presented to other end users.

Modern power system has many challenges that should be met in order to deliver quality power in a reliable manner. There are many causes and reasons in which affect the power quality in the power system. The power quality can be affected by internal and external factors. We can also classify PQ issues as natural and man-made and manifested in voltage, current, or frequency deviations that results in failure or mal-operation of equipment. Lightening and storms are natural causes of poor PQ. Whereas man-made causes are loads and operations [23]. The occurrence of such problems in the power system network is almost indispensable. Therefore, taking proper mitigation technique is mandatory to maintain good power quality. Some power quality problems are explained below [36, 24, 23].

2.3.1 Transients

This any unusual that happen in power system that shafts the steady state operating condition to another with a rise time less than 1μs up to a few milliseconds [24]. Transient is undesirable and momentary an event in nature. The name surge is used interchangeably with the transient. Transients can be classified as oscillatory or non-oscillatory (impulsive) [37]:

A. Impulsive transient

It is a sudden non power frequency change in steady state conditions of voltage, current, or both. Impulsive transients are unidirectional in polarity either positive or negative. Lightning strike on the power system transmission line is the most common cause of this impulsive transient.

B. Oscillatory transient

It is a sudden non-power frequency change in steady state conditions of voltage, current, or both that includes both positive and negative polarity values. The energizing Back-to-Back capacitor can cause an oscillatory current transient in tenth of kilohertz. A local system response to impulsive transient often result in oscillator transient. This power quality problem can led to equipment failure [24].

2.3.2 Short-Duration Voltage Variations

This category encompasses the IEC category of voltage dips and short interruptions. Each type of variation can be designated as instantaneous, momentary, or temporary, depending on its duration. The main consequences of short duration voltage variation are effects on data storage system, malfunction of sensitive devices like PLC's, malfunction of Adjustable Speed Drives ASD's, failure of contactors and switchgear, and malfunction of ASD.

The short-duration voltage variations are caused by fault conditions, operation of large loads which require high starting currents, intermittent loose connections in power wiring, and switching actions to isolate the faulted sections. Depending on the fault location and the system conditions, the fault can cause voltage interruption, sag and swell in the system.

A. Short interruptions (complete loss of voltage)

The fault condition can be close to or remote from the point of interest. In either case, the impact on the voltage during the actual fault condition is of the short-duration variation until protective devices operate to clear the fault.

B. Voltage Sag (temporary voltage drops)

According to IEEE standard 1159-1995 voltage sag is defined as a temporary reduction of RMS supply voltage ranging from 10% to 90% of the declared RMS voltage for a period of 0.5 cycle to 1 minute [23]. The voltage sag is the most frequently occurring problem caused by starting of electric motors, energizing of transformers, and short circuit in nearby network are the most common causes of voltage sag.

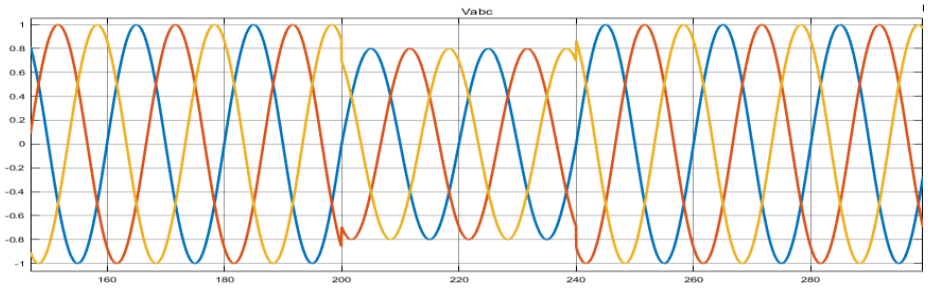

Figure 2. 3. Voltage sag

C. Voltage Swell (voltage rise)

Voltage swell is defined as a temporary increase in RMS voltage of more than 10% of the declared RMS voltage for a period of 0.5 cycle to 1 minute at power system frequency.

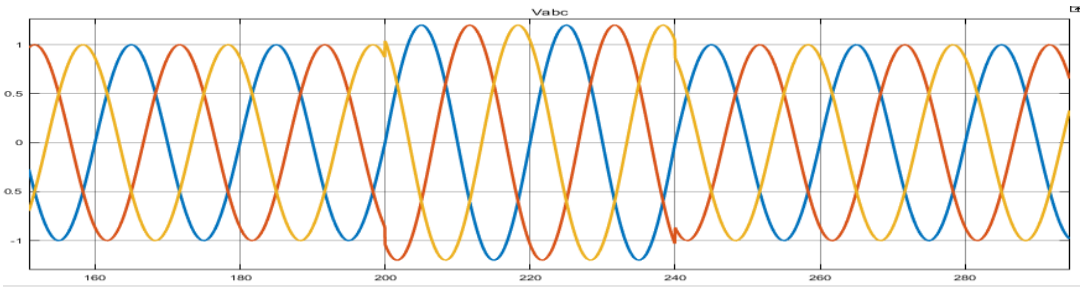

Figure 2. 4. Voltage swell

2.3.3 Voltage Fluctuations (Flickers)

A series of random or continues fluctuation of voltage due to arc welding machines, starting of high-power motors, disconnecting of large loads, and lightning is called voltage flickers. Voltage flicker cause a frequent luminous intensity variation of florescent lamps, incorrect operation of sensitive equipment, and shorten equipment life span [24]. According to ANSI C84.1, the magnitude of voltage flickers does not exceed the voltage range of 0.9 Pu to 1.1 pu.

2.3.4 Long Interruptions

If the duration for which the interruption occur is large ranging from few mille seconds to several seconds then it is called long interruption. This type of interruption leads to the stoppage of power completely for a period of time until the fault is cleared. The voltage signal during this type of interruption is shown in Fig. below. The main causes of long interruptions are power system faults, human error, and improper functioning of protective equipment

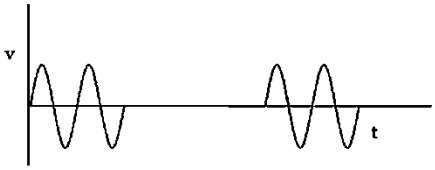

Figure 2. 5. Long interruption voltage signal

2.3.5 Waveform Distortion

Waveform distortion is defined as a steady-state deviation from an ideal sine wave of power frequency principally characterized by the spectral content of the deviation. Waveform distortion can be classified as DC offset, harmonics, inter-harmonics, notching, and noise.

Voltage harmonics are the second, third, fourth and so on multiple spectral component of the fundamental frequency voltage waveform, The main effects of harmonics in power system are intra-harmonics are and non-integral multiple of the fundamental frequency [38, 39]. The 3rd harmonic order is the most critical and contains three times the fundamental frequency. When non-linear single phase

loads operate, the 3rd harmonic is generated. Those devices are rectifiers, variable speed drives and converters [24]. Thermal stress (current effect), insulation stress (voltage effect), load rupture (abnormal operation), heat generated on transformers, telecommunication interference, increased losses in shunt capacitor banks and rotating machines, and harmonic over voltage are the main effects of waveform distortions.

The recommended practices and requirements for harmonic control in electrical power systems are control of the amount of harmonic and voltage current injected into the system and takes place at the end-user application. The voltage and current harmonics resonance can be classified as series resonant and parallel resonance. Series resonance appears when the circuit impedance gets lowest at certain frequency and this leads to excessive heating of transmission line and results in high power loss. Parallel resonance exists when the circuit impedance is getting the highest at certain frequencies resulting in excessive voltage excursion result in equipment malfunction [24].

2.3.6 System unbalance

A grid system to be considered balanced if the three phase current and voltage waveforms are sinusoidal at equal amplitude with 120° phase shift between consecutive phases. Voltage unbalance is the maximum voltage deviation from the average three phase voltages or currents divided by the three phase average voltage or current in percent. Voltage imbalance less than 2% single phase loads over three phase. For more than 5% imbalance can result from single phasing conditions without transposition. To check the voltage imbalance a negative –sequence component is used. Voltage unbalance can cause over heating of electrical machines.

2.3.7 Power frequency variations

It is the deviation of the supplied power fundamental frequency from its specified nominal value of 50 or 60Hz. The variation of the power frequency is directly related to the rotational speed of the generators supplying the system. It is possible to express the frequency (f_e) in hertz as a result of mechanical speed (n_m) in revolution per minute. Where p is the number of poles [40].

$$n_m = \frac{120\, f_e}{p} \rightarrow f_e = \frac{n_m p}{120}$$

According to EN-50160, under nominal 50 Hz operating condition the frequency deviation measured in 1 sec should 49.5 Hz to 50.5 Hz which is 50 Hz ± 1% for networks with synchronous connection to interconnected networks 99.5% of the year. In case of networks without synchronous connection to interconnected line from 49 Hz to 51 Hz which is 50% ± 2% for 99.5% of the year [24].

The dynamic balance mismatch between the load and generation lead to the slightly frequency variation. However, the variation exceed beyond the acceptable limit caused by faults on the power transmission system, a large block of load being disconnected, or a large generation going off-line.

2.3.8 Low power factor

Low power factor is caused due to high reactive power exchange between loads and three phase ac power grid. Hence, system voltage and current will have a phase shift due to the difference phase angle. The current in non-linear loads are not sinusoidal. The power factor is calculated by using the fundamental voltage and current. The main cause of low power factor are inductive loads.

The existence of higher reactive power results in voltage across the power transmission and distribution networks. The value of power factor ranges between 0 and 1. When it approached one it means that the system have a smaller phase shift and good power quality.

2.4 Power Electronic Technologies for Power Quality Problems

The conventional method of power system network control by using tap transformers adjustable load, phase-shifting transformers, and generator excitement control are slow and insufficient to effectively on controlling and responding to the modern power system disturbances especially for renewable energy integration. The integration of this renewable energy have negative impacts on the operation, control and protection of the grid system. The growth of power electronics device is the key factor for the development of FACTS. FACT devices utilize electrical energy power generation, conversion, and integration [18].

The power electronic application in utility is growing rapidly in modernizing the traditional power system, smart-grids, and flexibility of the AC transmission line. This promises to change the landscape of future power generation, operation and control by tackling key concerns related to reliability of power electronics, distributed generation, energy storage, smart cities, micro-grids, and power quality [32, 24]. The utility application of power electronics can be categorized as distributed generation (DG), power electronics in adjustable speed drives, transmission and distributions HVDC and FACTS, and power quality solutions. The three basic categories of power electronics in power quality solutions are emphasized below:

2.4.1 Static shunt compensators

The static shunt compensator uses shunt connected compensating devices to supply the reactive power demand of loads. The line current I is varied by varying the injected reactive current I_{sh}. The I_{sh} is adjusted by varying the shunt connected device impedance. Shunt connected, fixed or mechanically switched reactors are applied to minimize line overvoltage under light load conditions. Shunt connected, fixed or mechanically switched capacitors are applied to maintain voltage levels under heavy load conditions. Examples of static shunt compensators are thyristor controlled reactor and thyristor switched reactor (TCR and TSR), shunt connected Distribution STATCOM (DSTATCOM),and Thyristor switched capacitor and Thyristor controlled reactor (TSC-TCR)

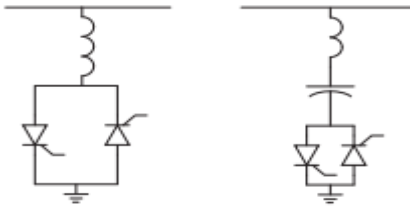

Figure 2. 6. Switched shunt inductor and capacitor [32]

2.4.2 Static series compensators

Such basic compensators may be connected in series to obtain the desired voltage rating and operating characteristics. The degree of series compensation is controlled in a step-like manner by increasing or decreasing the number of series capacitors inserted. Variable impedance type series compensators, and switching coverter type series compensators are the two methods of PE-based series compensators.

2.4.3 Combined compensators

The combined compensators are the combination of series- series or shunt-series compensators. The common examples of combined compensators are Dynamic Flow Controller (DFC), Interline Power Flow Controller (IPFC) and Unified Power Quality Conditioner (UPQC) [5].

The IPFC provides a dynamic compensation and power flow management in the transmission line. This device can be used to minimize transmission power loss [16].

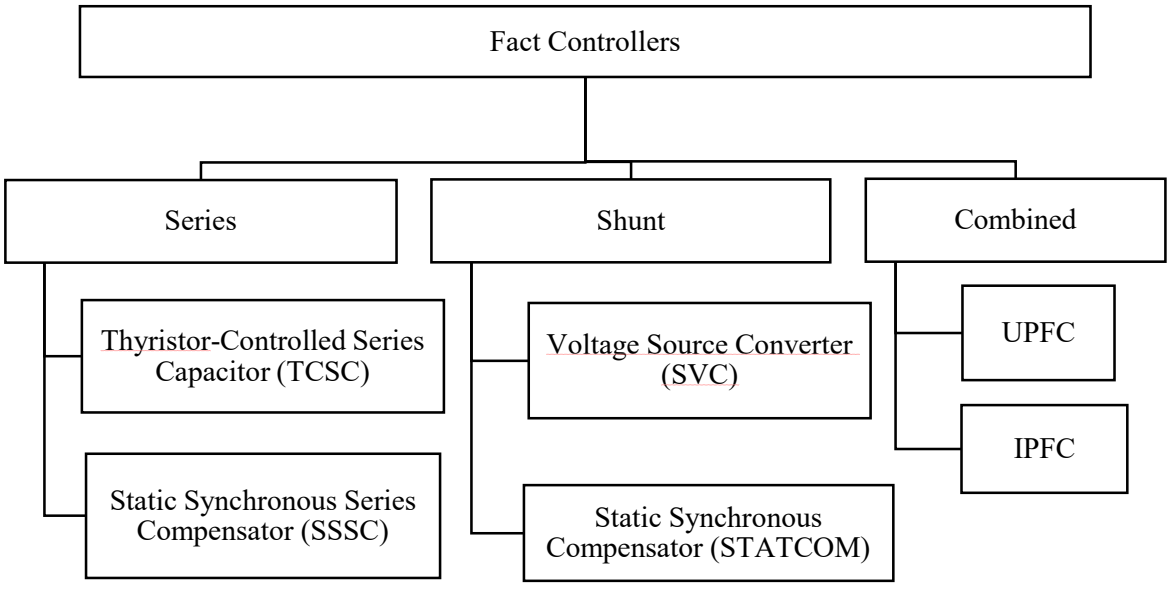

Figure 2. 7. FACT controller

The DVR is similar to SSSC while UPQC is similar to UPFC. In spite of the similarities, the control strategies are quite different for improving power quality. A major difference involves the injection of harmonic currents and voltages to isolate the source from the load. For example, a DVR can work as a

harmonic isolator to prevent the harmonics in the source voltage reaching the load in addition to balancing the voltages and providing voltage regulation. A UPQC can be considered as the combination of DSTATCOM and DVR. A DSTATCOM is utilized to eliminate the harmonics from the source currents and also balance them in addition to providing reactive power compensation (to improve power factor or regulate the load bus voltage).

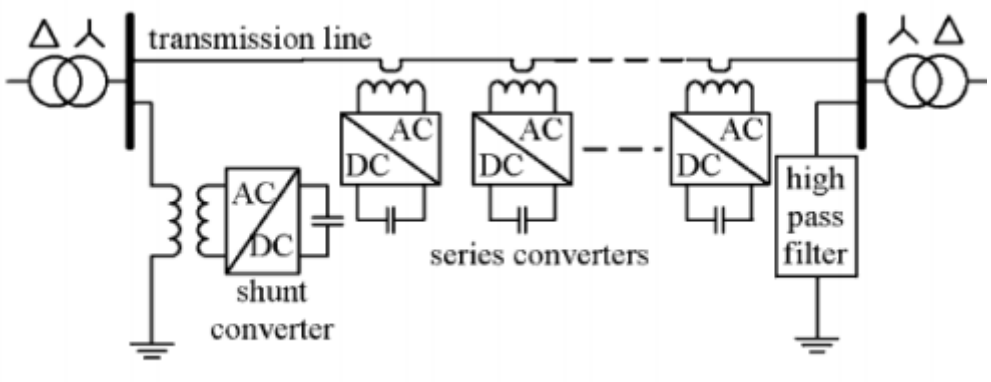

Figure 2. 8. DPFC system configuration [38, 39]

The main barrier in the development and delivery of wind energy is grid integration difficulty. For grid integration and synchronization high voltage must maintain the same voltage, frequency and phase angle. Otherwise the system will face disturbances. For high penetration of wind energy the power quality, low voltage rid and active and reactive power control must be kept within the standards. In addition to this for efficient operation, the grid power must satisfy the power quality requirements.

There are general steps that are associated with investigating of Power quality problems. The quality of electric power delivered is characterized by two factors namely- “continuity” of supply and the “quality” of voltage. As indicated by IEEE standard 1100 [37]

Chapter Three

Data Collection and System Modeling

3.1 Data collection and analysis

The existing problem identification and characterization of Ashegoda wind farm is done based on the collected data. Most of the data were obtained from the Ashegoda wind farm SCADA system as well as from the operation and maintenance manuals. Then by reviewing related literature and manufacturer data, cost benefit analysis is done based on the total capital, operation and maintenance costs against its benefits. Finally using MATLAB Simulink 2018a and Excel-2013 modelling and simulation of the distributed power flow controller and CBA are done.

3.1.1 Ashegoda wind turbine type

A. Vergnet GEV-HP turbine

The GEV-HP wind turbine is a two blades aero generator with adjustable speed, 1MW rated maximum power with front wind. GEV-HP turbine has a teetering hub and power control made by electrical pitch and electronic controller.

B. ECO-74 wind turbine

The Alstom ECO-74 is a wind turbine rated 1.67MW at 74m rotor diameter and employs three-blade for optimal aerodynamic performance. The cut-in and rated wind speed of the turbine are 3m/s and 13m/s respectively. The rotor speed varies between 10 and 19 rpm under active pitch control. Overall, Appendix A combines all the equipment specifications utilized in the wind farm.

Table 3. 1. Rated transmission line conductor specification [41]

№	Voltage (KV)	Station	Station	Conductor type	Size (mm^2)	Conductor configuration	Line rating (MVA)	Length (km)
1	230	Ashegoda	Alamata	AAAC	180	Double	318	125
2	230	Ashegoda	Mekelle	AAAC	180	Double	318	15

Table 3. 2. Rated residential and commercial power demand of tied substations

№	Substation name	P-load (MW)	Q-load (Mvar)	Remark
1	Mekelle	17.8936	8.6663	Distribution load demand neglecting big industries like Mesebo cement factory
2	Alemata	1.872	0.906	

The below load curves demonstrates daily load curve at Ashegoda wind power plant substation bus measurements. The data's are for Alamata-substation and Lachi-substations on some randomly selected day logged. For more detailed information see appendix.

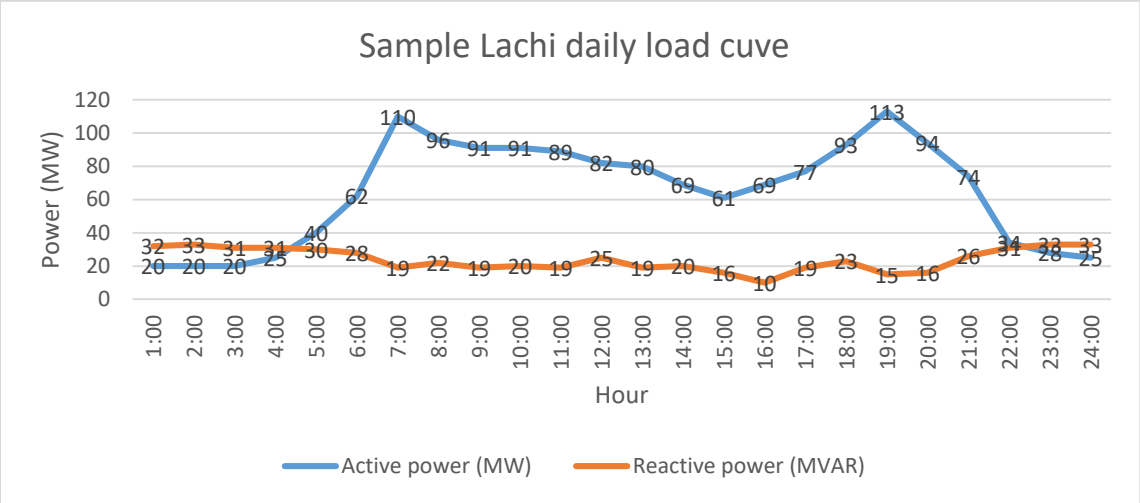

Figure 3. 1. Sample daily load curve from Lachi-substation

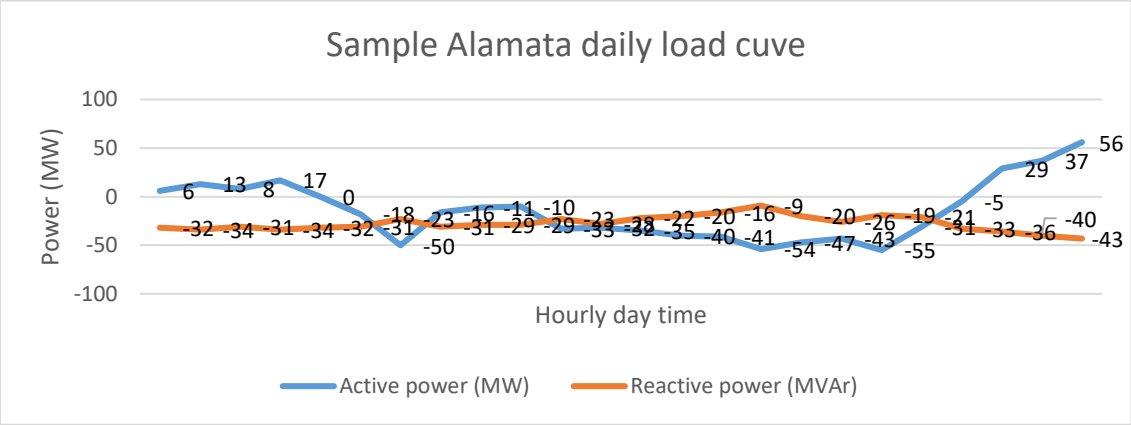

Figure 3. 2. Sample daily load curve from Alamata-substation

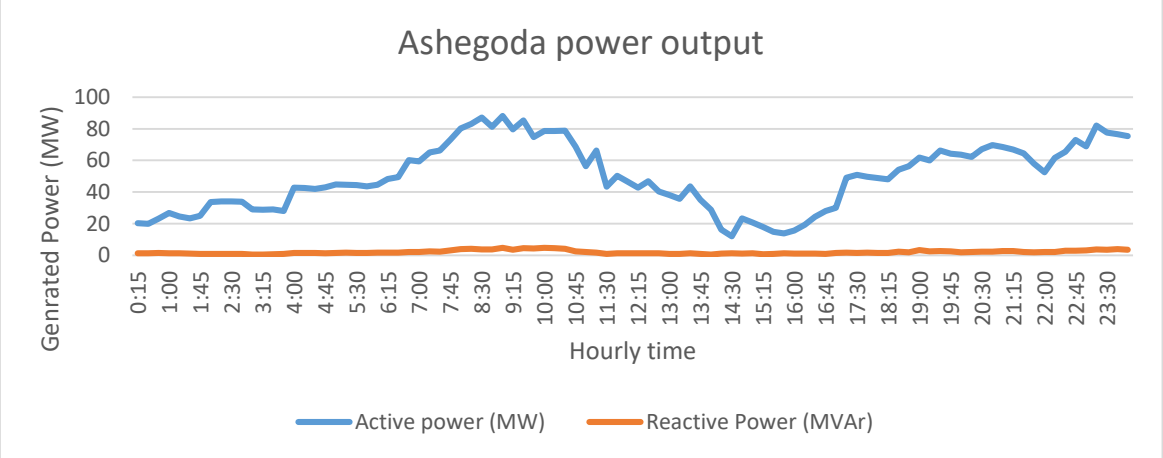

Figure 3. 3. Ashegoda wind farm power output

Based on the collected data the researcher identified that there is a high demand of reactive power from the substation. Not only reactive power demand there is harmonic distortion on the system due to harmonic sensitive equipment failure. The substation uses a power transformer tap changing mechanism to support voltage fluctuation. As a matter of fact such method causes transformer heating, slow response, and equipment tire and wear. This shorten the operating time of the transformer.

Table 3. 3. Power consumption description

Bus type	Positive active power(P>0)	Negative active power (P<0)	Positive reactive power (Q>0)	Negative reactive power (Q<0)
Generator side	Generator supplying real power	Generator absorbing real power	Generator supplying inductive VAR power	Generator absorbing reactive power
Load side	Load consuming real power	Load supplying real power	Load consuming inductive VAR power	Load supplying reactive power

3.2 DFIG modeling and control

The dynamic modeling of the DFIM can be done by transforming the three axis variable into two axes to reduce system design complexity. With stator reference frame the stator and rotor voltage is given by the Clarke transformation as [42]:

$$V_{\alpha s} = R_{si}\alpha_s + \frac{d\varphi\alpha_s}{dt} \tag{3.01}$$

$$V_{\beta s} = R_{si}\beta_s + \frac{d\varphi\beta_s}{dt} \tag{3.02}$$

$$V_{\alpha r} = R_{ri}\alpha_r + \omega_m\varphi\beta_r + \frac{d\varphi\alpha_r}{dt} \tag{3.03}$$

$$V_{\beta r} = R_{ri}\beta_r - \omega_m\varphi\alpha_r + \frac{d\varphi\beta_r}{dt} \tag{3.04}$$

Where $V_{\alpha s}$, $V_{\beta s}$, $V_{\alpha r}$, $V_{\beta r}$ are the $\alpha\beta$ stator and rotor voltage transformation.

$\varphi_{\alpha s}$, $\varphi_{\beta s}$, $\varphi_{\alpha r}$, $\varphi_{\beta r}$, are the stator and rotor flux linkages.

R_r, R_s , are the rotor and stator resistance.

L_r, L_s, are the rotor and stator inductance.

ω_m, is mechanical angular frequency.

The current equation for the stator and rotor winding is given by:

$$i_{\alpha s} = \left(\frac{1}{{L_m}^2 - L_s L_r}\right)(-L_r\varphi\alpha_s + L_m\varphi\alpha_r) \tag{3.05}$$

$$i_{\beta s} = \left(\frac{1}{{L_m}^2 - L_s L_r}\right)(-L_r \varphi\beta_s + L_m \varphi\beta_r) \tag{3.06}$$

$$i_{\alpha r} = \left(\frac{1}{{L_m}^2 - L_s L_r}\right)(-L_m \varphi\alpha_s + L_s \varphi\alpha_r) \tag{3.07}$$

$$i_{\beta r} = \left(\frac{1}{{L_m}^2 - L_s L_r}\right)(-L_m \varphi\beta_s + L_r \varphi\beta_r) \tag{3.08}$$

Where $i_{\alpha s},\ i_{\beta s},\ i_{\alpha r},\ i_{\beta r}$ are the $\alpha\beta$ stator and rotor Clark current transformations.

We can get the Park transformation from the Clark transformation by using the below equation.

$$\begin{bmatrix} f_d \\ f_q \end{bmatrix} = \begin{bmatrix} \cos\theta & \sin\theta \\ -\sin\theta & \cos\theta \end{bmatrix} \begin{bmatrix} f_\alpha \\ f_\beta \end{bmatrix} \tag{3.09}$$

To simply calculate the dq transformation it is possible to multiply the $\alpha\beta$ by $e^{-j\theta s}$ and $e^{-j\theta r}$. The stator and rotor dq voltage transformation is given by:

$$V_{ds} = R_s i d_s - \omega_s \varphi q_s + \frac{d\varphi d_s}{dt} \tag{3.10}$$

$$V_{qs} = R_s i q_s - \omega_s \varphi d_s + \frac{d\varphi q_s}{dt} \tag{3.11}$$

$$V_{dr} = R_r i d_r - \omega_r \varphi q_r + \frac{d\varphi q_r}{dt} \tag{3.12}$$

$$V_{qr} = R_r i q_r + \omega_m \varphi d_r + \frac{d\varphi q_r}{dt} \tag{3.13}$$

Where $V_{ds},\ V_{qs},\ V_{dr},\ V_{qr}$ are the dq stator and rotor Park voltage transformation.

$\varphi_{ds},\ \varphi_{qs},\ \varphi_{dr},\ \varphi_{qr}$, are the stator and rotor, dq flux linkages.

The rotor and stator Park transformation is given by:

$$i_{ds} = \frac{1}{\sigma L_s}\varphi d_s - \frac{L_m}{\sigma L_s L_r}\varphi d_r \tag{3.14}$$

$$i_{qs} = \frac{1}{\sigma L_s}\varphi q_s - \frac{L_m}{\sigma L_s L_r}\varphi q_r \tag{3.15}$$

$$i_{dr} = \frac{1}{\sigma L_r}\varphi d_r - \frac{L_m}{\sigma L_s L_r}\varphi d_s \tag{3.16}$$

$$i_{qr} = \frac{1}{\sigma L_s}\varphi q_r - \frac{L_m}{\sigma L_s L_r}\varphi q_s \tag{3.17}$$

Where, $\sigma = {(L_s L_r - L_m^2)}/{L_s L_r}$

$i_{ds},\ i_{qs},\ i_{dr},\ i_{qr}$, are the dq stator and rotor Park current transformations.

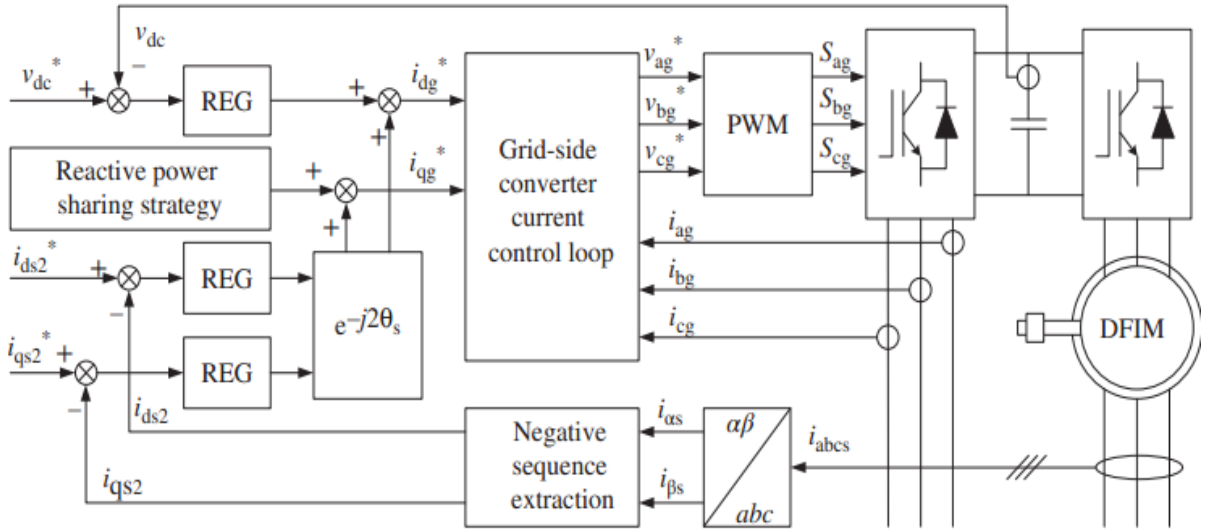

Figure 3. 4. Grid-side converter structure block diagram [43].

Assuming zero machine power loss the active and reactive power can be calculated by:

$$P_s = \frac{3}{2}\left(V_{ds}id_s + V_{qs}iq_s\right) \tag{3.18}$$

$$Q_s = \frac{3}{2}\left(V_{ds}id_s - V_{qs}iq_s\right) \tag{3.19}$$

$$P_r = \frac{3}{2}\left(V_{dr}id_r + V_{qr}iq_r\right) \tag{3.20}$$

$$Q_r = \frac{3}{2}\left(V_{dr}id_r - V_{qr}iq_r\right) \tag{3.21}$$

$$P_{total} = P_s + P_r \tag{3.22}$$

$$Q_{total} = Q_s + Q_r \tag{3.23}$$

Where, P_s, P_r, Q_r, Q_s are the stator and rotor active and reactive power under Park transformation for three phase doubly fed induction machine.

3.2.1 Power converter modeling

DFIG vector control mechanism is used to control the stator and grid power with proportional integral (PI) controller for wind energy conversion. A back-to-back power electronic converter are used. The main role of this converter is to control active and reactive power [42]. DFIG back-to-back converter mainly have two parts which are the rotor side converter and grid side convertor.

The rotor side converter is responsible for controlling the generator speed, torque, active and reactive power. Whereas the grid side converter is responsible to maintain constant DC-link voltage to ensure stable power flow. The Dc-link capacitor is used to store electrical energy.

3.2.2 DFIG control system

Due to its ability to control active and reactive power vector control is selected. The stator flux-oriented control is used to control the rotor side converter (RSC) and stator voltage oriented control is used for grid side converter (GSC) in the DFIG field-oriented control.

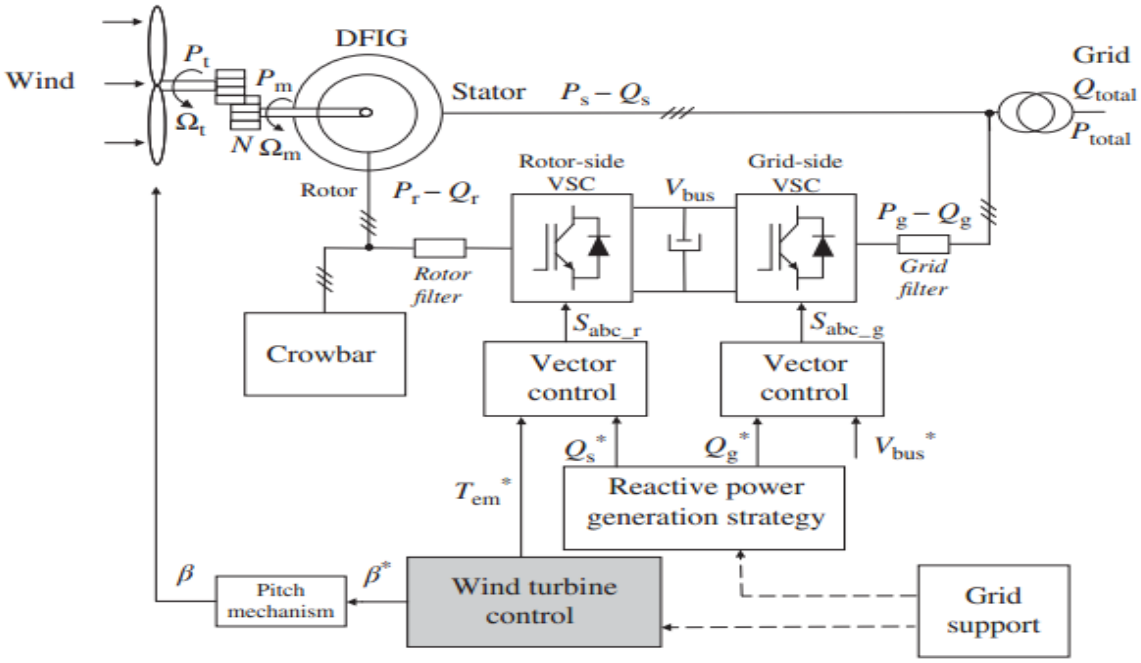

Figure 3. 5. Overall grid control DFIG system [43]

The rotor current control plays a vital role in controlling the active and reactive power of the stator. The mathematical equation for rotor dq control is given by:

$$i_{qr} = -\frac{2}{3V_g L_m} P_s L_s \tag{3.24}$$

$$i_{dr} = \frac{\varphi_s}{L_m} - \frac{2}{3V_g L_m} Q_s L_s \tag{3.25}$$

The grid currents which are responsible for grid active and reactive power. The dq transformation for grid control is given by:

$$i_{dg} = -\frac{2}{3V_g} P_g \tag{3.26}$$

$$i_{qg} = -\frac{2}{3V_g} Q_g \tag{3.27}$$

3.3 DPFC modeling and designing

DPFC topology and operating principle two methods are applied to the UPFC to improve its reliability.

- First eliminating the common dc-link between the shunt and series converters of the UPFC
- Second distributing the series compensating device.

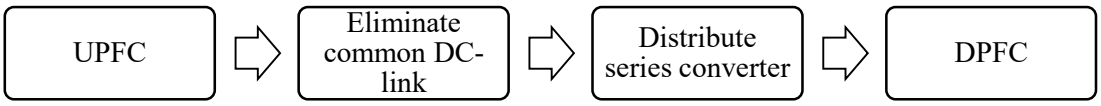

By combining these two approaches, the new FACTS device DPFC is earned. The main role of the series converter is to charge its own capacitor and generate the desired real and reactive power. The DPFC consists of one shunt and several other series connected converters. The shunt device is analogous to a STATCOM, whereas the series device employs the D-FACTS which is to use multiple single part devices rather than one massive rated converter. The DPFC is able to control all system parameters. The active power exchange between the shunt and the series converter is through the transmission line at the third-harmonic frequency.

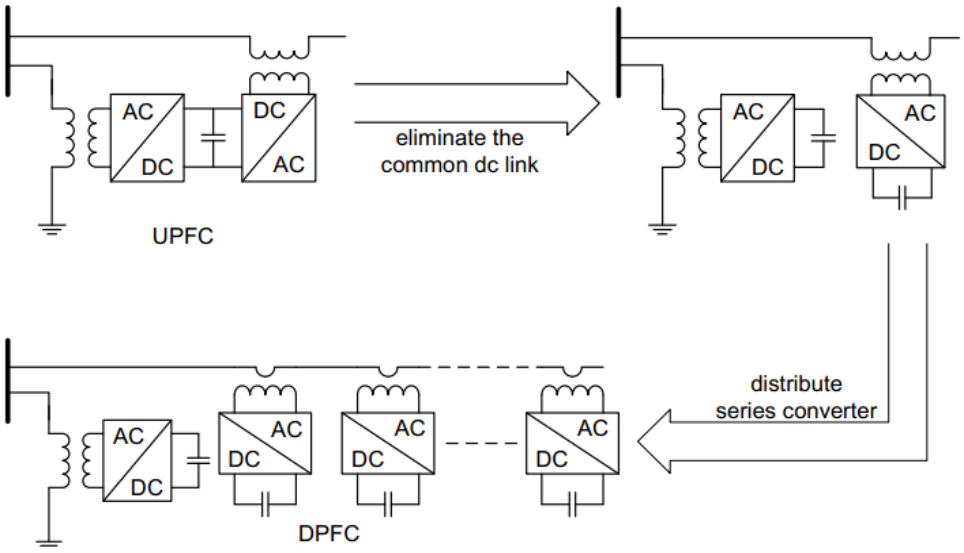

Figure 3. 6. UPFC system configuration [6, 9]

The DPFC device additionally needs a shunt connected high-pass filter at the opposite side of the shunt connected FACT controller. To enable independent operation the DPFC eliminates the common DC-link which is responsible for active and reactive power transfer between the series and shunt controller. It uses the transmission line through 3^{Rd} harmonics frequency [7]. This means according to Fourier analysis the non-sinusoidal voltage and current can be expressed as the total sum of sinusoidal amplitudes at different frequencies. Since the integrals of all the vector or cross product of terms with different frequencies are zero. Hence, the active power will be expressed by [9],

$$P = \sum_{i=1}^{\infty} V_i I_i \cos \emptyset_i \tag{3.28}$$

V_i , is voltage at the i^{th} harmonic frequency order.

I_i , is current at i^{th} harmonic frequency order and $\emptyset_i$ is the angle between current ant voltage.

From the equation above power can be generated at different frequency independent of the other frequency orders. This means converters can generate active power at one frequency and absorb this

power from other frequencies. The high-pass filter (HPF) allows high frequency signal (harmonic frequency) to pass and attenuating low frequency signals (fundamental frequency). This HPF is grounded and creates a closed loop for harmonic current.

In a three-phase system the 3rd, 6th, are 9th harmonics are identical in each phase, which are a zero-sequence components. The zero-sequence harmonic can be blocked by Y- Δ transformers connections. The 3rd harmonic is lowest frequency among all zero-sequence harmonics. This is the main reason in selecting the 3rd harmonics for active power exchange. This helps in eliminating the need of HPF required to prevent harmonic leakage. By using zero-sequence harmonic, HPF can be replaced by a cable that connect the neutral point of the Y- Δ transformer with the ground. In this the Δ winding act like open circuit to the 3rd harmonics and all harmonic flow through the grounding cable [9]. Hence, the large HPF is eliminated.

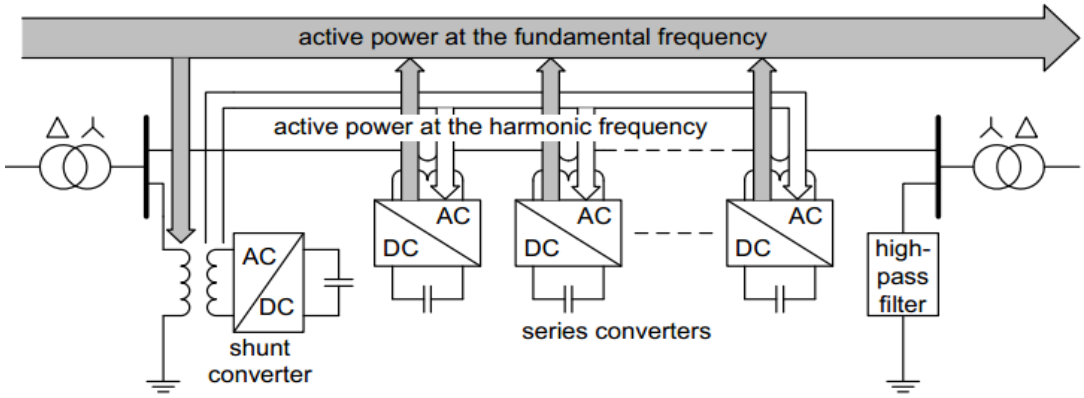

Figure 3. 7. Active power exchange [44]

The power exchange at the i^{th} harmonic frequency, P_i generated by the converter can be expressed as:

$$P_i = \frac{|V_{sh,i}||V_{se,i}|}{X_i} \, sin(\theta_{sh,i} - \theta_{se,i}) \tag{3.29}$$

Where: X_i is the i^{th} frequency line impedance which limits the power exchange capacity.

$|V_{sh,i}|$ *and* $|V_{se,i}|$, are the 9th voltage magnitude of the shunt and series converter

$\theta_{sh,i} - \theta_{se,i}$, is the angle difference between the series and shunt voltages.

To exchange the same amount of active power, line with high impedance requires higher voltage. Because the transmission lines mostly have inductive impedance and it is directly proportional to the system frequency. Higher frequency creates high system impedance and results in high voltage in the converters. Hence, the 3rd harmonic frequency is selected. Because it is the lowest of zero-sequence harmonics.

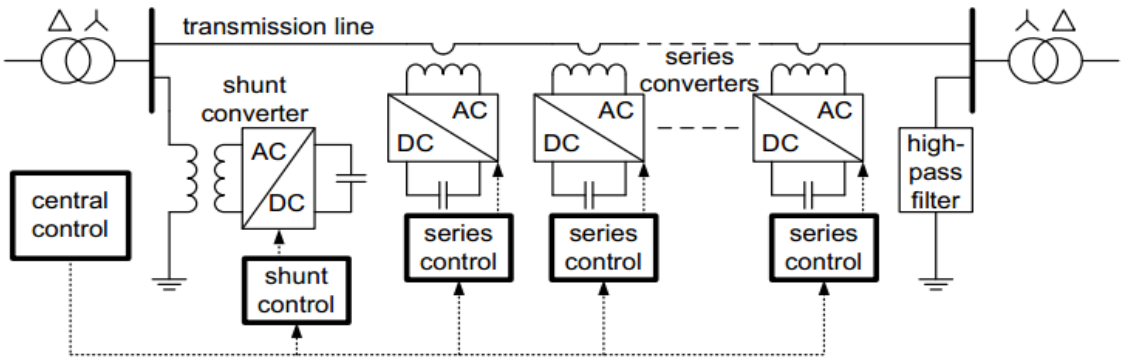

Figure 3. 8. Control block diagram of DPFC [9]

The main functions of the central converter is to generate a reference signal for the series and shunt converter. It provides a voltage reference signal at fundamental frequency component for the series converters and reactive current reference signal for shunt converter.

The series converter uses Dc voltage capacitor and provides a series voltage at fundamental frequency by using 3rd harmonics. The shunt controller injects a constant reactive current at fundamental frequency and by using 3rd harmonic current it supply active power for the series converter. The DC voltage of the shunt converter is maintained constant by absorbing active power from the grid at fundamental frequency.

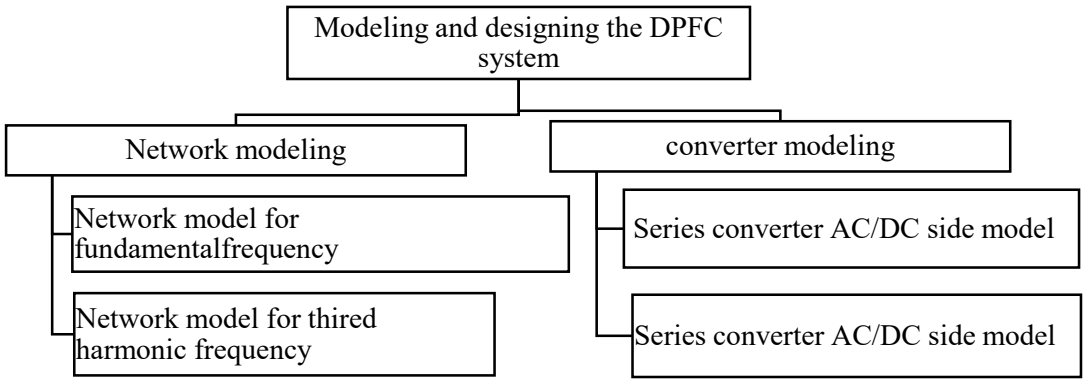

Figure 3. 9. DPFC modeling process

3.2.1 Fundamental frequency model

Assumptions taken into account:

- The voltages sources are fully controllable.
- The grounding is treated as ideal conductor with zero impedance.
- The mutual impedance between phases are neglected due to enough conductor spacing.
- The transformers are connected in delta-Y at both ends of the transmission line.

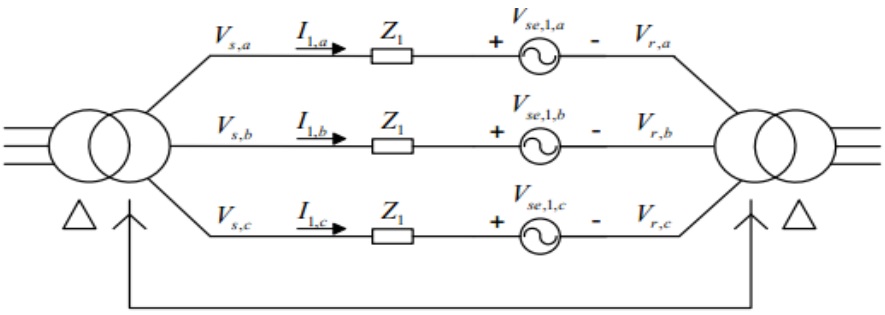

Figure 3. 10. Fundamental frequency circuit diagram [45]

The fundamental frequency is modeled as three single phase system with a phase angle deference of 120°. Based on the above circuit diagram:

$$V = ZI \tag{3.30}$$

$$\begin{bmatrix} V_{sa} \\ V_{sb} \\ V_{sc} \end{bmatrix} - \begin{bmatrix} V_{ra} \\ V_{rb} \\ V_{rc} \end{bmatrix} - \begin{bmatrix} V_{se1a} \\ V_{se1b} \\ V_{se1c} \end{bmatrix} = \begin{bmatrix} Z_1 & 0 & 0 \\ 0 & Z_1 & 0 \\ 0 & 0 & Z_1 \end{bmatrix} \begin{bmatrix} i_{1a} \\ i_{1b} \\ i_{1c} \end{bmatrix} \tag{3.31}$$

Where. V_{se1}, is series fundamental frequency voltage injected.

Z_1, is the line I.

V_s, sending end voltage and V_r, receiving end voltage.

The above equation shows by varying the series injected voltage we can vary the current through the transmission line. During the network modeling V_s and V_r are trited as input voltages.

3.2.2 Third harmonic frequency network model

The shunt connected power controller inject a 3rd harmonic order current to the neutral point of the Y-Δ transformer connection. This current distributed over the three phase system. The zero sequence reactance of both transformers and the line impedance can be combined as Z3 and the neutral impedance is assumed zero. Hence the equation for the above circuit is given by:

$$\begin{bmatrix} V_{sh3} - V_{se3a} \\ V_{sh3} - V_{se3b} \\ V_{sh3} - V_{se3c} \end{bmatrix} = \begin{bmatrix} Z_3 & 0 & 0 \\ 0 & Z_3 & 0 \\ 0 & 0 & Z_3 \end{bmatrix} \begin{bmatrix} i_{3a} \\ i_{3b} \\ i_{3c} \end{bmatrix} \tag{3.32}$$

In each phase contains 3rd harmonic current by the 3rd harmonic voltage injected by series and shunt converter which is V_{sh3} and V_{se3}.

3.2.3 Converter Model

A. Series converter model

There series converters are controlled by single phase PWM. The loss of PWW converter is neglected and the switching behavior is beyond this scope.

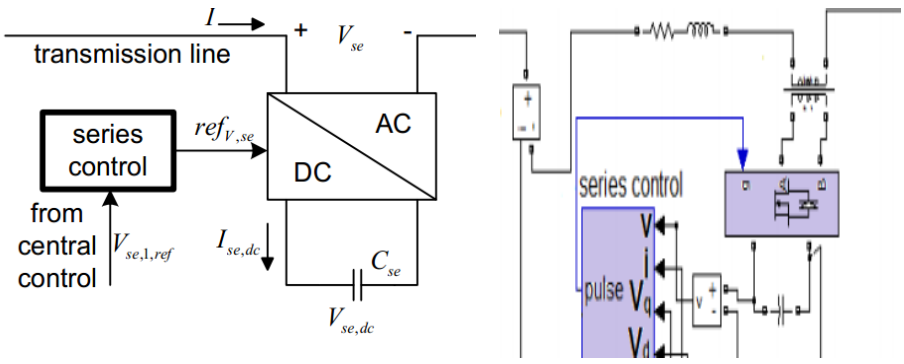

Figure 3. 11. DPFC series converter block and Simulink diagram

V_{se}, is the series converter AC - voltage.

V_{seDC} , is the series converter DC - voltage.

$refV_{se}$, AC signal modulation amplitude.

The AC current and voltage have the fundamental frequency donated by 1 and 3rd harmonic frequency that is donated 3.

$$V_{se} = V_{se1} + V_{se3} \tag{3.33}$$

The series AC voltage is given by:

$$V_{se} = refV_{se} . V_{seDC} \tag{3.34}$$

From the above equation the series converter voltage V_{se} is the product of the Ac reference voltage and Dc capacitor voltage. By applying superposition theorem equation 3.7 can be described as:

$$\begin{bmatrix} V_{se1} \\ V_{se3} \end{bmatrix} = \begin{bmatrix} refV_{se1} \\ refV_{se3} \end{bmatrix} . V_{DCse} \tag{3.35}$$

V_{DCse} Can be described by using I_{DCse}:

$$I_{DCse} = C_{se} \frac{dV_{seDC}}{dt} \tag{3.36}$$

$$I_{DCse} = refV_{se} . I \quad \text{(Approximation)}$$

$$I_{DCse} = (refV_{se1} + refV_{se3}) . (I_{se1} + I_{se3}) \tag{3.37}$$

$$C_{se} \frac{dV_{seDC}}{dt} = (refV_{se1} + refV_{se3}) . (I_{se1} + I_{se3}) \tag{3.38}$$

The above equation can be expressed in the dq-rotating reference farm as:

$$C_{se} \frac{dV_{seDC}}{dt} = (refV_{se1d} \sin\theta + refV_{se1q} \cos\theta + refV_{se3d} \sin 3\theta + refV_{se1q} \cos 3\theta) . (I_{se1d} \sin\theta + I_{se1q} \cos\theta + I_{se3d} \sin 3\theta + I_{se3d} \sin 3\theta) \tag{3.39}$$

The above equation can be approximated to:

$$C_{se} \frac{dV_{seDC}}{dt} = \frac{1}{2}(refV_{se1d}I_{se1d} + refV_{se1q}I_{se1q}) + \frac{1}{2}(refV_{se3d}I_{se3d} + refV_{se1q}I_{se3q}) \tag{3.40}$$

The DC side model are $refV_{se1}$, $refV_{se3}$, I_{se1}, I_{se3}.

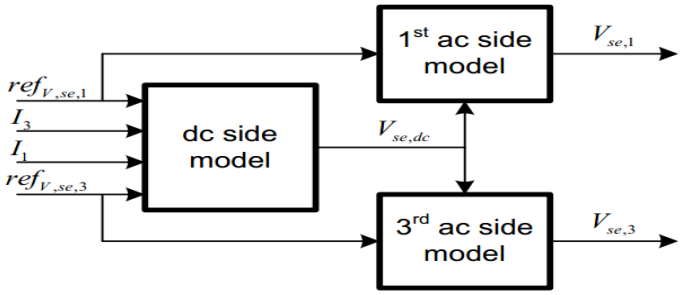

Figure 3. 12. Series controller model diagram [43]

The series converter is controlled by its own controller locally with identical configuration for each converter. To control the fundamental and 3rd harmonic a separate loop control is proposed. The 3rd harmonic control loop is used for capacitor DC voltage control.

The generated reference voltage to control the fundamental frequency is fed into each converter through communication line. The 3rd harmonic control is the major control loop in the series converter control strategy.

To control the DC voltage vector control is selected and the 3rd harmonic current is used due to easily measurability. A 3rd band filter is needed to extract the 3rd harmonic current from the fundamental frequency. The single phase PLL (phase lock loop) creates dq reference frame for the 3rd harmonic. In this, the d component of the 3rd harmonic voltage used to control the DC voltage. And the q cause a reactive power injection into the AC network and its keep zero during the operation [9].

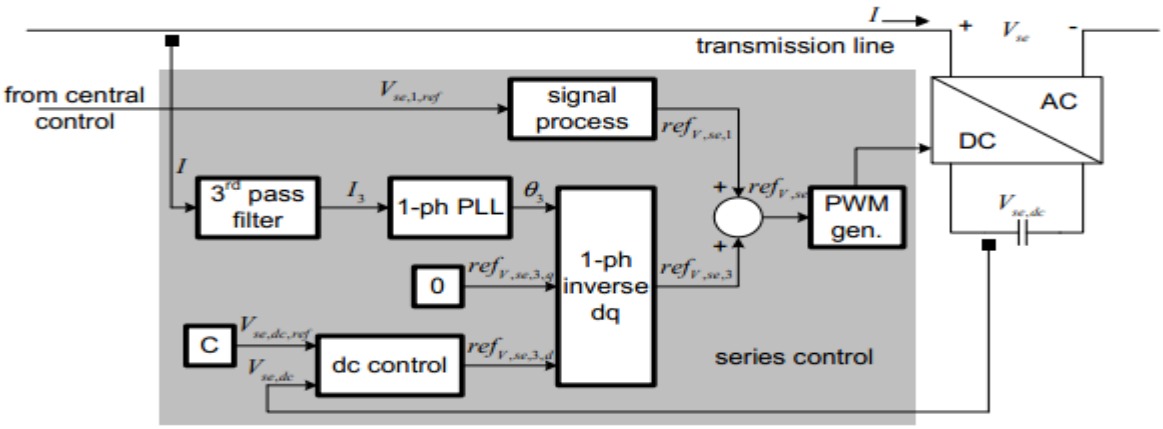

Figure 3. 13. Series converter control diagram [9]

To maintain the series DC capacitor voltage, DC voltage control loop is applied. Here both the frequency component are used in rotating reference frame for Park's transformation. By projecting the current to themselves I_{se1q} *and* I_{se3q} become zero. Because they are perpendicular to the current. Hence equation (3.11) can be rewrite as:

$$C_{se}\frac{dV_{seDC}}{dt} = \frac{1}{2}(\text{ref}\,V_{se1d}I_{se1d} + \text{ref}\,V_{se3d}I_{se3d}) \quad (3.41)$$

The fundamental frequency is treated as disturbance because the 3rd harmonic current with the line is constant and I_{se3d} is treated as constant. By using the Laplace transformation the time domain is converted into frequency domain for controller design. By selecting $\text{ref}\, V_{se3d}$ as control parameter and V_{seDC} as control objective, can be transformed as:

$$G(s) = \frac{V_{seDC}(s)}{\text{ref}\, V_{se3d}(s)} = \frac{I_{se3d}}{2C_{se}s} \tag{3.42}$$

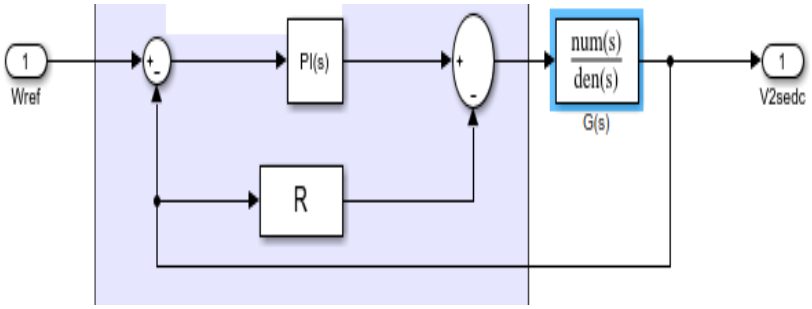

Figure 3. 14. Series DC voltage controller

In the above diagram R is controller active damping feedback and F(s) is the control function for the PI controller.

$$G'(s) = \frac{G(s)}{1+RG(s)} = \frac{I_{se3d}}{2sC_{se}+RI_{se3d}} \tag{3.43}$$

The G(s) is a first order system and its control function is given by:

$$F(s) = \frac{\alpha_d}{s} G'(s)^{-1} \tag{3.44}$$

α_d is the desired bandwidth of the closed loop system

$$F(s) = \frac{2C\alpha_d}{I_{se3d}} + \frac{R\alpha_d}{s} \tag{3.45}$$

The controller active damping R can be calculating by making the inner feedback loop as fast as the system close loop. Hence, by placing G′(s) pole at $-\alpha_d$ the active damping will be:

$$\frac{RI_{se3d}}{2C} = \alpha_d \tag{3.46}$$

$$R = \frac{2C\alpha_d}{I_{se3d}} \tag{3.47}$$

Similarly the PI controller parameters k_p and k_i can be calculates as:

$$k_p = \frac{2C\alpha_d}{I_{se3d}}, \qquad k_i = \frac{2C{\alpha_d}^2}{I_{se3d}} \tag{3.48}$$

C. Shunt converter model

The shunt converter is a three phase converter connected with a single phase converter using a back-to-back connection. Like STATCOM, the three phase converter is connected on the low-voltage side of the Y-Δ transformer and it absorbs active power from the grid. The 3rd harmonic is injected to the

network using the single phase converter output which is connected to the neutral point of Y-Δ transformer.

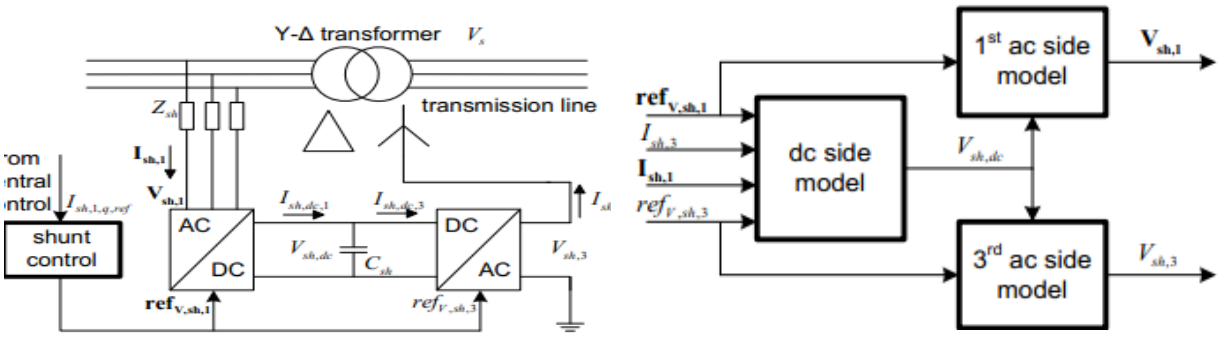

Figure 3. 15. Connection diagram of the shunt device and its controller [9]

The primary converter contains the fundamental frequency and the single phase converter generates the 3rd harmonic frequency. Similarly with series converter the Ac side voltage can be calculated as:

$$\mathrm{V_{sh1}} = ref\mathrm{V_{sh1}} \,.\, \mathrm{V_{shDC}}$$

$$\mathrm{V_{sh3}} = ref\mathrm{V_{sh3}} \,.\, \mathrm{V_{shDC}} \tag{3.49}$$

The modulation index for $ref\mathrm{V_{sh1}}$ and $ref\mathrm{V_{sh3}}$ is $[-1\ to\ 1]$. Capacitor Dc voltage given by:

$$C_{sh}\frac{d\mathrm{V_{sdDC}}}{dt} = \mathrm{I}_{shDC1} - \mathrm{I}_{shDC3} \tag{3.50}$$

The DC current at the three phase side can be calculated by applying parks transformation to the fundamental frequency.

$$\mathrm{I}_{shDC1} = \frac{3}{2}(ref\mathrm{V_{sh1d}}\mathrm{I}_{sh1d} + ref\mathrm{V_{sh1q}}\mathrm{I}_{sh1q}) \tag{3.51}$$

The 3rd DC current can be calculated by using single phase park transformation to the 3rd harmonic frequency. This is given by:

$$\mathrm{I}_{shDC3} = (ref\mathrm{V_{sh3d}}\ \sin 3\theta + ref\mathrm{V_{sh3q}}\ \cos 3\theta).(\mathrm{I}_{sh3d}\sin 3\theta + \mathrm{I}_{sh3q}\cos 3\theta)$$

$$\mathrm{I}_{shDC3} = \frac{1}{2}(ref\mathrm{V_{sh3d}}\,\mathrm{I}_{sh3d} + ref\mathrm{V_{sh3q}}\ \mathrm{I}_{sh3q}) \tag{3.52}$$

Zero average value are not considered to calculate the approximate DC voltage of the capacitor. Because they have no contribution on the capacitor voltage. They are treated as DC voltage ripples. Hence,

$$C_{sh}\frac{d\mathrm{V_{sdDC}}}{dt} = \mathrm{I}_{shDC1} - \mathrm{I}_{shDC3}$$

$$C_{sh}\frac{d\mathrm{V_{sdDC}}}{dt} = \frac{3}{2}(ref\mathrm{V_{sh1d}}\mathrm{I}_{sh1d} + ref\mathrm{V_{sh1q}}\mathrm{I}_{sh1q}) - \frac{1}{2}(ref\mathrm{V_{sh3d}}\,\mathrm{I}_{sh3d} + ref\mathrm{V_{sh3q}}\ \mathrm{I}_{sh3q}) \tag{3.53}$$

This three phase shunt converter maintain constant DC voltage and feed reactive power into the grid and the single phase converter feeds 3rd harmonic current in to the gird. Those converters have their own controller.

As the single phase converter inject a 3rd harmonic current it needs a current controller. The 3rd harmonic current is locked with the bus voltage at fundamental frequency. To capture the bus frequency PLL is applied. To create a virtual rotating reference frame for the 3rd harmonic current, the PLL θ_1 is multiplied by 3 and the DC voltage of the back-to-back converter is assumed to be zero. The series and shunt converter voltage is can be represented as voltage sources. The 3rd harmonics is represented as series and shunt voltage sources connected in series with resistor and inductor as shown below.

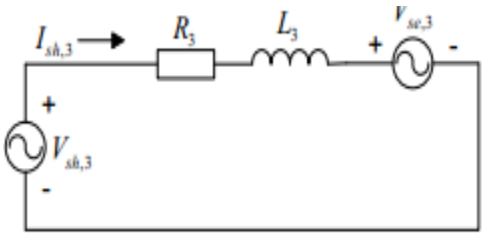

Figure 3. 16. Third harmonic circuit [46]

R_3 and L_3 the 3rd harmonic network resistance and inductance respectively. The voltage equation of the above circuit will be:

$$V_{sh3} = L_3 \frac{dI_{sh3}}{dt} + R_3 I_{sh3} + V_{se3} \tag{3.54}$$

By applying Parks transformation equation (3.54) becomes;

$$V_{sh3d} = L_3 \frac{dI_{sh3d}}{dt} + R_3 I_{sh3d} - \omega_3 L_3 I_{sh3q} + V_{se3d}$$

$$V_{sh3q} = L_3 \frac{dI_{sh3q}}{dt} + R_3 I_{sh3q} - \omega_3 L_3 I_{sh3d} + V_{se3q} \tag{3.55}$$

ω_3, is 3rd harmonic angular velocity and cause a coupling of both equations. To decouple the dq the coupling term will cross added. V_{sh3}, and I_{sh3} are the same and can be transformed to frequency domain.

$$G(s) = \frac{1}{R_3 + sL_3} \tag{3.56}$$

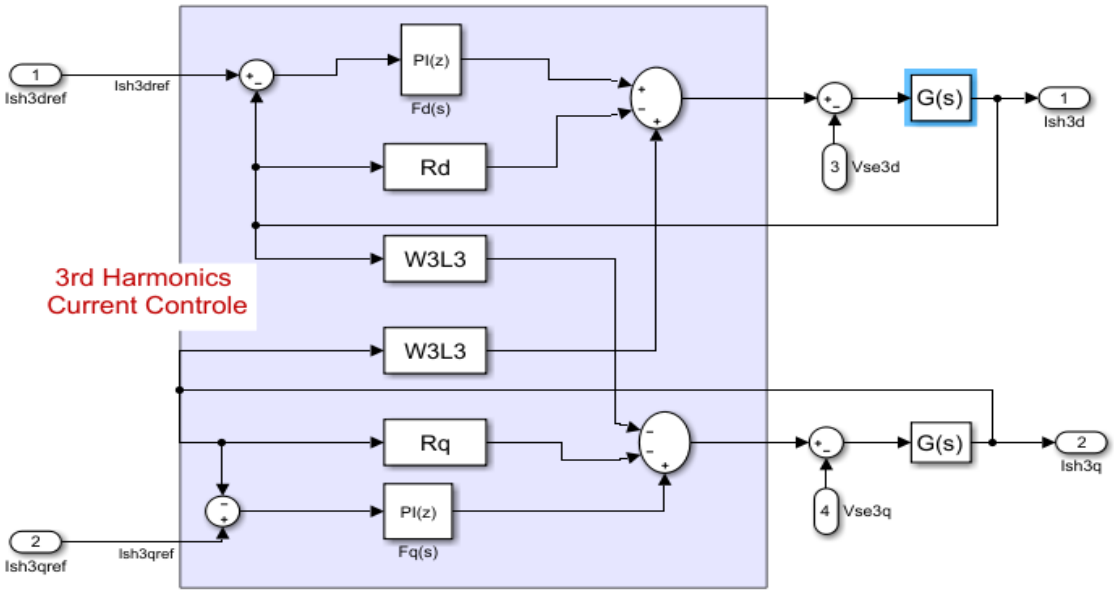

Figure 3. 17. Shunt converter 3rd harmonic current controller

The F(s) can be calculated as:

$$F_d(s) = \alpha_d L_3 + \frac{\alpha_d(R_3 + R_d)}{s}$$

$$F_q(s) = \alpha_q L_3 + \frac{\alpha_q(R_3 + R_q)}{s} \quad (3.57)$$

α_d , and α_q are the dq bandwidths. Then the reactive damping can be calculated as:

$$R_d = \alpha_d L_3 - R_3 \text{ , and } R_q = \alpha_q L_3 - R_3 \quad (3.58)$$

The aim of fundamental frequency control is to inject controllable reactive current to the grid and maintain constant DC voltage. This consists the reactive current control and DC voltage control. The PLL is created from the bus voltage as an input.

The fundamental current control is same as 3rd harmonic current control except there is no active damping R because of Vs is available and there is no disturbance theoretically. The rotating reference frame is generated from this Vs both d and q components of $ref\mathrm{V_{sh}}$ are non-zero values. This make the system difficult to control.

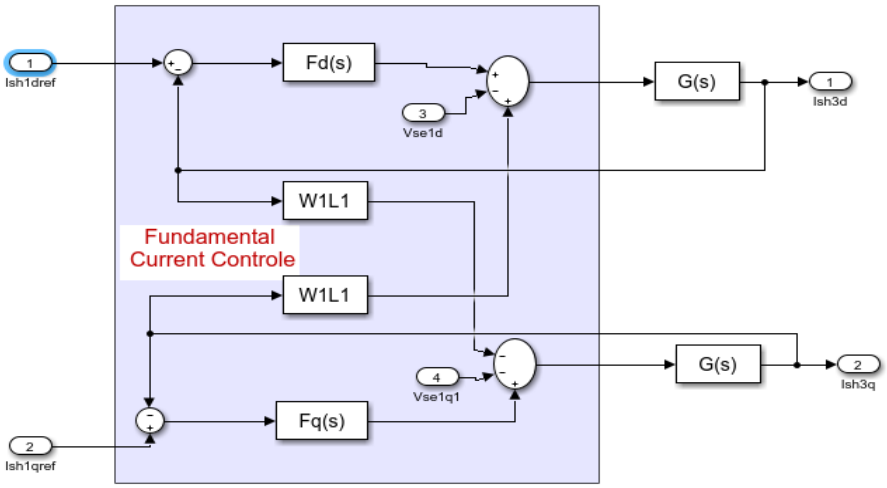

Figure 3. 18. Fundamental current controller

$$F_d(s) = \alpha_d L_1 + \frac{\alpha_d R_1}{s} \quad (3.59)$$

$$F_q(s) = \alpha_q L_1 + \frac{\alpha_q R_1}{s}$$

The capacitor Dc voltage control can be calculated same as the series DC voltage and is given by:

$$C_{se}\frac{d\mathrm{V_{seDC}}}{dt} = \frac{1}{2}\left(ref\mathrm{V_{se1d}}\mathrm{I}_{se1d} + ref\mathrm{V_{sh1q}}\mathrm{I}_{se1q}\right) + \frac{1}{2}\left(ref\mathrm{V_{se3d}}\,\mathrm{I}_{se3d} + ref\mathrm{V_{se3q}}\,\mathrm{I}_{se3q}\right) \quad (3.31)$$

To control the DC voltage the capacitor is treated as energy storage device.by neglecting the capacitive loss the instantaneous power can be calculated by:

$$\frac{1}{2}C_{sh}\frac{dV^2{}_{\text{shDC}}}{dt} = P_1 - P_3 \tag{3.60}$$

Due to the non-linearity of the equation with V_{shDC} W= $V^2{}_{shDC}$ is introduced. V_s is the rotating reference frame and the q component of V_s become zero by projecting V_s to itself.

$$\frac{1}{2}C_{sh}\frac{dW}{dt} = \frac{3}{2}V_{sd}\, I_{sh1d} - P_3 \tag{3.61}$$

In the above equation $V_s$is constant and P_3 is treated as disturbance. Hence, the Laplace transformation will be:

$$\boldsymbol{G(s) = \frac{W(s)}{I_{sh1d}} = \frac{3V_{sd}}{sC_{sh}}} \tag{3.62}$$

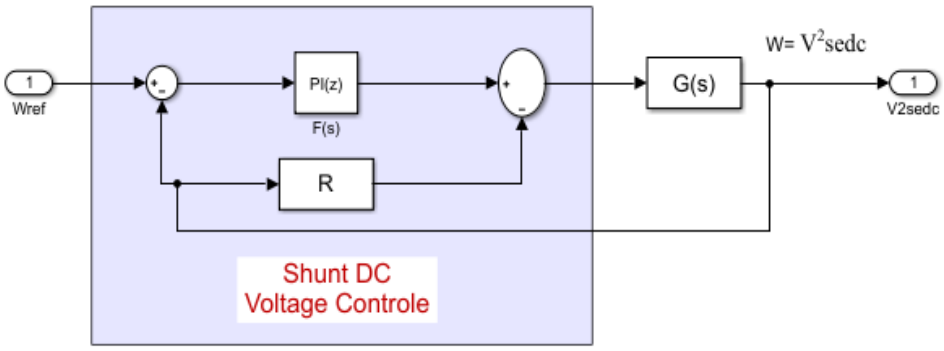

Figure 3. 19. DC shunt voltage controller

By using IMC method the PI control parameters can be calculated by:

$$R = \frac{\alpha C}{3V_{sd}}, k_p = \frac{\alpha C}{3V_{sd}}, and\ k_i = \frac{\alpha^2 C}{3V_{sd}} \tag{3.63}$$

3.4 DPFC converter specification

Table 3. 4. Transmission line conductor specifications

№	Voltage (KV)	Substation	Substation	Conductor type	Size (mm^2)	Conductor configuration	Line rating (MVA)	Length (km)
1	230	Ashegoda	Alamata	AAAC	180	Double	318	125
2	230	Ashegoda	Mekelle	AAAC	180	Double	318	15

Table 3. 5. Load demand neglecting industrial loads

№	Substation name	P-load (MW)	Q-load (Mvar)	Remark
1	Mekelle	17.8936	8.6663	Distribution load demand neglecting big industries like Mesebo cement factory
2	Alemata	1.872	0.906	

It is possible to calculate the max current capacity of the conductor based on the system given data.

- Transmission line rated voltage, $V = 230KV$
- Transmission line power capacity, $S = 318MVA$
- Generation station rated capacity, $P = 120MW$
- Assuming power factor, $\cos(\theta)$=0.92
- Generation power capacity, $S = 130MVA$

  To calculate the $Qmin$ and $Qmax$

$$Q = \sqrt{S^2 - P^2} = \sqrt{130^2 - 120^2} = 50MVAr$$

  Hence, $Qmin$ is -50MVAr and $Qmax$ is 50MVAr, and those are the base values.

$$P_{capacity} = \sqrt{3} * V_{rated} * I_{rated} \cos\theta$$

$$I_{rated} = I_{line} = \frac{P_{capacity}}{\sqrt{3} * V_{rated} * \cos\theta}$$

$$I_{line} = \frac{120MW}{\sqrt{3} * 230KV * 0.92} = \frac{120}{338.62} KA = 354A$$

Hence the line is wye(Y) connected line current and phase voltage are equal.

$$I_{rated} = I_{line} = I_{phase} = 354A$$

The voltage and current rating of the shunt and series converters depends on the range of DPFC control. The control range of the DPFC are:

A. Series converter rating

The series converter is responsible for controlling active and reactive power by injecting series voltage with transmission line. Hence the rating of the converter can be calculated as:

$$S_{series} = n.V_{injected}.I_{rated}$$

Where: n is the number of distributed series converters

$V_{injected}$, is the voltage injected by each converter

I_{line}, is the system line current.

Using Ashegoda substation line data the voltage fluctuation is supported by the OLTC power transformer mechanism. To support the transformer load and minimize the heating effect, tiring and wearing of power transformer equipment, the researcher selected 0.1pu of the nominal phase voltage because it stabilizes the system voltage. Hence, the injected voltage can be calculated as:

$$V_{injected} = 0.1 * V_{line} = 0.1 * 230KV = 23KV$$

Assuming one module per line the above equation becomes:

$$S_{series} = n.V_{injected}.I_{rated} = 23KV * 354A = 8MVA$$

The series converter converters inject a controllable AC voltages like a single phase inverters and it injects 23KV (rms).

$$V_{ACpeak} = \frac{2V_{Dc}}{2} = V_{Dc}$$

$$V_{ACpeak} = \sqrt{2}.V_{ACrms} = \sqrt{2} * 23KV = 32.53KV$$

$$V_{Dc\_se} = V_{ACpeak} = 32KV$$

From this, we can calculate series capacitor value.

$$P_{series} = \frac{1}{2}.C.V_{DC}^2.\frac{\Delta V_{dc}}{\Delta t} \quad (3.64)$$

Where, Δt is time to supply power which is 10ms and ΔV_{dc} is allowed DC voltage ripple which is 3%.

$$C\_se = \frac{2.P_c}{V_{DC}^2}.\frac{\Delta t}{\Delta V_{dc}} = \frac{2 * 8MVA}{(32KV)^2}.\frac{0.01}{0.03} = 0.52mF$$

B. Shunt converter rating

The shunt converter is place at the low-voltage side of Ashegoda substation 33KV side to feed the reactive power, and fed active power to the series converter ($\boldsymbol{S_{series}}$) line a, b, and c.

$$S_{shunt} = \sum S_{series} = S_{seA} + S_{seB} + S_{sec} \quad (3.65)$$

$$S_{shunt} = 3.S_{series} = 3 * 8MVA = 24MVA \approx 25MVA$$

The shunt converter is connected with the 33KV three phase network and feed the single phase converter to support series converter active power. Hence, the DC voltage level for three phase inverter become:

$$V_{Dc} = \frac{2*V_{ACline}}{\sqrt{3}} \quad (3.66)$$

$$V_{DC\_sh} = \frac{3\sqrt{3}\,V_{ACpeak}}{\pi} = 1.65\,V_{ACpeak} = 1.65 * 33 * \sqrt{2}KV = 77KV$$

From this, we can calculate shunt capacitor value.

$$P_{shunt} = \frac{1}{2}.C.V_{DC}^2.\frac{\Delta V_{dc}}{\Delta t}$$

Where, Δt is time to supply active power which is 10ms and ΔV_{dc} is allowed DC voltage ripple which is 3%.

$$C\_sh = \frac{2.P_{cshunt}}{V_{DC}^2}.\frac{\Delta t}{\Delta V_{dc}} = \frac{2 * 25MVA}{(38.10KV)^2}.\frac{0.01}{0.03} = 0.00281F = 2.8mF$$

3.4 Optimal sizing and placement of the DPFC system

The Metaheuristic optimization technique is selected. The technique is widely used due to its ability to handle no-linear and multi-objective problems effectively.

Under the Metaheuristic optimization the Genetic Algorithm is used because of best performance for multi-objectives. OPF aims to optimize a certain objective, subject to the network power flow equations and system and equipment operating limits. The optimal condition is attained by adjusting the available controls to minimize an objective function subject to specified operating and security requirements. Some well-known objectives can be identified as below:

Active power objectives

i. Economic dispatch (minimum cost, losses, MW generation or transmission losses)
ii. Environmental dispatch
iii. Maximum power transfer

Reactive power objectives

MW and MVAR loss minimization

Active power loss minimization, and VAr planning to minimize the cost of reactive power support are the objectives functions used to optimal size and place the DPFC system. The mathematical description of the OPF problem is presented below:

OPF objective function for cost minimization: the OPF problem can be formulated as an optimization problem to minimize the active power loss and voltage profile improvement. Total Generation cost function is expressed as:

$$F(P_G) = \sum_{i=1}^{N_G}\left(\alpha_i + \beta_i P_{Gi} + \gamma_i P_{Gi}^2\right) \tag{3.67}$$

The objective function is expressed as:

$$Min\ F(P_G) = f(x,u) \tag{3.68}$$

Subjects to satisfy Nonlinear Equality Constraints:

$$g(x,u) = 0 \tag{3.69}$$

And Nonlinear Inequality Constraints:

$$h(x,u) \leq 0 \tag{3.70}$$

$$u_{min} \leq u \leq u_{max}$$

$$x_{min} \leq x \leq x_{max}$$

F (P_G) is total cost function f(x, u) is the scalar objective, g(x, u) represents nonlinear equality constraints (power flow equations), and h(x, u) is the nonlinear inequality constraint of vector arguments x, u.

OPF objective function for power loss minimization: the objective functions to be minimized are given by the sum of line losses in the transmission line.

$$P_L = \sum_{K=1}^{Nl} P_{lk} \tag{3.71}$$

Individual line losses P_{lk} can be expressed in terms of voltages and phase angles as:

$$P_{lk} = g_k\left[V_i^2 + V_j^2 - 2V_iV_j\cos(\delta_i - \delta_j)\right] \tag{3.72}$$

The objective function is a quadratic form and is suitable for implementation using the quadratic interior point method and can now be written as:

$$Min\ P_k = \sum_{i=1}^{Nl} g_k\left[V_i^2 + V_j^2 - 2V_iV_j\cos(\delta_i - \delta_j)\right] \tag{3.73}$$

Constraints for objective function of power loss minimization: the controllable system quantities are generator MW, controlled voltage magnitude, reactive power injection from reactive power sources and transformer tapping. The objective use herein is to minimize the power transmission loss function by optimizing the control variables within their limits. There is no violation on the transmission power flow capacity and bus voltage magnitude occurs in a normal system operating conditions. These are system constraints to be formed as equality and inequality constraints in the above. To calculate the per-unit quantities of the line impedance the actual and base quantities are required. The per-unit quantity are calculated by: There are three bus in the network as shown in the figure below.

$$Per - unit\ quantity = \frac{actual\ quantity}{base\ value\ of\ quantity} \tag{3.74}$$

$$Z_{pu} = \frac{Z}{Z_B},\ Z_B = \frac{V_B}{I_B},\ I_B = \frac{S_B}{V_B} \tag{3.75}$$

$$S\ base\ = 130MVA, \qquad V\ base = 230KV$$

$$I_B = \frac{S_B}{V_B} = \frac{130MVA}{230KV} = 565A$$

$$S_{pu} = V_{Pu}.I_{Pu}^* = P_{pu} + jQ_{Pu}$$

$$V_{pu} = Z_{pu}I_{pu}$$

$$Z_{actual} = R_{actual} = X_{actual}$$

$$Z_B = \frac{230KV}{565A} \approx 400\Omega$$

The ac resistance of the ACCC conductor at $@\ 75\,℃\ \rightarrow R = {}^{0.171\Omega}/_{km}$, $Xc = 0.22\ M\Omega.km$, $and\ \ Xl = 0.258\Omega\ per\ km$, is given at 0.3m radius of conductor according ACCC manufacturers data sheet [47, 48].

$$A_{conductor} = \pi r^2$$

Where r is the radius of the conductor.

$$r = \sqrt{\frac{A_{conductor}}{\pi}} = \sqrt{\frac{180_{mm^2}}{\pi}} = 7.57mm \tag{3.76}$$

$$Xl = 7.57mm * \frac{0.258\Omega}{0.3m} = 6.51m\Omega\ per\ km$$

$$Xl = 2\pi fL, \quad L = \frac{Xl}{2\pi f} = 0.207mH$$

$$Xc = 7.57mm * \frac{0.22M\Omega}{0.3m} = 5.55k\Omega.km$$

$$X_c = \frac{1}{2\pi fc}, \qquad C = \frac{1}{2\pi fX_c} = \frac{1}{5.55 * 2 * \pi * 50\ k\Omega.km} = 0.573\mu F/km$$

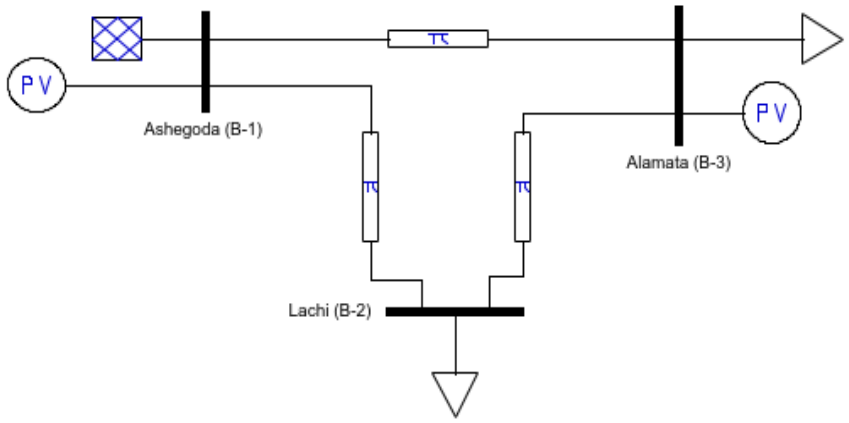

Figure 3. 20. PSAT (mdl) model of the existing network

Table 3. 6 Network transmission line parameters

Line	Bus name	Z actual per km	Total length(Km)	Z actual total	Z pu - total
Z12	Ashegoda – Lachi	0.171 + j 0.0065	15	2.565 + j0.09	0.0064 + j0.0002
Z23	Alamata – Lachi	0.171 + j 0.0065	141	24.111 + j0.846	0.0602 + j0.0021
Z13	Alamata – Ashegoda	0.171 + j 0.0065	125	21.375 + j0.75	0.0534 + j0.0018

Table 3. 7 PSAT load flow result

From bus	To bus	Line	P Flow [p.u.]	Q Flow [p.u.]	P Loss [p.u.]	Q Loss [p.u.]	MW loss	MVar loss
Ashegoda (B-1)	Alamata (B-3)	1	-0.1775	0.4447	0.0056	-0.0289	0.728	-3.757
Ashegoda (B-1)	Lachi (B-2)	2	0.2918	0.9685	0.0025	-0.0023	0.325	-0.299
Alamata (B-3)	Lachi (B-2)	3	0.2129	-0.3700	0.0039	-0.0295	0.507	-3.835

3.5 Cost benefit analysis of the system

Cost benefit analysis is done based on the investment and operational and maintenance costs of the overall DPFC system against the system operational and financial benefits. This operational benefits

are reduction in transmission loss, congestion relief, increase wind farm's lifetime, and improvement network voltage stability.

The cost benefit analysis calculations of the distributed power flow controller system are done based on the cost comparison of implementation against the economic befits that bring to the power system. The steps that the researcher flow is listed below.

Step 1. Defining the scope of cost benefit analysis

- System configuration based on the number of buses, lines, and base MVA and KV (230kv).
- Type of DPFC rating of the series and shunt converter (8MVA and 25 MVA).
- Duration of the project which is economic life span (20 years.)

Step 2. Estimate the total cost of DPFC

a. Initial investment (capital) cost
   - Series units – 8MVA per line
   - Shunt converter – 25MVA per 3-phase
   - Transformer, protection, installation, testing and commissions – 10%

b. Operating and maintenance cost (O&M) cost
   - Annual O&M = capital cost * O&M rate

Step 3. Quantifying benefits

a. Power loss reduction

Calculate the real power loss

$$P_{loss} = 3.I^2.R_{total}$$

Convert to energy loss and by energy cost ($/kWh).

$$E_{saved} = P_{loss}.hours/year$$

b. Increase transfer capacity

Helps to reduce network reinforcement costs.

c. Improve reliability
   - By implementing, the system face fewer blackouts and improve system stability
   - Minimize the value of loss load (VoLL) by avoiding outage durations

Step 4. Financial evaluation

a. Net present value (NPV)

$$NPV = \sum_{t=1}^{T} \frac{B_t - C_t}{(1+r)^t} \quad (3.78)$$

Where, B_t - Benefit in a year t

C_t - Cost in a year t, and r - Discount rate (7-10%)

t – Total life span (20 years)

b. Benefit –cost ratio

$$BCR = \frac{Total\ present\ value\ of\ benefit}{Total\ present\ value\ of\ cost} \quad (3.79)$$

If $BCR > 1$, it is going to be economical fusible.

Microsoft Excel is used to calculate the cost benefit analysis for a 20 year lifespan of the DPFC system. Detailed calculations and all the costs related to DPFC system integration and installations are tabulated in Appendix D1 and D2. Based on manufacturer industries data and research publications the cost of DPFC are listed below. From the table the main costs are [49, 50, 51, 52]:

Table 3. 8. Series Converter cost

Type	Cost per kVa (USD$)	Size	Total cost
IGBT module	50	8 MVA	$ 400,000.00
DC capacitor	28		$ 224,000.00
Gate driver and sensor	16		$ 128,000.00
Cooling system	12		$ 96,000.00
Series transformer	35		$ 280,000.00
Filter component	8		$ 64,000.00
control Hardware	10		$ 80,000.00
protection system	8		$ 64,000.00
Total cost			$ 1,336,000.00
Overall cost(x3)			$ 4,008,000.00

Table 3. 9. Shunt converter cost

Type	Cost per kVa (USD$)	Size	Total cost
IGBT module	45	25 MVA	$ 1,125,000.0
DC capacitor	25		$ 625,000.0
Gate driver and sensor	14		$ 350,000.0
Cooling system	10		$ 250,000.0
Series transformer	32		$ 800,000.0
Filter component	7		$ 175,000.0
Control Hardware	9		$ 225,000.0
Protection system	7		$ 175,000.0
Total cost			$ 3,725,000.0

Table 3. 10. DPFC annual benefits

Annual benefits		
Loss reduction (MW)		3
Hours per year		8760
Energy saved (MWh /year) = Loss reduction * Hours per year		26280
Energy saved (kWh/year) = Energy saved * 1000		26280000
Residential customer tariff (based on March 2025)	51-100 kWh	0.010
	101-200 kWh	0.018
	201-300 kWh	*0.026*
Energy price (USD/kwh) = Energy saved * tariff (201-300 kWh)		683,280

According to Addis Insight, The cost of electricity I Ethiopia varies base on the type of consumers. In to power system those loads are residential, commercial and industrial. Not only this the tariff system also vary based on the amount of energy consumed [53].

Referring to the Appendix D, after 20 years the total NPV is USD $ 15,310,316.00 and the total initial investment is USD $ 7,883,000.00 By implementing the DPFC system the Ethiopian electric utility will simply get profit a USD $ 7.5 million without considering scrap value of DPFC after useful life. Hence, the DPDC system is economically feasible.

Chapter Four

Simulation Studies and Result Analysis

4.1 PSAT power flow report

The PSAT data result is used to analyze the DPFC optimal sizing and placement as input data and network loss calculation.

Table 4. 1. Load flow study

From bus	To bus	Line	P Flow [p.u.]	Q Flow [p.u.]	P Loss [p.u.]	Q Loss [p.u.]
Ashegoda (B-1)	Alamata (B-3)	1	-0.1775	0.4447	0.0055	-0.0288
Ashegoda (B-1)	Lach (B-2)	2	0.2918	0.9685	0.0025	-0.0023
Alamata (B-3)	Lach (B-2)	3	0.2129	-0.3700	0.0039	-0.0294

Table 4. 2. PSAT global summary report

Global summary report			
Power	Total generation	Total load	Total loss
Real power [p.u.]	0.5452	0.5332	0.012
Reactive power [p.u.]	0.7446	0.8053	-0.0606

4.2. Genetic Algorithm m-file result

DPFC has the benefits of voltage profile enhancement and decrease power loss. With the optimal sizing and placement we can optimize the voltage profile and energy loss. According to the m-file result, the series converters are placed at bus-2 which connects Lachi-substation with Ashegoda wind farm. Technically this is due to the higher reactive power demand at Lachi-substation. The values of DPFC series and shunt converters are 7 MVA and 22.34 MVA respectively. By considering the converters loss and some future increase in load the researcher used the calculated values of 8 MVA and 25 MVA for series and shunt converters respectively. The list below are GA simulation results found by using MATLAB m-file code. Appendix F presents the M-file of the GA.

- Optimal Bus to Place Series DPFC: 2
- Series Converter Size: 7.00 MVA
- Shunt Converter Size: 22.34 MVA

4.3. MATLAB Simulink analysis

The graph below illustrates MATLAB/Simulink results corresponding to the operation of DFIG wind turbine at its rated capacity, highlighting system performance under normal and fault conditions.

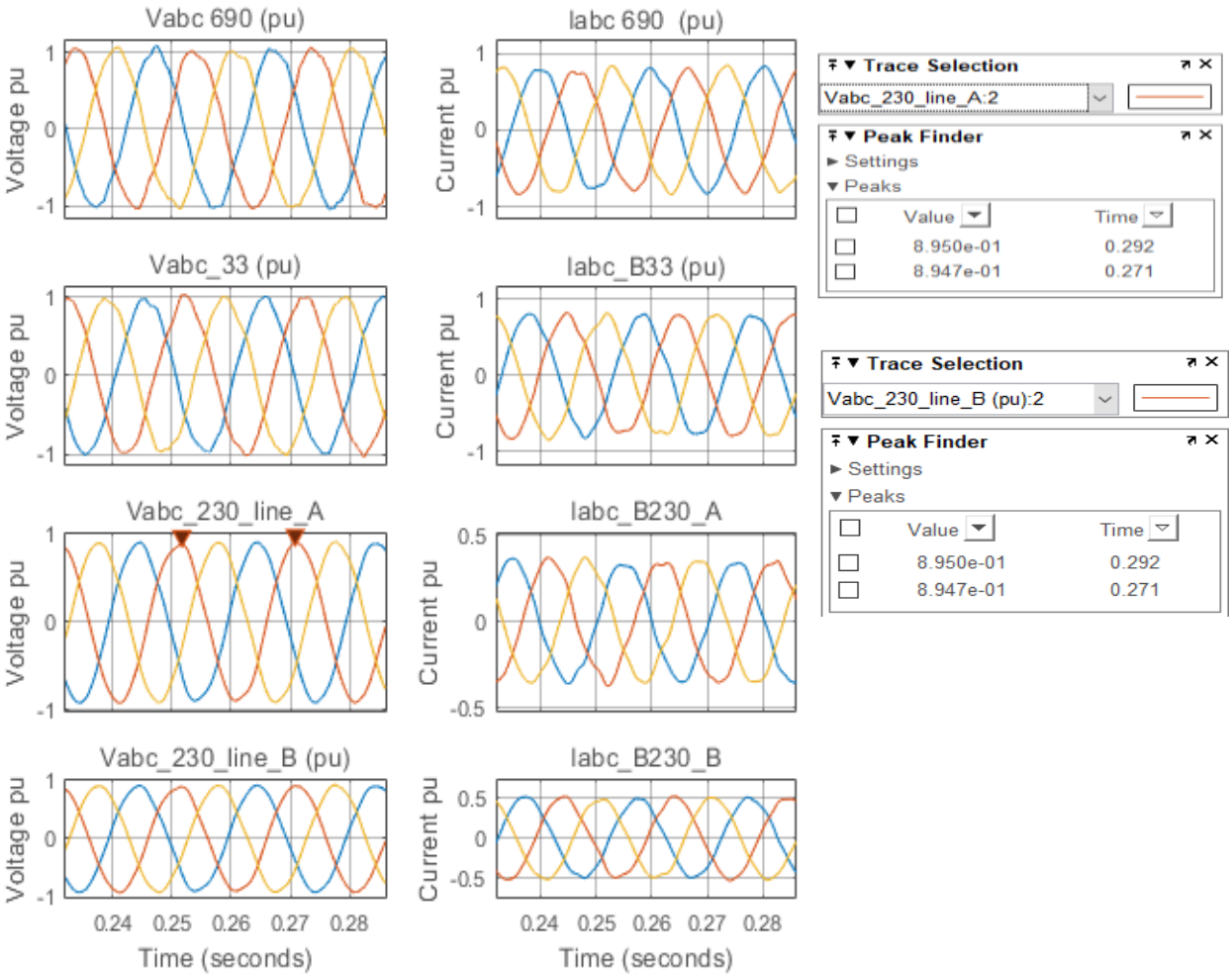

Figure 4. 1. Bus voltage level at rated capacity of DFIG without DPFC

The figure above illustrates the current and voltage pu magnitudes obtained from MATLAB Simulink model. The Bus voltage level at Vabc_ 230_line_A and Vabc_ 230_line_B experienced long duration under-voltage due to the high reactive power demand at Lachi-substation and the high voltage long distance transmission line between Alamata and Ashegoda wind farm, which is 141km.

According to IEEE standard, voltage magnitude below 0.9 pu for longer than 1 min is under-voltage [35]. Hence, the high voltage buses operates at 0.89 pu, which violate the international standard and needs a proper compensation to stabilize the voltage level. In addition to the time domain analysis a Fast Fourier Analysis (FFT) was done to evaluate the voltage and current total harmonic distortion (THD) analysis on bus Vabc_690. This is the bus which connect turbine-IGBT generated voltage with the cluster 33kv voltage.

The voltage THD at Vabc_690 without DPFC is 4.77% at 0.963 fundamental voltage magnitude. The voltage magnitude is in the tolerable limit. According to the manufacturer the maximum allowable current and voltage distortion is 3% [10]. This exceeds the standard limit and lead to equipment overheating, protection malfunction and reduce the lifespan of sensitive equipment. It also results in the reliability and system loss.

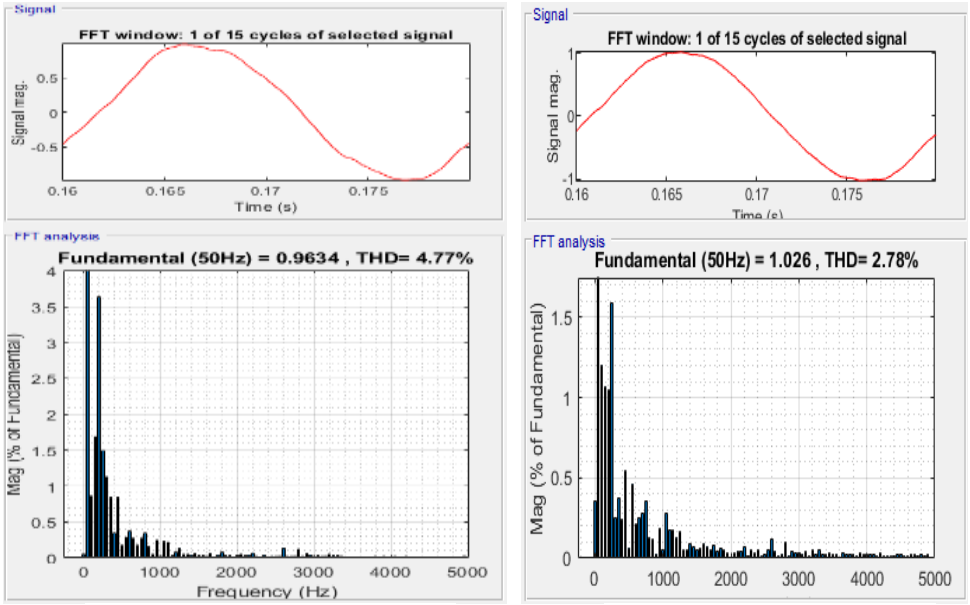

a. Voltage THD without DPFC b. Voltage THD with

Figure 4. 2. Total voltage harmonic distortion when the DFIG work at rated capacity

As shown in the below figure, the total current harmonic distortion reached 4.97%; which exceed the acceptable limit. Due to this the IGBT converter experience heating and sometimes burning. As a result, integrating DPFC device is mandatory to minimize the THD. After the installation of the DPFC device the current and voltage THD become 1.84% and 2.78%.

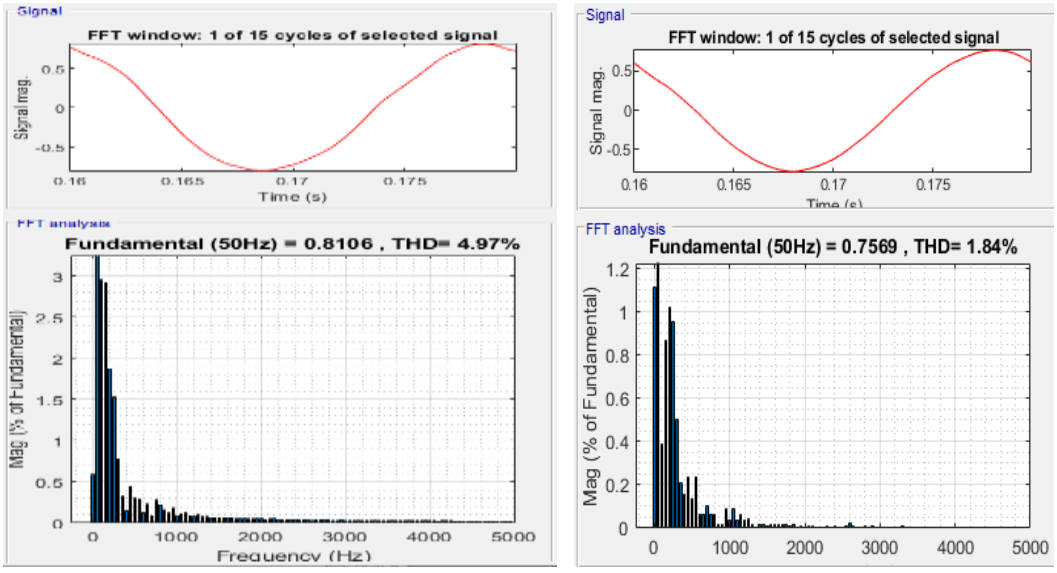

a. Voltage THD without DPFC b. Voltage THD with DPFC

Figure 4. 3. Total current harmonic distortion when the DFIG work at rated capacity

Long duration voltage drop under nominal value often caused by poor reactive power support, feeder loss and overloading. Such phenomena can be mitigated by the use of DPFC. DPFC injects reactive power to the power system at the point of common coupling to support bus voltage.

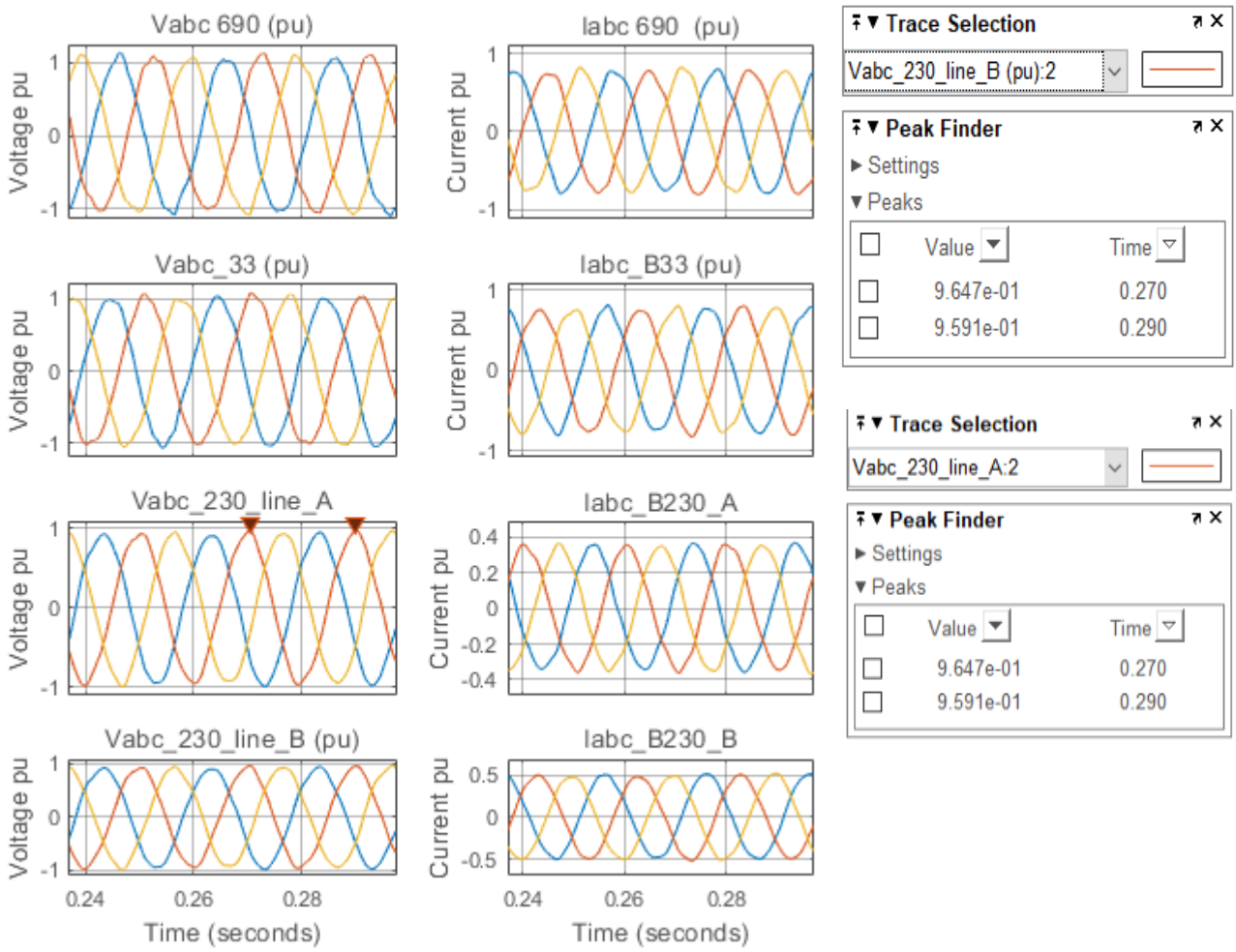

Figure 4. 4. Bus voltage with DPFC at different voltage buses

The shunt converter supplied the required reactive power, while the series distributed converter redistribute the active power to relive the active power stress on the system. As a result, the system voltage restored their voltage magnitude to the acceptable limits of 0.96 pu as shown in above. The DFIG active and reactive power response under DPFC and without DPFC analyzed below.

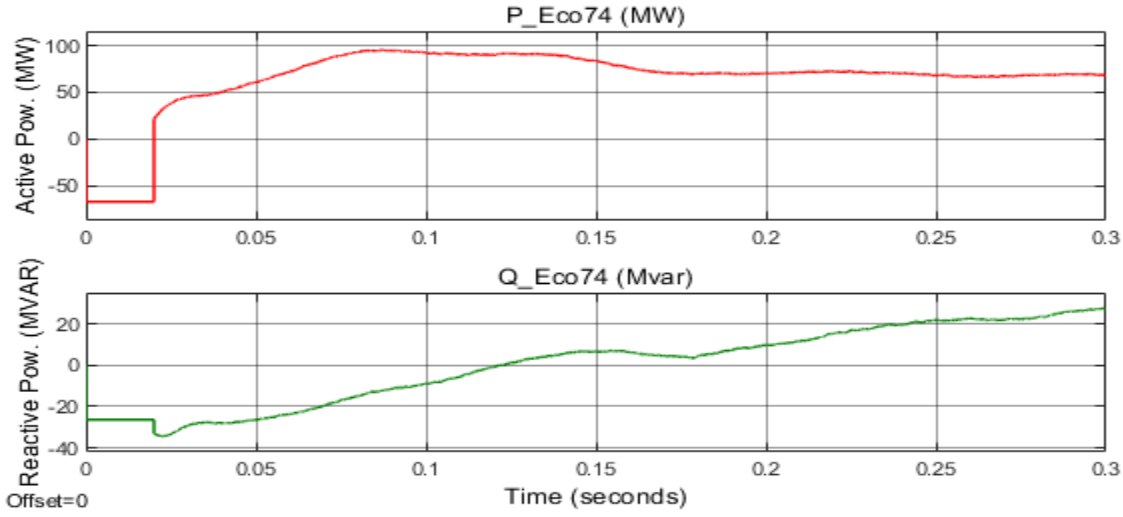

a. Active and reactive power output of DFIG without DPFC

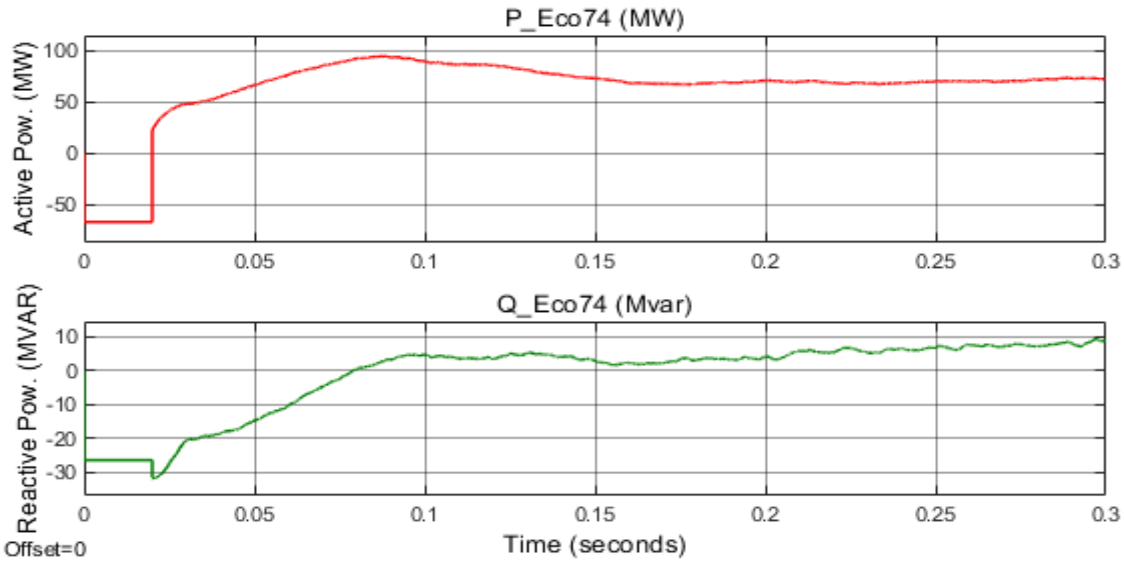

b. Active and reactive power output of DFIG with DPFC

Figure 4. 5. DFIG ECO74 active and reactive power output

The above figure shows DFIG active and reactive power response with and without DPFC converter. Under steady state operation the active power output is about 70 MVA and around 17 MVA reactive power without application of any FACT device. However, with the help of shunt connected converter DPFC at the wind farm DFIG generates approximately 73 MVA and 8 MVA active and reactive power respectively.

According to the system model at appendix H, Reactive power flow from the voltage source of shunt converter to the bus of B-33Sh if the magnitude of the voltage source Vsh **is** greater than the Vabc_33, and the phase of them are the same. If the phase angle of the voltage source Vsh leads the phase angle of the Vabc_33, and the magnitude of Vsh is greater than Vabc_33, then real and reactive power flow from the Vsh to the bus B33sh.

Contrariwise, if the magnitude of the Vsh is less than the Vabc_33 but the phase angle difference between them is zero, then only reactive power will flow from the bus Vabc_33 to the bus V-33sh. In this process the Vsh is consuming reactive power.

If the phase angle of Vabc_33 leads the phase angle of Vsh, and the Vsh magnitude is less than V-33sh then real and reactive power flow from Vabc_33to Vsh and the shunt converter is consuming real and reactive power. If the phase angle difference between the voltage at bus Vabc_33 and Vsh is maintained to zero then by varying the magnitude of Vsh reactive power can be generated or consumed by Vsh. Generally, by controlling the magnitude and phase angle of the shunt converter Vsh the direction of real and reactive power flow to the bus Vabc_33 can be controlled.

4.3.1. Voltage sag and swell analysis

DPFC mitigates voltage sags and swells. Voltage sags are controlled by injecting reactive power and series compensating voltage to improve bus voltage. Similarly voltage swells can be mitigated by absorbing reactive power and injecting counter voltages to support voltage swell. Using the Simulink model the sag and swell are inserted from 0.20 to 0.24 seconds.

As figuratively illustrated in the below, sags are a short duration RMS voltage drop usually from 0.1 to 0.9 pu. The main causes of voltage sags are short-circuit faults, starting of motor, or sudden heavy load connections. Voltage sags are mitigated by injecting reactive current to support bus voltage. The distributed series converters injecting compensating voltage in series with line. From figure 4.6, the DPFC system improve the voltage sag by around **0.1** pu.

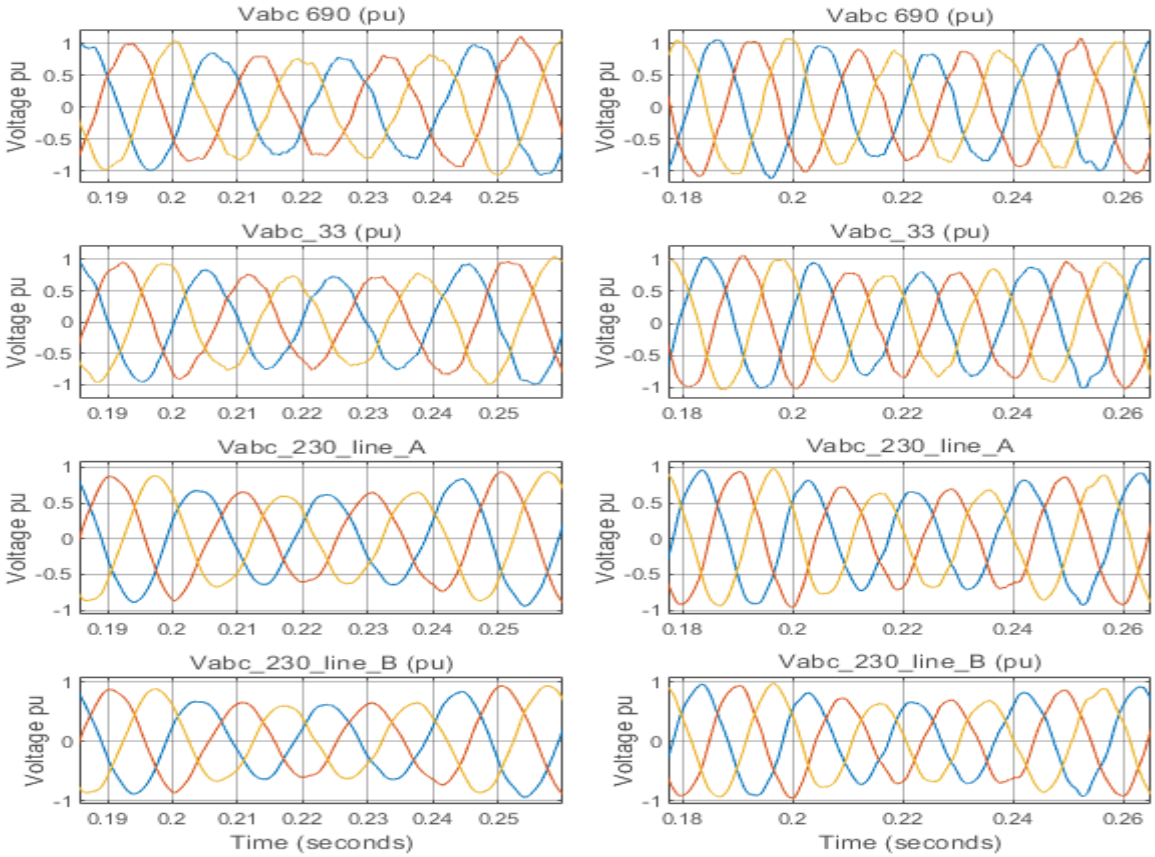

a. Voltage sag without DPFC b. Voltage sag with DPFC

Figure 4. 6. Sag response with and without DPFC controller

Voltage swell is a short duration raise in RMS voltage usually from 1.1 to 1.8 pu. Swells are caused by sudden load outage and sudden switching of capacitor bank. The DPFC shunt converter absorbs excess reactive power during swell. This reduces the voltage magnitude on the bus. The series converter injects opposite voltage to the swell voltage. In this manner the voltage swell can be limited and equipment overstress are prevented. From the below figure the DPFC system decreased the voltage swell by 0.1 pu. For more detailed IEEE standard on voltage sag and swell see appendix E.

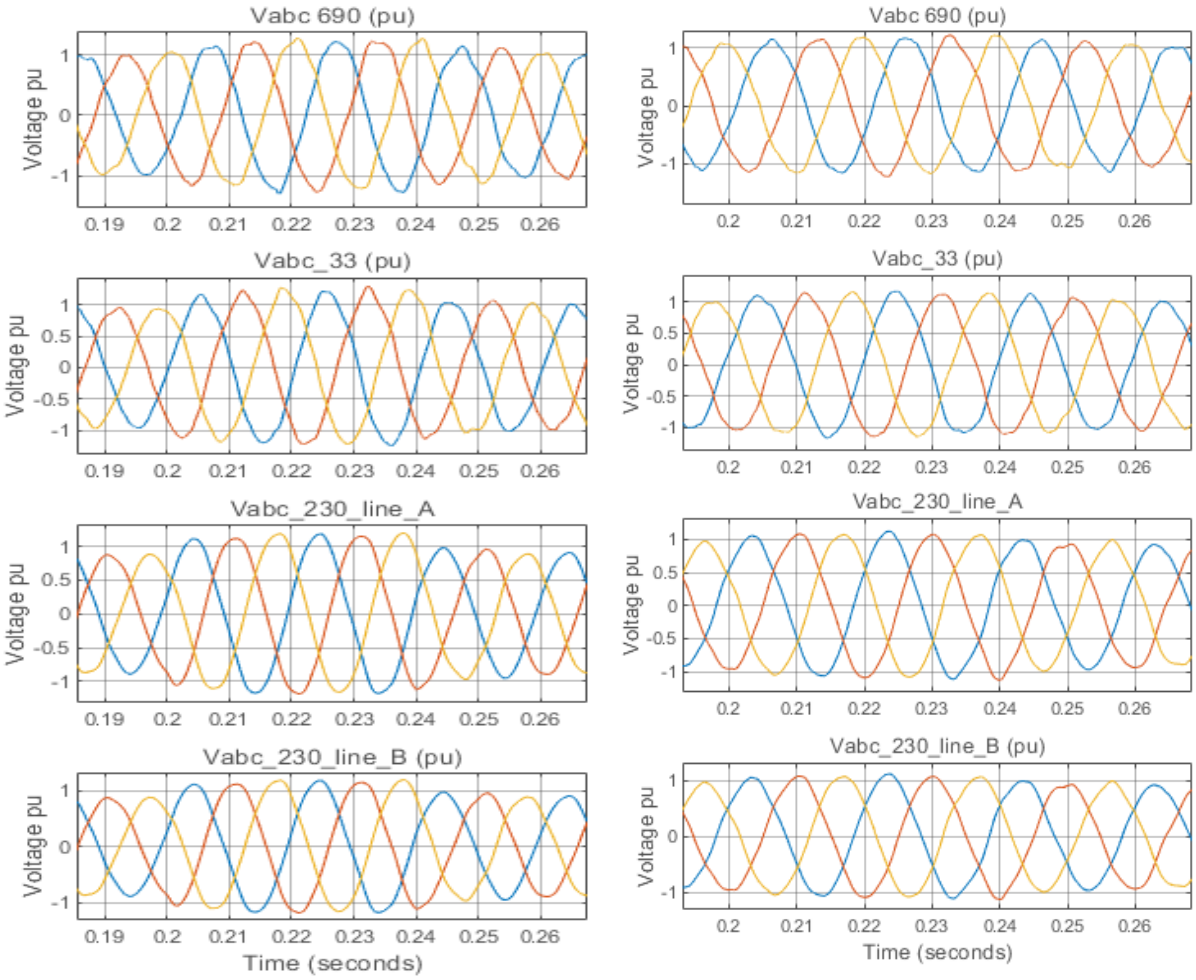

a. Voltage swell without DPFC

b. Voltage swell with DPFC

Figure 4. 7. Swell response with and without DPFC controller

4.3.2 Power system stability analysis

Fault or short circuit is a failure of power system which interferes the normal flow of current. After the occurrence of fault the operation of the system departs from steady state operation. Faults give excessive current and voltage at certain point of the system and cause a severe equipment damage [54]. There are two types of fault. Namely unsymmetrical and symmetrical faults.

During power system short-circuit fault the system current rise to several times the normal current. The high fault current can cause high thermal stress, voltage sag, and equipment damage. Hence, without compromising system stability the DPFC can limit the fault current.

The series converters play a vital role in fault current reduction. The series converter DPFC injects a voltage that opposes the fault current which is series voltage drop. This increases the apparent impedance of the line. As the impedance increase the faulted current passing through the line. The shunt converter supports voltage recovery during system faults.

As shown from the below simulation results, DPFC can work as current limiter and FACT device. This can ensure dual benefits in voltage support and limiting current during faults. Fault current is inserted from 0.24 to 0.26 seconds.

4.3.3. Single line-to-ground fault (SLG)

The below figure represents a single line-to-ground fault at Ashegoda – Lachi network at 1Km distance from Ashegoda farm. The current per-unit value of faulted line reached 0.91, 1.03, and 0.55 Pu for line to ground fault with ground at bus Vabc-690, Vabc-33, and Vabc-230 respectively without the use of any FACT device controller.

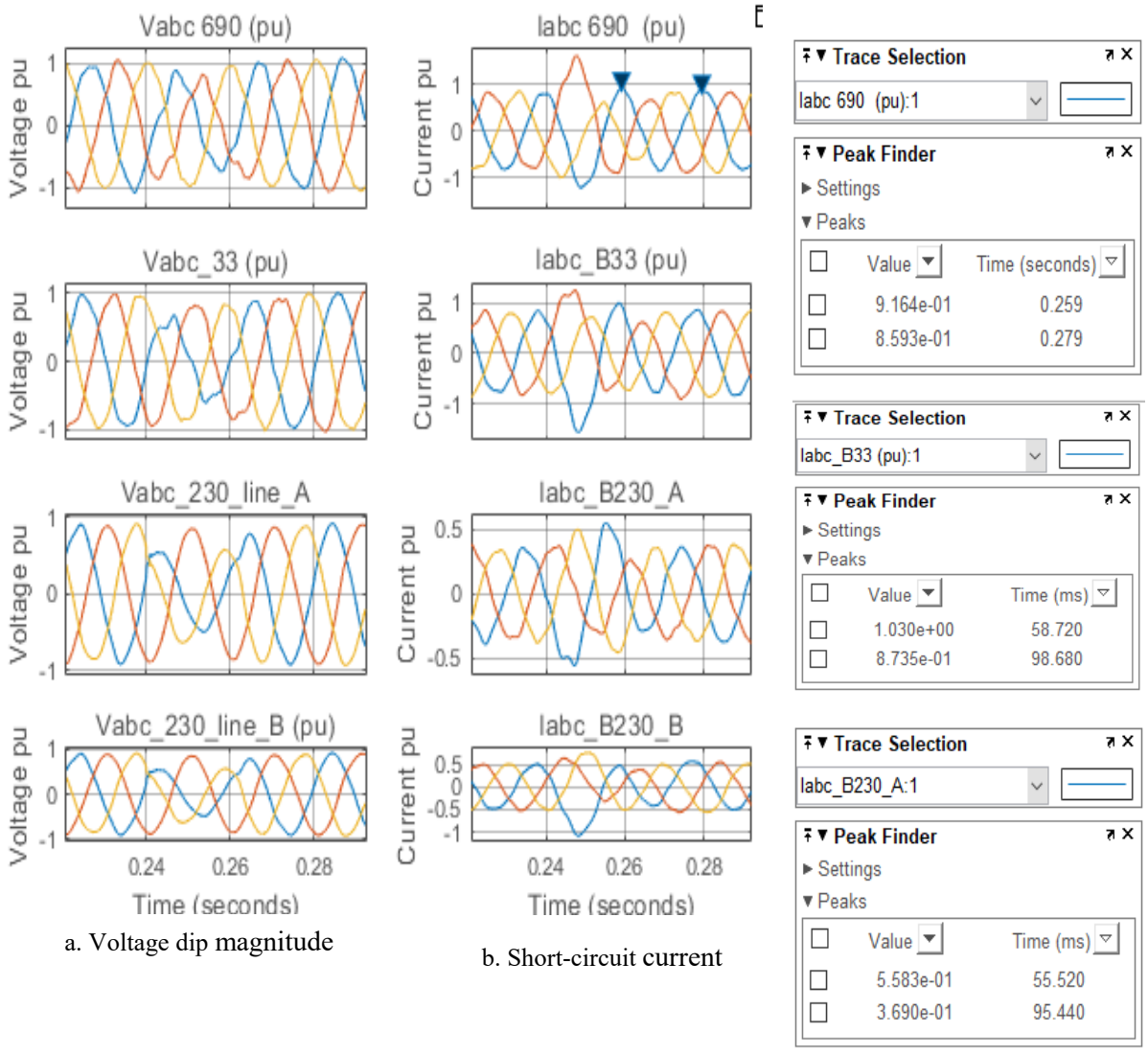

a. Voltage dip magnitude

b. Short-circuit current

Figure 4. 8. Single line-to-ground fault response without DPFC

After proper integration of DPFC controller the fault current for line-1 get minimized. This is due to the series converter ability of adjusting the line impedance. The fault current are minimized to 0.85 at bus Iabc_B690, 0.88 at bus Iabc_B33, and 0.38 Pu at bus Iabc_B230 as shown in the below figure 4.9.

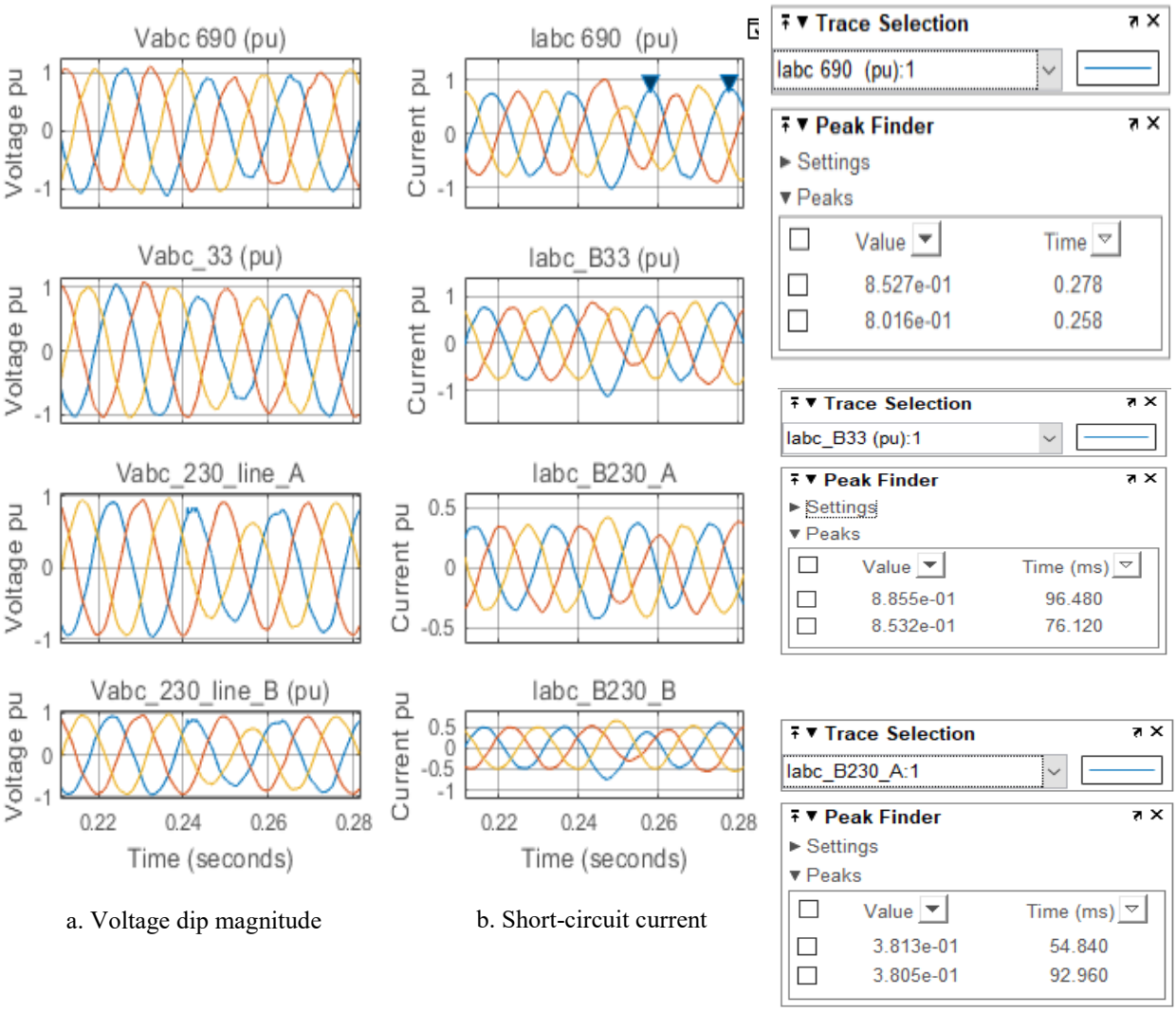

a. Voltage dip magnitude b. Short-circuit current

Figure 4. 9. Single line to ground fault response with DPFC

4.3.4. Double line to ground fault (L-L-G)

A double line to ground fault happen when two conductors make contact with the ground at the same time and create a parallel path fault. It is more saver than singe line to ground fault. The distributed nature of DPFC can provide an effective mitigation capability on multiple faulted paths simultaneously.

Figure 4.10 illustrates the network response to double line to ground fault condition. The current per-unit value reached 2.13 pu, 2.20 pu, and 0.62 Pu for double line to ground fault without DPFC at bus Iabc_B690, Iabc_B33, and Iabc_B230 respectively.

The system response to double line to ground fault in the presence of DPFC is shown in figure 4.11. The fault currents are limited to 1.3 pu, 1.21 pu, and 0. 45 pu on the above respective buses of Iabc_B690, Iabc_B33, and Iabc_B230.

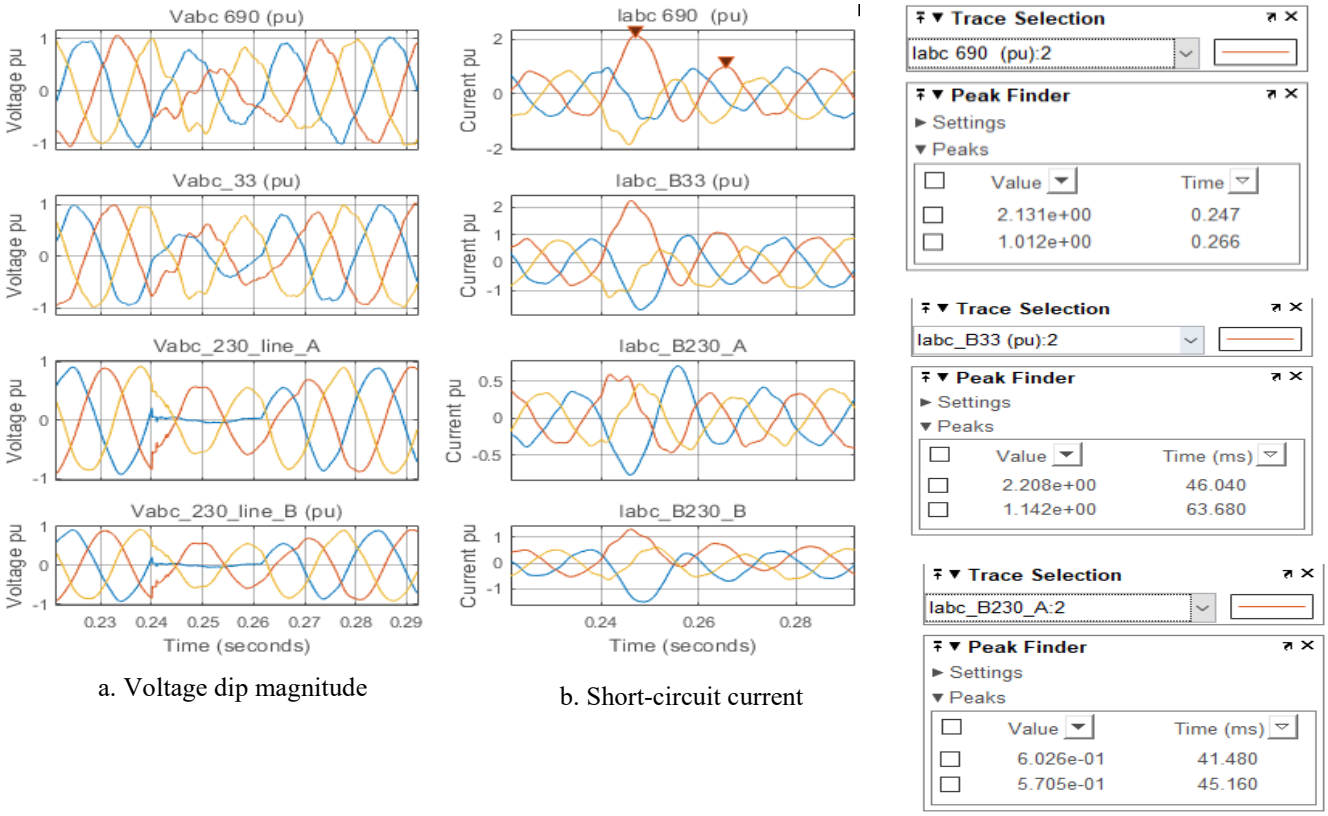

a. Voltage dip magnitude

b. Short-circuit current

Figure 4. 10. Double line to ground fault without DPFC

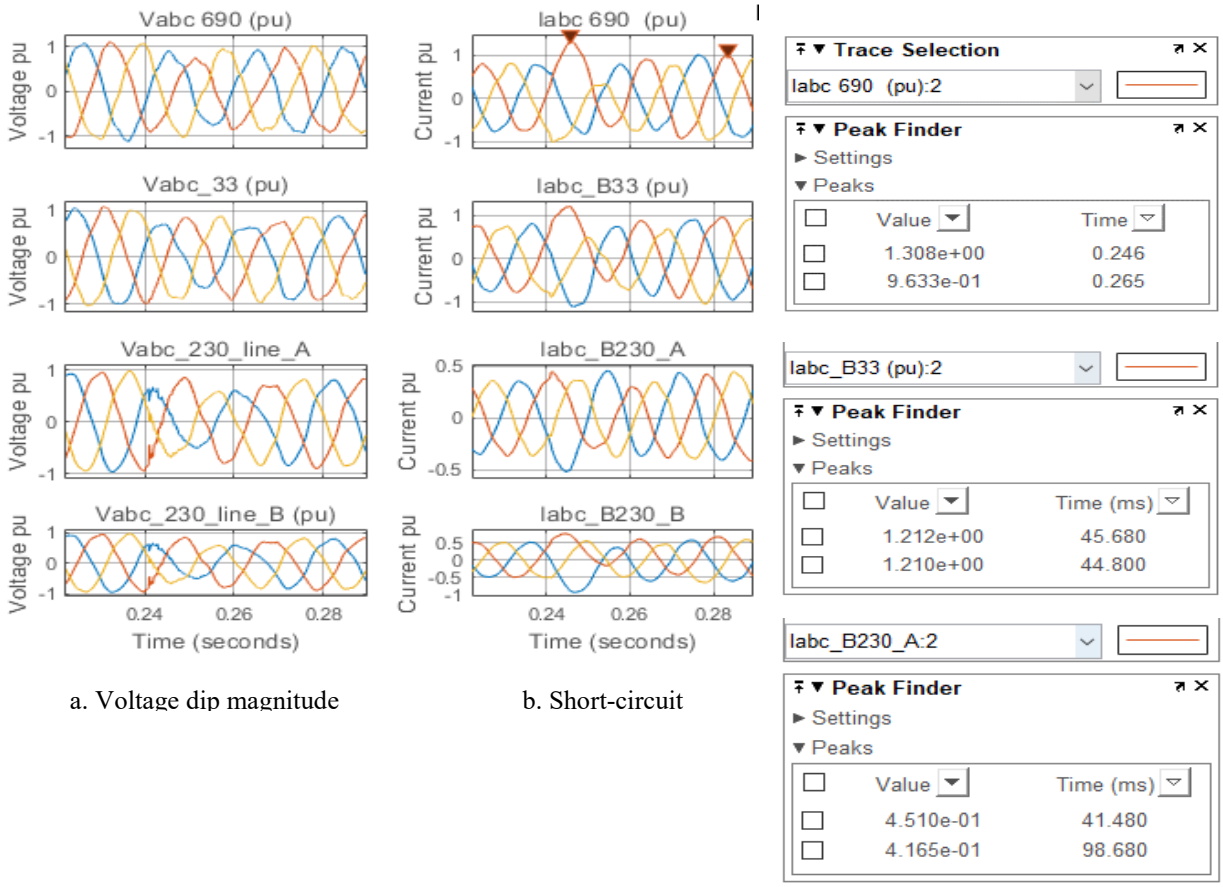

a. Voltage dip magnitude

b. Short-circuit

Figure 4. 11. Double line to ground fault response with DPFC

4.3.5. Symmetrical fault analysis

The simulation result as shown below, symmetrical faults are an equal fault current in the three phase lines with equal 120° phase displacement among the fault current. This type of fault occur when 3-phase line connected together at the same time. This type of faults are the most severe as it causes a simultaneous three phase voltage drop to nearly zero at the faulted location and large symmetrical faulted current will flow through all the three phase lines.

The peak current during three phase- to- ground fault without compensation at bus Iabc_690 is 2.05 pu, 2.26 pu at bus Iabc_B33, and 0.73 pu at bus Iabc_B230.

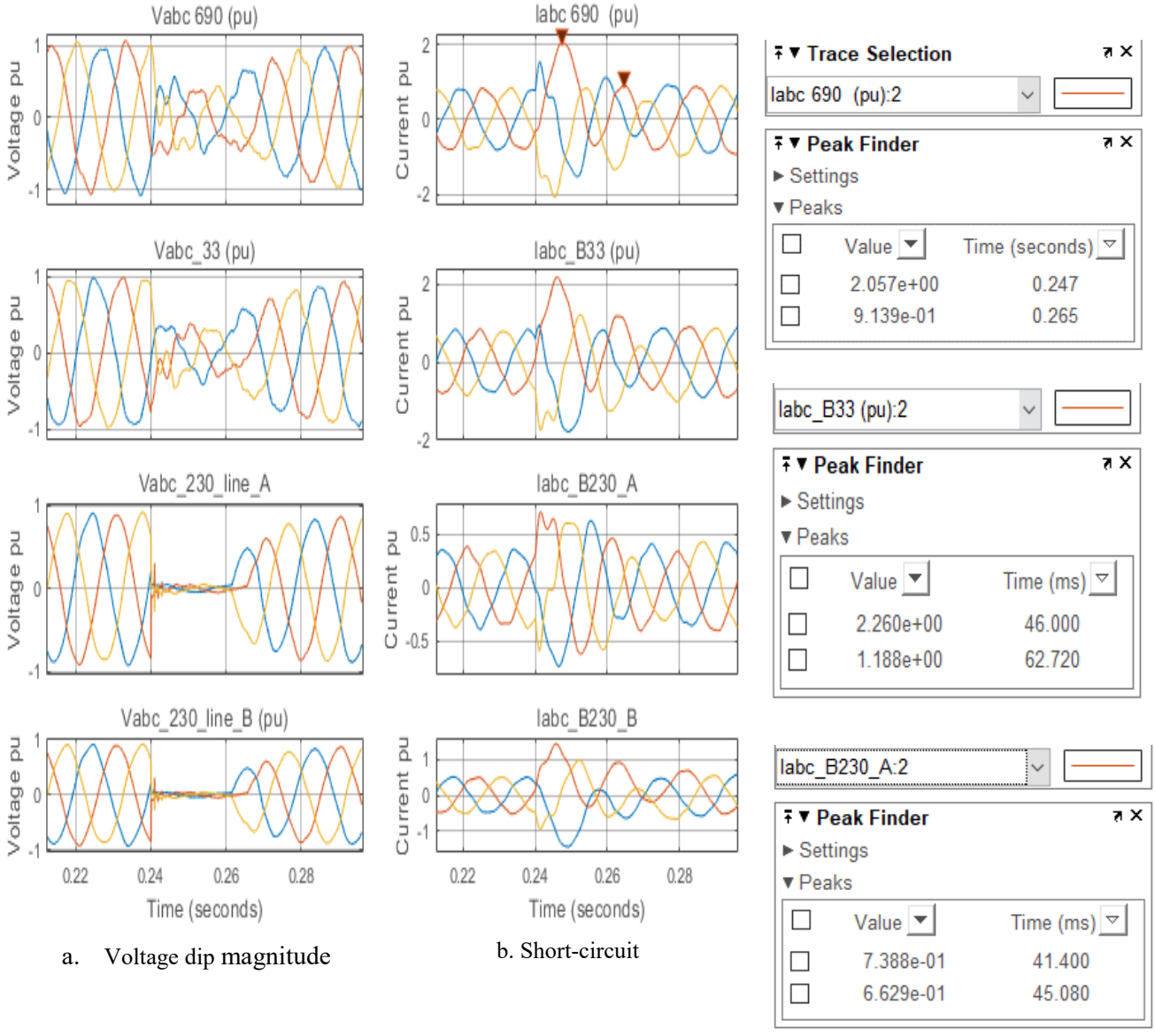

a. Voltage dip magnitude

b. Short-circuit

Figure 4. 12. Symmetrical fault at Lachi-Ashegoda line without DPFC

With the help of DPFC controller as shown in the below Simulink result, the short circuit fault current is minimized to 1.2 pu, 1.08 pu, and 0.45 pu for Iabc_690, Iabc_B33, and Iabc_B230 respectively. The

series converter injects a series voltage to particularly restore the three phase voltage during the fault. The fault current is limited by dynamically controlling line impedance.

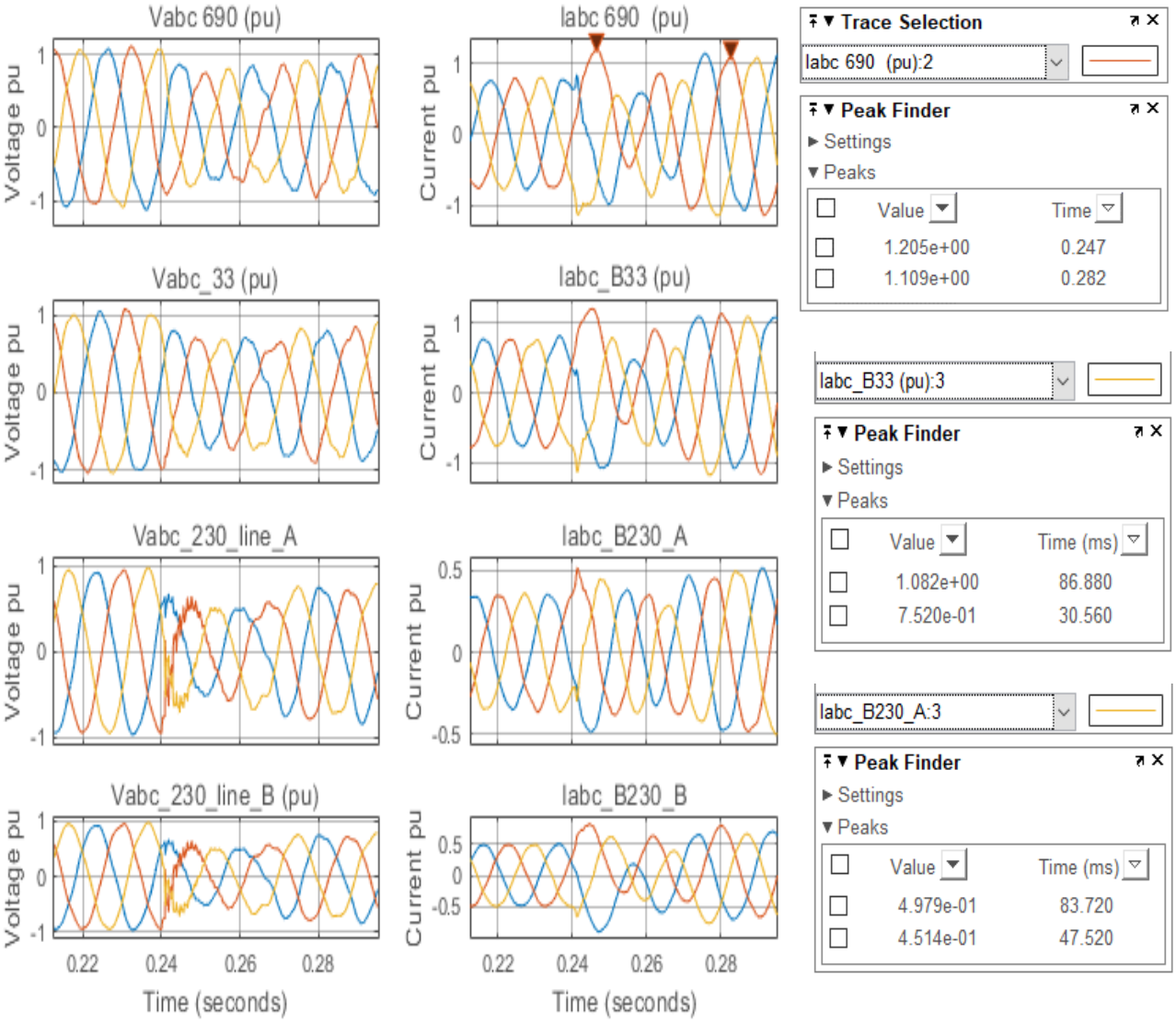

a. Voltage dip magnitude b. Short-circuit current

Figure 4. 13. Symmetrical fault at Lachi-Ashegoda line with DPFC

Chapter Five

Conclusion and Recommendation

Based on the result obtained from MATLAB simulation under DPFC performance and the cost benefit analysis, the following conclusion and recommendation have been made and possible future works are addressed.

5.1. Conclusion

This study analyzed and modeled the integration, impact, cost benefit analysis, and Genetic Algorithm (GA) based optimal sizing and placement of DPFC for Ashegoda wind farm. The installed capacity of Ashegoda wind farm is 120 MW, with 54 DFIG three blade WECs rated at 1.67MW. In the analyzed system, both transmission lines experienced inductive reactive power flow approximately 43MVAr and more than 3% current total harmonic distortion (THD), which leads to additional power loss, voltage drop, equipment overheating, and network congestions. On the other hand, the on-load tap changer (OLTC) transformer used to support voltage sag, swell, under-voltage, and over-voltage has slow response time up to 10 seconds per tap, and creates transformer overheating and mechanical fatigue.

The incorporation of a distributed power flow controller (DPFC) with in the system is necessary for mitigating integration challenges and improving power quality. The DPFC is the most reliable and cost efficient system for power system quality improvement and optimal power flow control. Integrating DPFC exhibited excellent performance in maintaining voltage stability and limiting short-circuit current levels under different fault scenarios.

The result indicated that, without DPFC the 230kv system operated at under-voltage of 0.89 pu with 5% current THD at bus 690v. After integration of 8MVA series and 25MVA shunt DPFC controller, the voltage profile is improved to 0.96 pu and current THD is minimized to 1.8%. Integrating DPFC exhibited excellent performance in maintaining voltage stability and limiting short-circuit current levels under different fault scenarios. The cost benefit analysis was carried out over a 20-year period, showed Ethiopian electric utility gain around $7.5 million US dollars profit without considering scrap value.

5.2. Recommendation

The increase in electrical energy demand and consumption opened a new era for renewable energy. Due to the price and climatic concern caused by the non- renewable energy like fossil fuels, the world is digging to ride through these problems. Manufacturing industries and utilities are working on the improvement and optimal application of renewable energy sources. It has not been employed yet at full-scale.

The presence of high inductive reactive power in high voltage transmission lines can cause voltage drops, poor voltage regulation, increase line loss and reduce power transfer capability. Only applying

OLTC cannot mitigate the above problems. Hence, integrating DPFC or other FACT devices effectively reduce the power quality problems and enhance power transfer capability.

5.3 Future Work

Future researchers on the area of interest, might consider protection system improvement and sizing caused due to DPFC and load forecasting. Active power loss minimization, and VAr planning to minimize the cost of reactive power support are the objectives functions used for optimal size and place the DPFC in this paper. Considering environmental dispatch and maximum power transfer for future GA based optimization is recommended.

References

[1] E. G. a. N. Fulghum, "Global Electricity Review 2025," Creative Commons ShareAlike Attribution Licence (CC BY-SA 4.0), 2025.

[2] A. A. a. e. a. Julian Prime, "Renewable Energry Statistics 2024," International Renewable Energy Agency (IRENA) , Abu Dhabi, 2025.

[3] THAMATAPU ESWARA RAO et al., "Performance Improvement of Grid Interfaced Hybrid System Using Distributed Power Flow Controller Optimization Techniques," *IEEE Access,* vol. 10, pp. 12742-12752, 2022.

[4] G. K. S. Subhashree Choudhury, "A critical analysis of different power quality improvement techniques in microgrid," *e-prime - Advances in Electrical engineering, electronics and energy,* vol. 8, pp. 1-21, 2024.

[5] Aamir Farooq et al., "Influence of Unified Power Flow Controller on Flexible Alternating Current Transmission System Devices in 500 kV Transmission Line," *Journal of Electrical and Electronic Engineering,* vol. 6, no. 1, pp. 12-19, 2018.

[6] MALOTH HUSSEN and AND THIRUMALAIVASAN RAJARAM, "A Comprehensive Review of Voltage Source Converters-Based FACTS Controllers in Hybrid Microgrids," *IEEE Access,* vol. 13, pp. 62961-62999, 2025.

[7] Mahesh Shende and Prof. Redharaman Shaha, "Improvement of Power Quality in Distrinution System Using Photovoltaic Bassed DPFC," *Journal of Emerging Technologies and Innovative Research (JETIR),* vol. 7, no. 12, pp. 100-102, 2020.

[8] V. K. G. e. Biplab Bhattacharyya, "UPFC with series and shunt FACTS controllers for the economic operation of a power system," *Ain Shams Engineering Journal,* no. 5, pp. 775-787, 2014.

[9] Zhihui Yuan and Sjoerd W.H. et al, "A FACTS Device: Distributed Power-Flow Controller (DPFC)," *IEEE Transcations on power electronics,* vol. 25, no. 10, pp. 2564-2572, 2010.

[10] A. w. Farm, Operating and maintanance manual, Vernet.

[11] A. T. Guide, "ON-Load Tap Changer for Power Transformer," ABB, 2018.

[12] B. K.Divya, "Dynamic Performance of Distriuted Power Flow Controller for Power Quality Improvment," *IEEE Transaction on Power Delivery,* vol. 25, no. 4, pp. 2864-2872, 2010.

[13] M. H. a. e. a. Jawad Hussain, "Power Quality Improvement of Grid Connected Wind Energy System Using DSTATCOM - BESS," *INTERNATIONAL JOURNAL of RENEWABLE ENERGY RESEARCH,* vol. 9, no. 3, 2019.

[14] G. e. al., "Research on the three-phase load imbalance control of the active distribution network based on the distributed power flow controller," *Frontiers in Energy Research,* vol. 10, no. 3389, pp. 01-13, 2024.

[15] a. D. a. e. a. R. Thilepa, "POWER QUALITY IMPROVEMENT BY VOLTAGE CONTROL USING DSTATCOM IN MATLAB," *ARPN Journal of Engineering and Applied Sciences,* vol. 10, no. 6, 2015.

[16] R. A. a. e. al., "Power Flow Analysis Using interline Power Flow Controller," *Journal of Multidisciplinary Engineering Science and Technology (JMEST),* vol. 7, no. 5, pp. 13871-13876, 2020.

[17] B. L. a. e. a. Qiuyu Li, "A Novel Location Method for Interline Power Flow Controllers Based on Entropy Theory," *Protection and control of modern power systems,* vol. 9, no. 3, pp. 70-81, 2024.

[18] Djamel Eddine Tourqui and et al., "Improving the Electrical Stability by Wind Turbine and UPFC," *Improving the Electrical Stability by Wind Turbine and UPFC,* pp. 1-12, 2018.

[19] D. S. Y.N.Vijayakumar, "APPLICATION OF INTERLINE POWER FLOW CONTROLLER (IPFC) FOR POWER TRANSMISSION SYSTEM," *INTERNATIONAL JOURNAL OF INNOVATIVE RESEARCH IN ELECTRICAL, ELECTRONICS, INSTRUMENTATION AND CONTROL ENGINEERING ,* vol. 2, no. 10, pp. 2138-2142, 2014.

[20] S. Singh, "Technical Aspects of Different Grid Connected Wind Energy Conversion System Configurations in Wind Farm," *International Journal of Engineering and Advanced Technology (IJEAT),* vol. 9, no. 1, pp. 3949-3955, 2019.

[21] a. C. S. R. Vemuri Sowmya Sree, "Distributed power flow controller based on fuzzy-logic controller for solar-wind energy hybrid system," *International Journal of Power Electronics and Drive Systems (IJPEDS),* vol. 13, no. 4, pp. 2148 - 2158, 2022.

[22] S. W. d. H. e. Braham Ferreira, "Utilizing Distributed Power Flow Controller (DPFC) for Power Oscillation Damping," *IEEE TRANSACTIONS ON POWER ELECTRONICS,* vol. 6, no. 9, pp. 4241-4244, 2009.

[23] Anita Y. Solanki and Dr. Sanjay R. Vyas, "A Review on Power Quality Enhancement Using Custom Power Devices," *International Research Journal of Engineering and Technology (IRJET),* vol. 08, no. 02, pp. 287- 290, 2021.

[24] M. T. a. e. a. Joao L. Afonso, "A Review on power electronics technologies for power quality improvement," *Energies,* vol. 14, p. 8585, 2021.

[25] Jiying Shi et al., "IIWO Based Sliding Mode Extremum Seeking Control for MPPT in Wind Energy Conversion System," *ScienceDirect,* vol. 158, pp. 85-90, 2019.

[26] V. W. a. e. a. Prem Kumar Chaurasiya, "Wind Energy development and policy in India, A review," *Energy Strategy Reviews/ Elsevier,* no. 24, pp. 342-357, 2019.

[27] G. U. a. e. a. B Kandavel, "Comparative Study of Total Harmonic Distortion in Multilevel Inverrters Based WECS," *International Journal of Engineering & Technology,* vol. 7, pp. 42-45, 2015.

[28] Simon Watson et al., "Future emerging technologies in the wind power sector: A European perspective," *Renewable and Sustainable Energy Reviews/ ScienceDirect,* vol. 113, pp. 1-21, 2019.

[29] S. N. a. M. G. Daniel Fallows, "Harmonic Reduction Methods for Electrical Generation: A Review," *IET Generation Transmission & Distribution,* vol. 24821037, 2018.

[30] H. A. Kazem, "Harmonic Mitigation Techniques Applied to Power Distribution Networks," *Advances in Power Electronics,* vol. 591680, p. 10, February 2013.

[31] G. U. M. M. B. Kandavel, "Comparative Study of Total Harmonic Distortion in Multi level converters Based WECS," *International Journal of Engineering & Technology,* vol. 7, pp. 42-45, 2018.

[32] Ned Mohan, Power Electronics A First Course, United States of America: John Wiley & Sons, Inc., 2012.

[33] F. S. a. e. Wikus Kruger, "Energy and Economic Growth Research Program/ Ethiopia Country Report," University of Cape Town, 2019.

[34] Luca Marena et al, "INTEGRATION OF VARIABLE RENEWABLE ENERGY IN THE NATIONAL ELECTRIC SYSTEM OF ETHIOPIA," RES 4Africa Foundation and Ethiopian Electric Power (EEP), 2019.

[35] M. S. Bollen, Understanding Power Quality Problems, USA New York: IEEE Press Series on power Engineering, 2000.

[36] S. Kumar, "Power Quality Issues and its Mitigation Techniques," in *National Institute of Technolgy*, Orissa, India, 2014.

[37] Roger C. Dugan and Mark F.MCGranaghan and et al., Electrical Power Systems Quality, Second Edition, Digital Engineering Library: McGraw Hill Professional Engineering, 2004.

[38] b. D. I. B. T. C. Augusto Matheus dos Santos Alonsoa, "A selective harmonic compensation and power control approach exploiting distributed electronic converters in microgrids," *Electrical Power and Energy System,* vol. 10, 2019.

[39] K. Padiyar, FACTS CONTROLLERS IN POWER TRANSMISSION AND DISTRIBUTION, New Delhi· Bangalore : NEW AGE INTERNATIONAL PUBLISHERS, 2007.

[40] S. J. Chapman, Electric Machinery Fundamentals, fourth edition, New York: McGraw-Hill, 2005.

[41] Miraja Fereja, Writer, *Existing and planned transmission network.* [Performance]. EEPCO, 2015.

[42] Mekdes Gemechu and Milkias Berhanu, "Power control of wind energy converssion system with doubly fed induction generator," *Journal of energy,* vol. 2022, pp. 1-12, 2022.

[43] H. A.-R. e. al., Power electronics for renewable energy systems, transportation and industrial applications, United Kingdom: IEEE press WIley, 2014.

[44] S. M. B. e. a. Ahmad Jamshidi, "Power Quality Improvement and mitigation case study using distributed power flow controller," *IEEE transactions,* vol. 978, no. 1, pp. 464-468, 2012.

[45] C. S. R. Vemuri Sowmya Sree, "Distributed power flow controller based on fuzzy-logic controller for solar-wind energy hybrid system," *nternational Journal of Power Electronics and Drive Systems (IJPEDS),* vol. 13, no. 4, pp. 2148-2158, 2022.

[46] Y. S. e. a. Aihong Tang, "Study on control Method of a Distributed Power Flow Controller," *IEEJ Transactions on elctrical and elctronics engineering,* pp. 1-7, 2019.

[47] E. C. a. Cables, Writer, *ACCC - All Conductor Composite Core.* [Performance]. EMTA Conductor and Cable INC..

[48] M. C. Ltd, Writer, *Energy Efficient High current OH conductors - Technical Data Sheet.* [Performance]. CTC Cable corporation, 2021.

[49] H. Y. a. S. A. e. al., "Valuation of reactive power support provided by photovoltaic system in distribution network," *International Transaction on Electrical Energy systems ,* vol. 31, pp. 1-18, 2020.

[50] J. ,. e. a. Smith, "Economic Assessment and Business case development for DPFC in modern transmission sytems," *IEEE Transaction on power systems,* vol. 38, no. 4, pp. 2897-2910, 2023.

[51] N. Y. s. g. m. intiative, "DPFC demonstration project," New York power authority (NYPA) and Electricpower research institute, New York, 2022.

[52] T. M. a. B. e. al., "Valuation of reactive power and voltage support service," *The Electricity Journal,* vol. 36, no. 2, 2023.

[53] A. Insight, "Addis Insight," 9 March 2025. [Online]. Available: https://www.addisinsight.net/2025/03/09/ethiopia-to-increase-electricity-tariffs-starting-april/. [Accessed 2 10 2025].

[54] R. M. V.K. Mehta, Writer, *principles of power system.* [Performance]. S.Chand and Company LTD, 2013.

[55] A. M. a. K. Mokariya, "HARMONICS IN POWER SYSTEM AND ITS MITIGATION TECHNIQUES," p. 4, 2016.

Appendix A

Appendix A represents the collected data of equipment rating in a tabular form.

Table A 1. GEV- HP wind turbine specifications

Specification	Parameter	category
1	Wind turbine type	GEV - HP
2	Hub high	70 m
3	Rotor diameter	62 m
4	Nominal rotor speed	22.5 rpm
5	Cut-in wind speed	2 m/s
6	Cut-out wind speed	25 m/s
7	Rated wind speed	12.5 m/s
8	Blade number	2
9	Blade length	30 m
10	Gearbox ratio	67.4
11	Min generator speed	809 rpm
12	Rated generator speed	1516 rpm
13	Generator type	Asynchronous
14	Rated power	1060 kw
15	Rated voltage	690 V
16	Rated current	1030 A
17	Nominal torque	6799 Nm
18	Frequency	50or 60 Hz
19	Max THD current	3%
20	Electronic type	Full scale IGBT
21	Total № of turbines	30

Table A 2. ECO74 wind turbine type specification

№	specification	class
1	Wind turbine type	ECO-74
2	Hub high	80 m
3	Rotor diameter	74 m
4	Rated rotor speed	19 rpm (low speed shaft)
5	Cut-in wind speed	3 m/s
6	Cut-out wind speed	25 m/s
7	Rated wind speed	13 m/s
8	Blade number	3
9	Blade length	30 m
10	Gearbox ratio	94.6
11	Generator speed range	(950-2100) rpm
12	Rated generator speed	1800 rpm
13	Generator type	DFIG
14	Rated power	1670 kw
15	Stator rated voltage	690 V
16	Rotor rated voltage	760 V
17	Rated current	630 A
18	Nominal torque	6799 Nm
19	Frequency	50 Hz
20	Electronic type	AC-DC-AC IGBT
21	Total № of turbines	54

Table A 3. Power transformer specification

№	specification	class
1	Transformer type	SFZ-65000/230
2	№ of Transformer	2
3	Rated power	65 MVA
4	Rated voltage LV	33 KV
5	Rated voltage HV	230 KV
6	Method of cooling	ONAN/ONAF
7	Rated current LV	875.6 / 1137.2 A
8	Rated Current HV	125.5 / 163.2 A
9	Number of phases	3
10	Voltage regulation by tap changer	± 10 taps@ 1.25%
11	№ of tap positions of on load tap changer	21
12	Rated frequency	50 Hz
13	Vector group	YNd11

Table A 4. Auxiliary transformer Specification

№	Specification	Class
1	Transformer type	DCU 3436
2	№ of Transformer	2
3	Rated power	250 KVA
4	Rated voltage LV	400 V
5	Rated voltage HV	33 KV
6	Method of cooling	ONAN
7	Rated current LV	360.8 A
8	Rated Current HV	4.37 A
9	Number of phases	3
10	Vector group	Dyn 11
11	Rated frequency	50 Hz

Table A 5. Earthing transformer Specification

№	Specification	Class
1	Transformer type	DCA 4236
2	№ of Transformer	2
3	Rated power	19053 KVA
4	Rated voltage LV	6300V
5	Rated voltage HV	33 KV
6	Method of cooling	ONAN
7	Rated neutral current	1000 A
8	Number of phases	3
9	Vector group	YNd5
10	Rated frequency	50 Hz

Table A 6. Transmission line specifications

№	Parameter	Value
1	Type of conductor	AAAC
2	Conductor cross sectional area	$180mm^2$
3	Maximum operating temperature	90-100°c
4	Overall diameter	18-20mm
5	Thermal expansion coefficient	$23*10^{-6}/°c$
6	AC resistance at 25°c	0.171 Ω/km
7	Reactance	0.258 Ω/km

Appendix B

Line-1 and line-2 Bus data at some randomly selected day.

Time Hrs.	System Frequency Hz	Bus Voltage KV	LINE- 1 Alamata				LINE- 2 Lachi			
			Real power MW	Reactive power MVAR	Voltage KV	Current Amp	Real power MW	Reactive power MVAR	Voltage KV	Current A
1:00	50.13	238	6	-32	238	81	20	32	239	92
2:00	50.11	239	13	-34	240	81	20	33	240	92
3:00	50.02	237	8	-31	237	79	20	31	238	93
4:00	50.15	238	17	-34	239	91	25	31	239	95
5:00	50.07	235	0	-32	235	80	40	30	235	121
6:00	50.03	228	-18	-31	228	91	62	28	228	171
7:00	49.97	226	-50	-23	226	136	110	19	226	282
8:00	50.14	230	-16	-31	231	89	96	22	231	245
9:00	50.07	224	-11	-29	224	80	91	19	224	228
10:00	50.03	226	-10	-29	225	74	91	20	226	134
11:00	49.98	225	-33	-23	225	103	89	19	225	233
12:00	50.01	229	-32	-28	229	99	82	25	230	208
13:00	50.13	230	-35	-22	230	104	80	19	231	205
14:00	50.21	234	-40	-20	234	109	69	20	234	175
15:00	50.07	231	-41	-16	232	108	61	16	232	157
16:00	50.01	225	-54	-9	225	140	69	10	225	177
17:00	50.04	229	-47	-20	230	126	77	19	230	198
18:00	49.98	230	-43	-26	230	127	93	23	231	237
19:00	50	231	-55	-19	231	143	113	15	231	128
20:00	50.06	236	-31	-21	237	89	94	16	237	229
21:00	49.92	230	-5	-33	230	85	74	26	231	195
22:00	50.07	239	29	-36	239	116	34	31	239	109
23:00	50.05	236	37	-40	236	136	28	33	237	105
24:00	50.14	237	56	-43	237	172	25	33	238	99

Appendix C

15-minunt station load data for the four clustered wind energy feeders.

TIME	TOTAL	
	MW	MVAR
0:15	20.31	1.29
0:30	19.87	1.32
0:45	23.02	1.51
1:00	26.72	1.22
1:15	24.55	1.18
1:30	23.4	1.11
1:45	24.99	0.90
2:00	33.67	0.89
2:15	34.13	0.90
2:30	34.01	0.90
2:45	33.87	0.89
3:00	28.99	0.45
3:15	28.76	0.48
3:30	28.98	0.64
3:45	27.91	0.76
4:00	42.81	1.35
4:15	42.60	1.34
4:30	41.95	1.34
4:45	43.04	1.29
5:00	44.76	1.45
5:15	44.60	1.64
5:30	44.34	1.41
5:45	43.59	1.50
6:00	44.55	1.67
6:15	48.20	1.61
6:30	49.44	1.53
6:45	60.13	2.08
7:00	59.35	2.11
7:15	65.02	2.4
7:30	66.19	2.22
7:45	73.11	3.04
8:00	80.16	3.91
8:15	83.17	3.96
8:30	87.09	3.72
8:45	81.18	3.74
9:00	88.25	4.67
9:15	79.69	3.46
9:30	85.33	4.37

9:45	74.83	4.33
10:00	78.64	4.75
10:15	78.60	4.48
10:30	78.89	3.99
10:45	68.73	2.51
11:00	56.33	2.01
11:15	66.37	1.53
11:30	43.39	0.72
11:45	50.22	1.27
12:00	46.59	1.13
12:15	42.79	1.16
12:30	46.87	1.20
12:45	40.33	1.15
13:00	38.09	0.87
13:15	35.59	0.83
13:30	43.63	1.15
13:45	35.04	0.90
14:00	28.82	0.50
14:15	16.28	1.02
14:30	11.92	1.16
14:45	23.24	1.07
15:00	20.65	1.27
15:15	17.93	0.6
15:30	14.72	0.86
15:45	13.82	1.20
16:00	15.58	1.00
16:15	19.23	1.05
16:30	24.42	1.07
16:45	28.04	0.81
17:00	30.08	1.47
17:15	49.14	1.64
17:30	50.81	1.47
17:45	49.65	1.60
18:00	48.88	1.42
18:15	47.95	1.49
18:30	54.06	2.14
18:45	56.41	1.83
19:00	61.73	3.17
19:15	59.92	2.53
19:30	66.28	2.72
19:45	64.15	2.48
20:00	63.62	1.84
20:15	62.16	2.07
20:30	67.15	2.27

20:45	69.68	2.24
21:00	68.46	2.69
21:15	66.88	2.61
21:30	64.43	2.03
21:45	57.91	1.85
22:00	52.41	1.96
22:15	61.60	1.99
22:30	65.40	2.75
22:45	73.03	2.90
23:00	68.85	3.12
23:15	81.98	3.72
23:30	77.61	3.51
23:45	76.57	3.83
0:00	75.35	3.49

Appendix D

Appendix D 1. DPFC CBA for Ashegoda wind farm

DPFC CBA for Ashegoda wind farm			
1	Parameter	Value	Unit
2	Base power	130	MVA
3	Base voltage	230	KV
4	Series unit rating	8	MVA
5	No. of series units	3	Units
6	Shunt unit rating	25	MVA
7	Series unit cost	$ 4,008,000.00	USD/unit
8	Shunt unit cost	$ 3,725,000.0	USD/unit
9	Installation cost	150000	USD/unit
10	Annual Ope&mai rate	0.02	%
11	Loss reduction	3	MW
12	Energy price	0.026	USD/kwh
13	Period of analysis	20	Years
14	Discount rate	0.08	
15	Loan interest	0.18	
Capital cost			
	Series converter total	$ 4,008,000.0	
	Shunt converter total	$ 3,725,000.0	
	Installation cost	$ 150,000.0	
	Total capital cost	$ 7,883,000.00	
Annual operating and maintenance cost			
	O&m cost per year	$ 157,660.00	

Appendix D 2. Total cost benefit analysis

year	Benefit (USD)	O&M (USD)	Net cash flow (USD)	Discount rate	NPV
0	$ -	$ 157,666	-157666	1.000	-157666.00
1	$ 683,280.0	$ 315,332	$ 367,948.00	0.847	$ 311,820.3
2	$ 1,366,560.0	$ 472,998	$ 893,562.0	0.718	$ 641,742.3
3	$ 2,049,840.0	$ 630,664	$ 1,419,176.0	0.609	$ 863,754.3
4	$ 2,733,120.0	$ 788,330	$ 1,944,790.0	0.516	$ 1,003,101.0
5	$ 3,416,400.0	$ 945,996	$ 2,470,404.0	0.437	$ 1,079,836.4
6	$ 4,099,680.0	$ 1,103,662	$ 2,996,018.0	0.370	$ 1,109,819.6
7	$ 4,782,960.0	$ 1,261,328	$ 3,521,632.0	0.314	$ 1,105,528.4
8	$ 5,466,240.0	$ 1,418,994	$ 4,047,246.0	0.266	$ 1,076,721.9
9	$ 6,149,520.0	$ 1,576,660	$ 4,572,860.0	0.225	$ 1,030,979.0
10	$ 6,832,800.0	$ 1,734,326	$ 5,098,474.0	0.191	$ 974,137.2
11	$ 7,516,080.0	$ 1,891,992	$ 5,624,088.0	0.162	$ 910,646.9
12	$ 8,199,360.0	$ 2,049,658	$ 6,149,702.0	0.137	$ 843,859.2
13	$ 8,882,640.0	$ 2,207,324	$ 6,675,316.0	0.116	$ 776,257.4
14	$ 9,565,920.0	$ 2,364,990	$ 7,200,930.0	0.099	$ 709,643.9
15	$ 10,249,200.0	$ 2,522,656	$ 7,726,544.0	0.084	$ 645,290.4
16	$ 10,932,480.0	$ 2,680,322	$ 8,252,158.0	0.071	$ 584,057.2
17	$ 11,615,760.0	$ 2,837,988	$ 8,777,772.0	0.060	$ 526,490.1
18	$ 12,299,040.0	$ 2,995,654	$ 9,303,386.0	0.051	$ 472,895.2
19	$ 12,982,320.0	$ 3,153,320	$ 9,829,000.0	0.043	$ 423,400.3
20	$ 13,665,600.0	$ 3,310,986	$ 10,354,614.0	0.037	$ 378,001.7
Total value at the end of 20th year					$ 15,310,316.9
Profit at the end of 20th year					$ 7,427,316.86

Appendix E

Power quality classification and characteristics

№	Category				Typical duration	Voltage magnitude
1	Transients	Impulsive	Nanosecond		< 50 ns	-
			Microsecond		50 ns – 1 ms	-
			Millisecond		> 1 ms	
		Oscillatory	Low frequency	< 50 kHz	0.3 – 0.5 ms	0 – 4 pu
			Medium frequency	5 – 500 kHz	20 μs	0 – 8 pu
			High frequency	0.5 – 5 MHz	5 μs	0 – 4 pu
2	Short-duration variations	Instantaneous	Interruption		0.5 – 30 cycles	< 0.1 pu
			Sag (dip)			0.1 – 0.9 pu
			Swell			1.1 – 1.8 pu
		Momentary	Interruption		30 cycles – 3 s	< 0.1 pu
			Sag (dip)			0.1 – 0.9 pu
			Swell			1.1 – 1.4 pu
		Temporary	Interruption		3 s – 1 min	< 0.1 pu
			Sag (dip)			0.1 – 0.9 pu
			Swell			1.1 – 1.2 pu
3	Long –duration variations		Interruption		> 1 min	0.0 pu
			Under-voltage		> 1 min	0.8 – 0.9 pu
			Over-voltage		> 1 min	1.1 – 1.2 pu
4	Voltage unbalance				Steady state	0.5 – 2%
5	Wave distortion		DC offset		Steady state	0 – 0.1%
			Harmonics		Steady state	0 – 20%
			Inter-harmonics		Steady state	0 – 2 %
			Notching		Steady state	
			Noise		Steady state	0 – 1%
6	Voltage fluctuations				Intermittent	0.1 -7%
7	Power frequency variations				< 50 ns	

Appendix F

MATLAB M-file code

```
%% Genetic Algorithm Optimization for DPFC Placement and Sizing for Ashegoda wind farm
% 3-Bus 230kV System - MATLAB Script

clc;
clear;

%% System base-values
S_base = 130e6;      % Base apparent power 130MVA
V_base = 230e3;      % Base system voltage 230KV
Z_base = 400;      % Base system impedance 400 ohm


%% line impedance specification base values

Z12 = 2.565 + 0.09i;      % line impedance between Lachi - Ashegoda
Z23 = 24.111 + 0.846i;        % line impedance between Lachi - Alamata
Z13 = 21.375 + 0.75i;      % line impedance between Alamata - Ashegoda

%% line impedance specification in per unit value Zpu = Zactual/ Zbase

Z12_pu = 0.0064 + 0.0002i;      % line impedance between Lachi - Alamata
Z23_pu = 0.0602 + 0.0021i;      % line impedance between Lachi - Ashegoda
Z13_pu = 0.053 + 0.0018i;      % line impedance between Alamata - Ashegoda


%% GA Setup
nvars = 3; % [busIndex, SeriesSize (MVA), ShuntSize (MVA)]
lb = [1, 1, 5];   % lower bounds
ub = [3, 25, 50]; % upper bounds

fitnessFcn = @(x) dpfc_fitness(x, Z12_pu, Z23_pu, Z13_pu, S_base, V_base);

options = optimoptions('ga', ...
    'PopulationSize', 29, ...
    'MaxGenerations', 100, ...
    'Display', 'iter', ...
    'PlotFcn', {@gaplotbestf});

[x_opt, fval] = ga(fitnessFcn, nvars, [], [], [], [], lb, ub, [], options);

fprintf('\nOptimal Bus to Place Series DPFC: %d\nSeries Converter Size: %.2f MVA\nShunt Converter Size:
%.2f MVA\n', ...
    round(x_opt(1)), x_opt(2), x_opt(3));


%% --- Objective Function ---
function cost = objfun_dpfc(x, Y, bus_data)
    bus = round(x(1));
    P_inj = x(1);
    Q_inj = x(3);
```

```
    bd = bus_data;
    bd(bus,1) = bd(bus,1) + P_inj;
    bd(bus,2) = bd(bus,3) + Q_inj;

    [V, success] = powerflow(Y, bd);

    if ~success || any(isnan(V))
        cost = 1.35e6;
        return;
    end

    I = Y * V;
    S = V .* conj(I);
    loss = sum(real(S));
    volt_dev = sum(abs(abs(V) - 1));

    cost = 0.7 * loss + 0.5 * volt_dev * 100;
end

%% --- Nonlinear Constraints ---
function [c, ceq] = nonlcon_dpfc(x, Y, bus_data)
    V_min = 0.90;
    V_max = 1.1;
    bus = round(x(1));

    bd = bus_data;
    bd(bus,1) = bd(bus,1) + x(2);
    bd(bus,2) = bd(bus,2) + x(3);

    [V, success] = powerflow(Y, bd);
    if ~success
        c = [1]; ceq = [];
        return;
    end

    Vmag = abs(V);
    c = [Vmag - V_max; V_min - Vmag];
    ceq = [];
end

%% Newton-Raphson Power Flow Solve for 3-bus)
function [V, success] = powerflow(Y, bus_data)
    max_iter = 20;
    tol = 1e-6;
    V = ones(3,1);
            .
            .
            .
```

Appendix G

General network diagram 2015 existing-model [41].

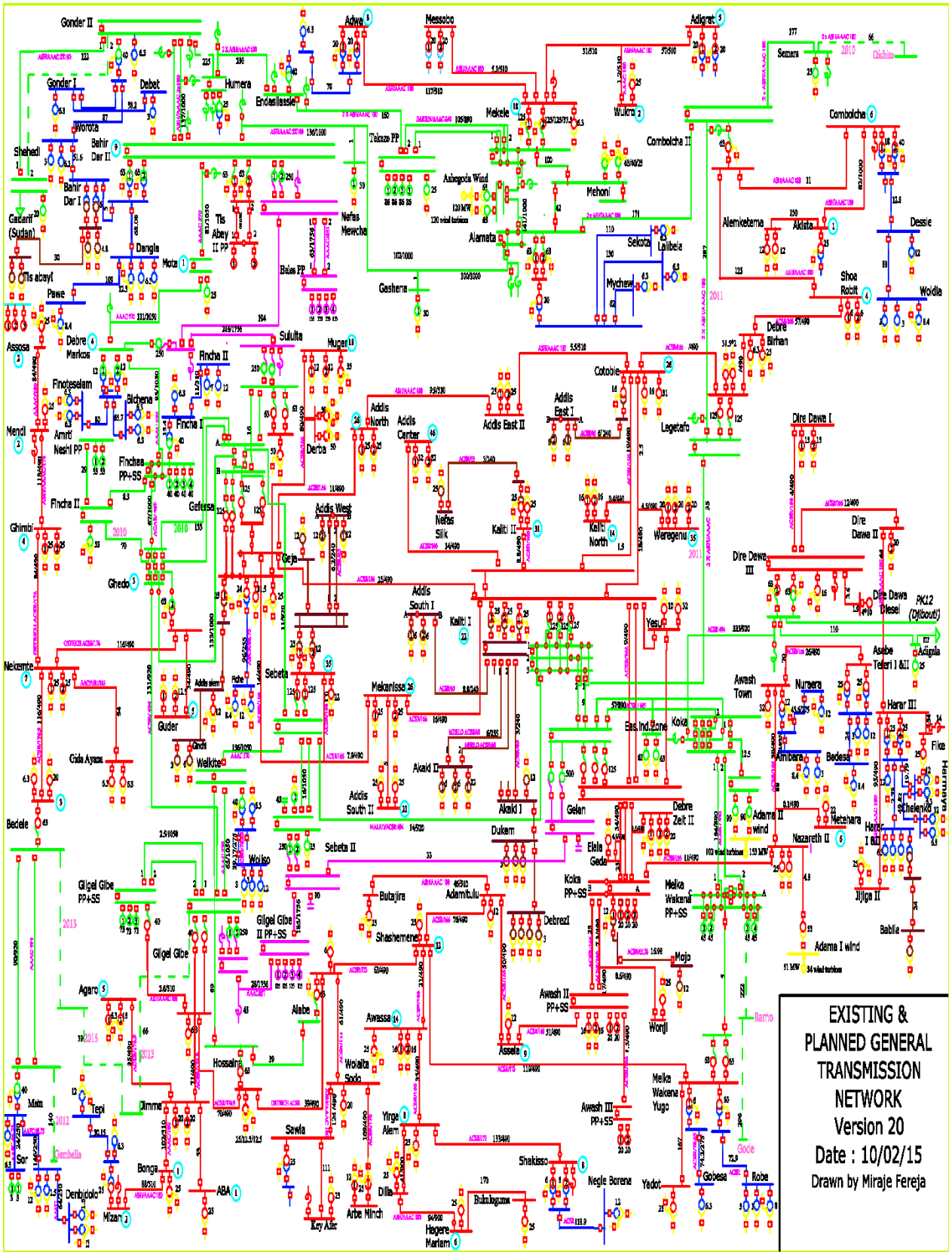

Appendix H

Over all MATLAB Simulink model.